NASA CR-165276

LOW-THRUST CHEMICAL ROCKET ENGINE STUDY

by J. A. Mellish

AEROJET LIQUID ROCKET COMPANY

Prepared for

NATIONAL AERONAUTICS AND SPACE ADMINISTRATION

NASA/Lewis Research Center
Contract NAS 3-21940

1. Report No. NASA CR-165276	2. Government Accession No.	3. Recipient's Catalog No.
4. Title and Subtitle Low-Thrust Chemical Rocket Engine Study		5. Report Date March 1981 6. Performing Organization Code
7. Author(s) J. A. Mellish		8. Performing Organization Report No. 10. Work Unit No.
9. Performing Organization Name and Address Aerojet Liquid Rocket Company Post Office Box 13222 Sacramento, CA 95813		11. Contract or Grant No. NAS 3-21940
12. Sponsoring Agency Name and Address National Aeronautics and Space Administration Washington, D.C. 20546		13. Type of Report and Period Covered Contractor Report, Final 14. Sponsoring Agency Code

15. Supplementary Notes

Project Manager, Mr. D. D. Scheer, Space Propulsion and Power Division, NASA-Lewis Research Center, Cleveland, OH 44135

16 Abstract

This program provides the engine data and information, required by NASA and vehicle contractors, to perform system studies on cargo orbit-transfer vehicles which would deliver large space structures to geosynchronous equatorial orbit. Low-thrust engine performance, weight, and envelope parametric data were established, preliminary design information was generated, and technologies for liquid rocket engines were identified.

Two major engine design drivers were considered in the study: (1) cooling and (2) engine cycle options. Both film-cooled and regeneratively cooled engines were evaluated. The propellant combinations studied were hydrogen/oxygen, methane/oxygen, and kerosene/oxygen. The fuels were used as the engine coolants. Pressure-fed and pump-fed engine cycle categories were investigated as candidates for the subject engine application, and data for various cycle options within each category were provided. The options considered include conventional pressure-fed, parallel accumulator, expander, turboalternator, auxiliary power source, and pump-filled feed system tank concepts.

Engine cooling and parametric evaluations were conducted over a range of thrusts from 445 N (100 lbF) to 13445 N (3000 lbF) and a range of chamber pressures from 1.36 atm (20 psia) to 68 atm (1000 psia). Feasible operating regimes for each coolant, coolant scheme, and engine cycle concept were established.

A 224 N (500 lbF) thrust, 34 atm (500 psia) chamber pressure hydrogen/oxygen pump-fed engine was selected for preliminary design. The engine is regeneratively cooled with hydrogen and uses a mixed expander and turboalternator engine cycle. The parametric data for this concept were updated to reflect the results of the preliminary design effort.

17 Key Words (Suggested by Author(s))	18. Distribution Statement
Low-Thrust Cargo Orbit-Transfer Vehicles Chemical Rocket Engines H_2/O_2, CH_4/O_2, RP-1/O_2 Propellant Combinations Pump-Fed and Pressure Fed Engines	Unclassified-Unlimited

19 Security Classif. (of this report)	20. Security Classif. (of this page)	21. No. of Pages	22. Price*
Unclassified	Unclassified	148	

* For sale by the National Technical Information Service, Springfield, Virginia 22161

NASA-C-168 (Rev 10-75)

PRECEDING PAGE BLANK NOT FILMED

FOREWORD

The work described herein was performed at the Aerojet Liquid Rocket Company (ALRC) under Contract NAS 3-21940 with Mr. Dean D. Scheer of the NASA/Lewis Research Center serving as the Project Manager. The ALRC Program Manager was Mr. Larry B. Bassham, and the Project Engineer was Mr. Joseph A. Mellish.

The study involved parametric, conceptual, and preliminary design analyses to provide engine system data and descriptions necessary for low-thrust cargo orbit-transfer vehicle (COTV) studies and to identify technology needs in the propulsion area.

The technical period of performance for this study was from 20 July 1979 to 12 December 1980.

The author wishes to acknowledge the efforts of the following ALRC Engineering personnel who contributed significantly to the study program and to this report:

K. L. Christensen
R. L. Ewen
R. A. Hewitt
G. R. Janser
J. E. Jellison
L. L. Lang
A. V. Lundback
P. J. Robinson
R. L. Sabiers
W. R. Thompson
B. E. Wallis

TABLE OF CONTENTS

TABLE OF CONTENTS (Cont.)

LIST OF TABLES

LIST OF FIGURES

LIST OF FIGURES (cont.)

LIST OF FICURES (cont.)

SECTION I

SUMMARY

A. STUDY OBJECTIVES AND SCOPE

The major objectives of this Low-Thrust Chemical Rocket Engine Study were to provide parametric data and preliminary designs on liquid rocket engines for low-thrust cargo orbit-transfer-vehicles (COTV) and to identify those items where technology is required to enhance the designs.

Specific study objectives were:

- Provide fundamental propellant property, combustion property, and performance data for O_2/H_2, O_2/RP-1, and O_2/CH_4 engine concepts.
- Establish the combined thrust level and chamber pressure range over which conventional film-cooled and regeneratively cooled low-thrust chamber designs are feasible.
- Identify potential operating conditions by considering advanced cooling schemes.
- Devise engine system concepts for the low-thrust application.
- Generate parametric performance, weight, and envelope data for viable concepts based upon historical data and conceptual evaluations.
- Select a concept and design point for preliminary design.
- Prepare a preliminary design of the selected engine concept.
- Update the parametric data and provide these data in a format suitable for use by COTV vehicle system contractors.

To accomplish the program objectives, two major engine design drivers were evaluated in the study: (1) cooling and (2) engine cycle. The propellant combinations, coolants, cooling methods, and parametric ranges investigated are summarized in Table I. Pressure-fed and pump-fed engine categories were investigated for this engine application. Parametric weight, envelope, and performance data are provided for various cycle options within each engine category. The cycle options evaluated include conventional pressure-fed, parallel accumulator, expander, turboalternator, auxiliary power source, and pump-filled feed tank concepts.

TABLE I. - LOW-THRUST ENGINE STUDY CASES

PROPELLANT COMBINATION	O/F	COOLING METHOD	COOLANT	THRUST STUDY RANGE N (LBF)		CHAMBER PRESSURE STUDY RANGE, ATM (PSIA)	
H_2/O_2	6.0	Regen	H_2	445-13345	(100-3000)	1.36-68	(20-1000)
H_2/O_2	6.0	Film	H_2	445-13345	(100-3000)	1.36-68	(20-1000)
RP-1/O_2	3.0	Regen	RP-1	445-13345	(100-3000)	1.36-68	(20-1000)
RP-1/O_2	3.0	Film	RP-1	445-13345	(100-3000)	1.36-68	(20-1000)
CH_4/O_2	3.7	Regen	CH_4	445-13345	(100-3000)	1.36-68	(20-1000)
CH_4/O_2	3.7	Film	CH_4	445-13345	(100-3000)	1.36-68	(20-1000)

B. RESULTS AND CONCLUSIONS

1. Regenerative Cooling Analysis Results

The study showed that cooling with kerosene, RP-1, was not feasible over the entire thrust and chamber pressure ranges using conventional design practice and criteria. The thermal data showed that the RP-1 bulk temperature exceeded the coking temperature limit of 1010°R. Therefore, design features to minimize the enthalpy rise of the coolant were investigated. A graphite thermal liner, short chamber lengths, and purified RP-1 were assumed to obtain the results shown in Figure 1. With these features, RP-1 was found to be a feasible coolant over combined thrust and chamber pressure ranges of 1100 N (250 lbF) and 1.36 atm (20 psia) to 13345 N (3000 lbF) and 47.6 atm (700 psia). These results were obtained assuming no benefit from carbon deposition. It was not considered prudent to base the design studies on the dependence of a carbon layer formation because of uncertainties in the experimental data base.

Methane, CH_4, provided a larger feasible cooling regime, as shown in Figure 1. The cooling limit shown on the figure was obtained for advanced designs using a thermal liner and short chamber lengths. Without advanced features, the minimum thrust level that is feasible to cool at 68 atm (1000 psia) chamber pressure was determined to be 7120 N (1600 lbF).

Hydrogen, H_2, provided the largest cooling operating map, as shown in Figure 1. Thermal liners are not required or desired with this coolant. The limit shown in the figure is for an advanced short chamber; however, even for longer chamber lengths, an engine with a thrust level as low as 4448 N (1000 lbF) was found to be feasible to cool at 68 atm (1000 psia).

Based upon the coolant investigations, the following regeneratively cooled systems were evaluated in the system concept studies:

Propellant Combination	Coolant	Regen Cooling Scheme
O_2/RP-1	RP-1	Advanced
O_2/H_2	H_2	Conventional and advanced
O_2/CH_4	CH_4	Conventional and advanced

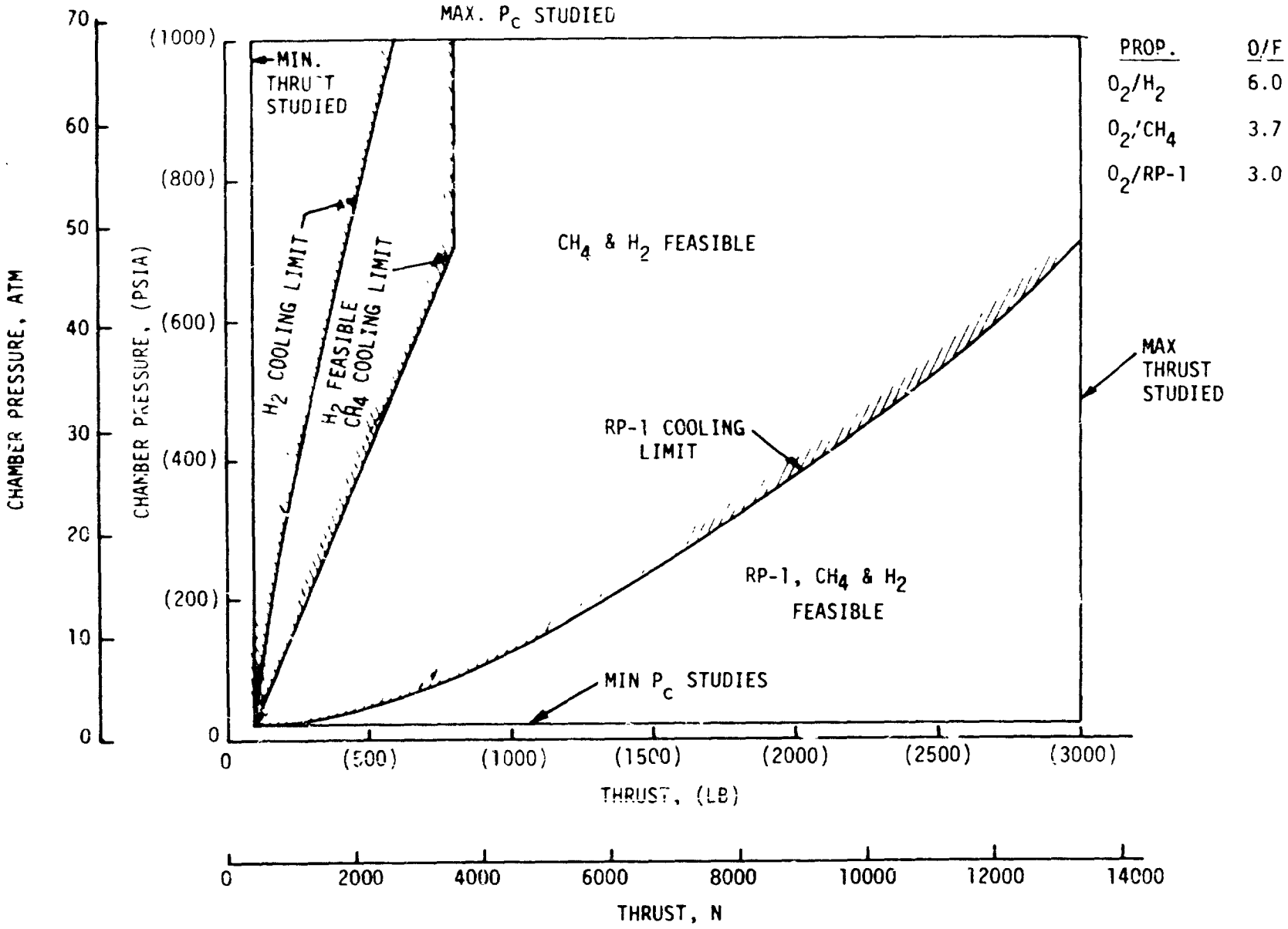

Figure 1. Regen Cooling Limits Summary

I, B, Results and Conclusions (cont.)

2. Film Cooling Analysis Results

The results of film cooling studies to establish the upper chamber pressure limit, based on a 10% performance degradation, are shown in Figure 2 for the three fuels. The performance degradation is based upon a comparison with the performance of an engine requiring no film cooling. Hydrogen and RP-1 provide small film cooling feasible regimes. Film cooling with methane was not found to be feasible unless it was assumed that the CH_4 decomposes. Since an analysis of the kinetics of CH_4 decomposition was beyond the scope of this study effort, CH_4 film cooling was dropped from the study. The RP-1 film cooling regime was deemed to be too small to be feasible; consequently only the O_2/H_2, H_2 film-cooled engines were carried into the concept evaluations.

3. Concept Evaluation Results

Various propulsion system concepts were screened to identify those most promising for the COTV. The basic engine system concepts evaluated are shown in Figure 3. Engine performance, weight and envelope parametric data, and system weight differences were established to aid in this screening process.

As shown by Figure 3, two pressure-fed concepts (i.e., conventional pressure-fed and parallel accumulator) and four basic pump-fed concepts were evaluated. A mixed expander/turboalternator cycle was also included in the O_2/H_2 engine investigations. This cycle has the fuel pump and alternator driven in the expander mode whereas the oxidizer pump is driven by an electric motor.

Based upon the coolant evaluations and system considerations, the concepts considered to be applicable for each candidate system and coolant are shown in Figure 4. More options are available with O_2/H_2 regeneratively cooled engines.

The ranking of the system concepts in the order of increasing weight is listed below:

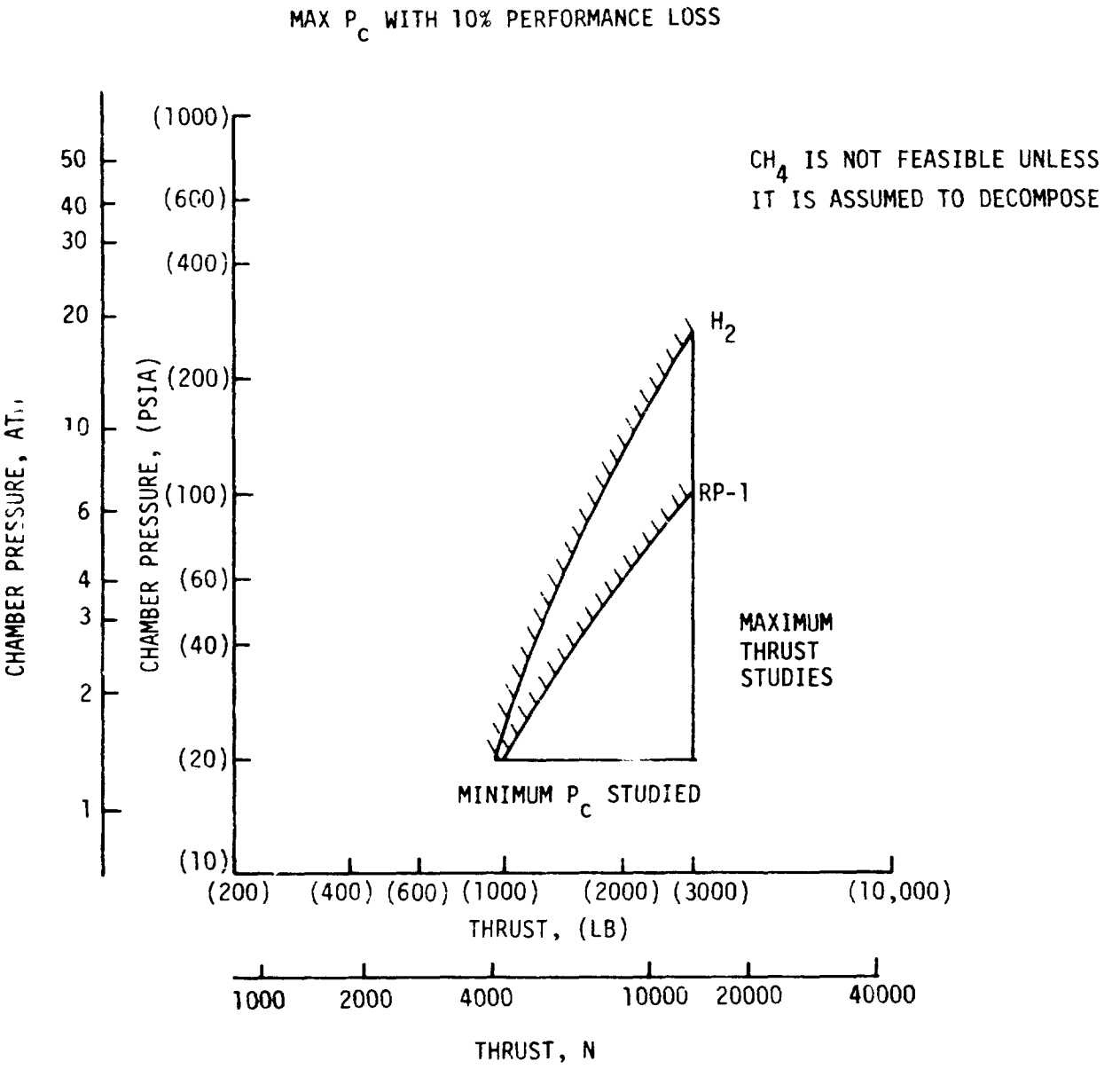

Figure 2. Film Cooling Analyses Results

CONVENTIONAL PRESSURE-FED

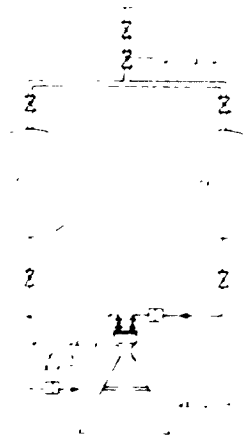

AUXILIARY POWER SOURCE

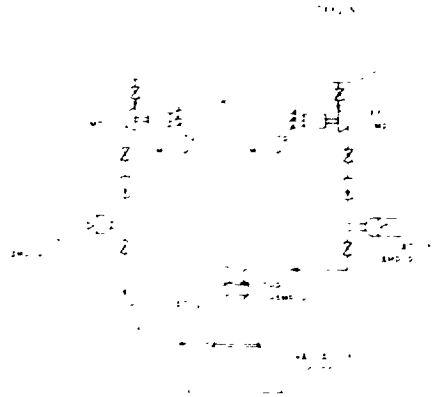

TURBOALTERNATOR

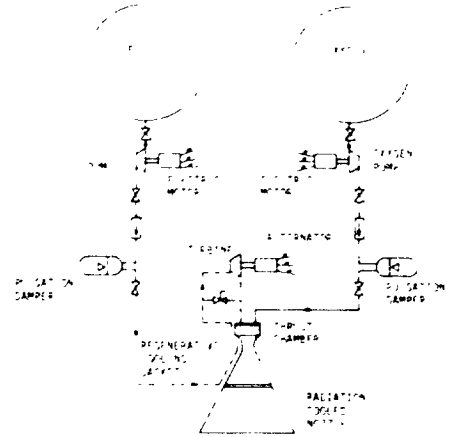

PARALLEL ACCUMULATOR

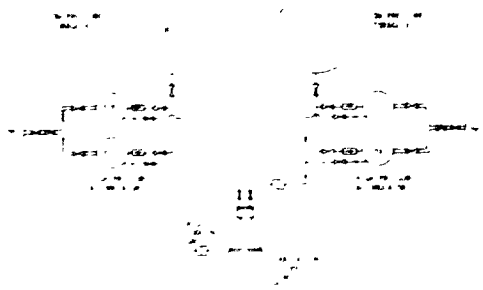

PUMP-FILLED FEED TANK

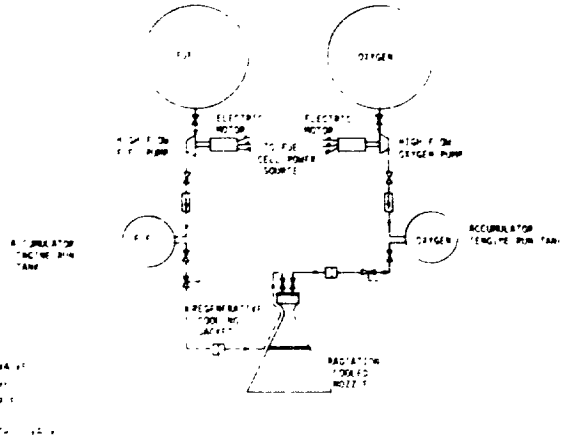

EXPANDER

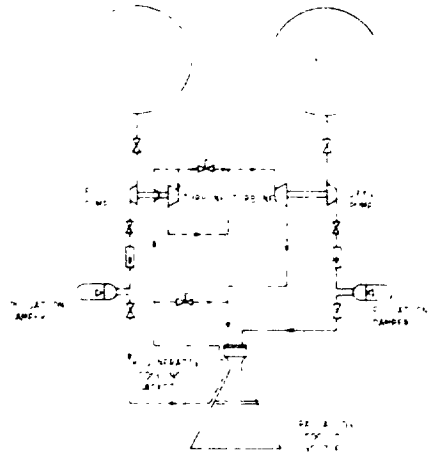

Figure 3. Basic Engine System Concepts

PROPELLANT COMBINATION / SYSTEM CONCEPT	FUEL REGEN - COOLED			FUEL FILM-COOLED
	$O_2/RP\text{-}1$	O_2/H_2	O_2/CH_4	O_2/H_2
SIMPLE PRESSURE-FED	X	X		X
PARALLEL ACCUMULATOR	X	X		X
AUXILIARY POWER SOURCE	X	X	X	X
TURBOALTERNATOR		X	X	
EXPANDER		X	X	
PUMP-FILLED FEED TANK	X	X		X
MIXED EXPANDER & TURBOALTERNATOR		X		

TOTAL OF 18 PARAMETRIC DATA CASES

Figure 4. Engine System Concept Matrix

I, B, Results and Conclusions (cont.)

Concept	Additional Weight Driver
1. Expander Cycle	-
2. Mixed Expander/Turbo-alternator Cycle	Electrical Components
3. Turboalternator Cycle	Electrical Components
4. Auxiliary Power Sorrce	Fuel Cells
5. Pump-Filled Feed Tanks	Accumulators
6. Parallel Accumulator	Accumulators and Pressurization
7. Conventional Pressure-Fed	Large Tanks and Pressurization

The results of the concept comparisons showed that film-cooled engine performance is too low. There is a 10% performance loss when compared to a regeneratively cooled engine at only moderate (i.e., 6.8 atm (100 psia) to 13.6 atm (200 psia)) operating chamber pressures. Film-cooled systems are also only applicable with the heavier-weight system options.

RP-1 systems are also only applicable with the heavier system concepts because heated RP-1 is not a good turbine drive fluid.

Methane regeneratively cooled pressure-fed systems are not practical because feasible cooling system designs could have only been obtainec if the coolant pressure had been maintained above the critical pressure of CH_4; 45.4 atm (667 psia). This makes the propellant tanks and pressurization system too heavy.

Hydrogen regeneratively cooled engines have the highest performance, demonstrating approximately a 120-sec advantage over RP-1 and a 95-sec increase in comparison to CH_4. Pump-fed, regeneratively cooled engines are also the lightest weight system options.

As a result of these concept evaluations, a pump-fed, regeneratively cooled, mixed expander/turboalternator O_2/H_2 engine was selected for preliminary design.

4. Preliminary Design Results

The engine design point and system schematic selected for preliminary design is shown in Figure 5.

The engine cycle selected is a mixed expander and turboalternator cycle. The expander/turboalternator concept incorporates some of the best features of the expander and turboalternator cycles. The hydrogen turbopump is driven in the expander mode, and the oxidizer turbopump is driven in the turboalternator mode. This eliminates a large electric motor and reduces the size of the alternator conventionally used for a turboalternator cycle. The lower horsepower oxygen pump is driven by an electric motor. The advantage over an expander cycle is the elimination of a hot-gas bipropellant seal, with only a minor weight penalty for the alternator and electric motor.

The design point thrust and chamber pressure were selected on the basis of the thermal and power balance results obtained as well as the vehicle study inputs provided by NASA/LeRC. It is on the low side of the system study recommendations but provides a reasonable base point for technology identification.

To meet the engine pressure schedule requirements, hydrogen is pumped to a pressure of approximately 62.6 atm (920 psia) for delivery to the thrust chamber. The hydrogen enters the thrust chamber coolant jacket at an area ratio of 23:1 and flows forward through a slotted copper chamber to the injector headend. Eighty percent of the hydrogen flow is used to drive the LH_2 TPA turbine and alternator assembly. The remaining heated hydrogen bypasses the turbine assembly and provides the cycle power balance margin and thrust control.

The oxygen is pumped to a pressure of approximately 43.5 atm (640 psia) and is delivered to the thrust chamber injector in the liquid state to be mixed and burned with the gaseous hydrogen.

The nozzle extension is radiation-cooled from an area ratio of 23:1 to the exit (ε = 400:1). FS-85 columbium with a silicide coating has been tentatively selected as the nozzle extension material because of its high temperature capability.

The engine preliminary design and resulting characteristics are summarized in Figure 6. Parametric weight, envelope, and performance data are shown as a function of nozzle area ratio in Figure 7 for the baseline engine concept.

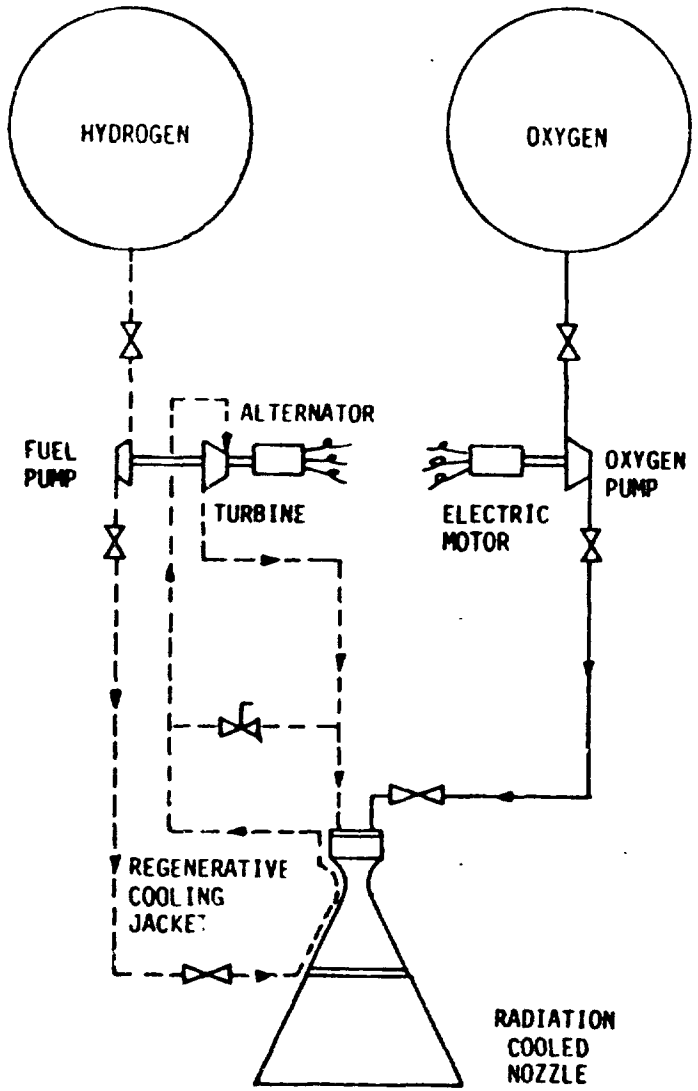

Propellant Combination	O_2/H_2
Engine Vacuum Thrust, N (lb)	2220 (500)
Thrust Chamber Pressure, atm (psia)	34 (500)
Engine Mixture Ratio	6.0
Nozzle Area Ratio	400:1
Thrust Chamber Coolant	H_2
Cooling Method	Regen
Engine Cycle	Mixed Expander & Turboalternator

FLOW CONTROL VALVE

SHUT-OFF VALVE

Figure 5. Engine Preliminary Design Point and System Schematic

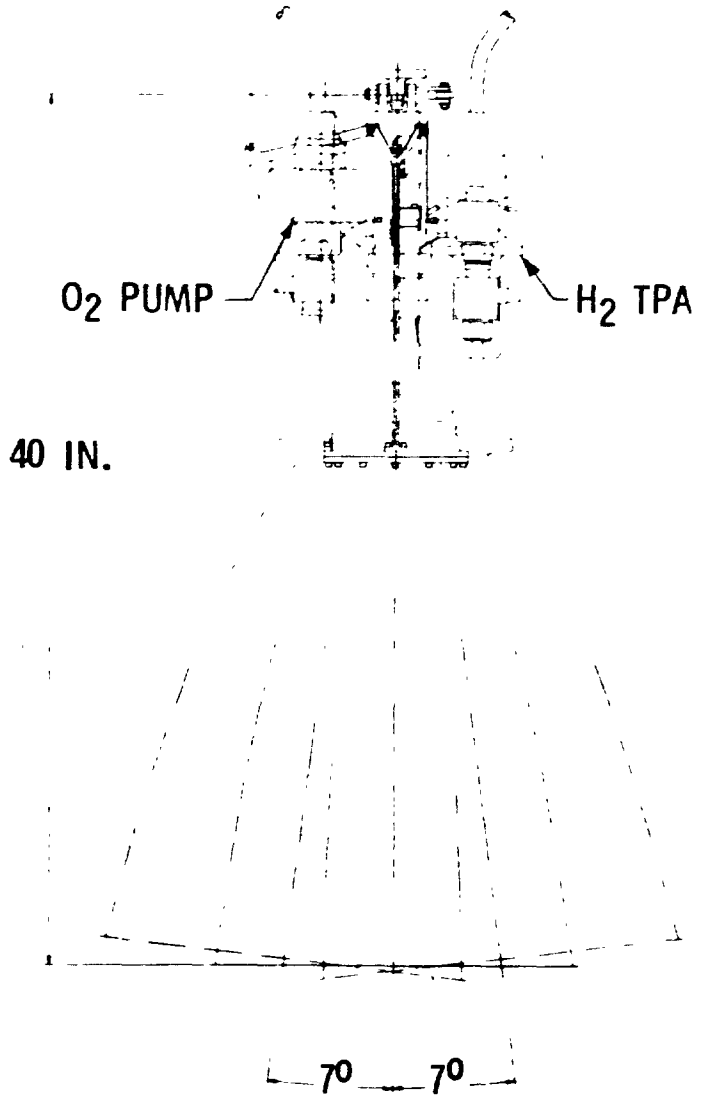

PROPELLANTS	O_2/H_2
VAC. THRUST, N (LB)	2224 (500)
CHAMBER PRESSURE, ATM (PSIA)	34 (500)
ENGINE O/F	6.0
NOZZLE AREA RATIO	400:1
COOLING METHOD	REGEN
COOLANT	H_2
VAC. DELIVERED I_s, SEC	465
ENGINE WEIGHT, kg (LB)	38.8 (85.4)
ENGINE LENGTH, Cm (IN.)	101.6 (40)
STATIC NOZZLE EXIT DIA.,Cm(IN.)	40.6 (16)

Figure 6. Engine Preliminary Design Summary

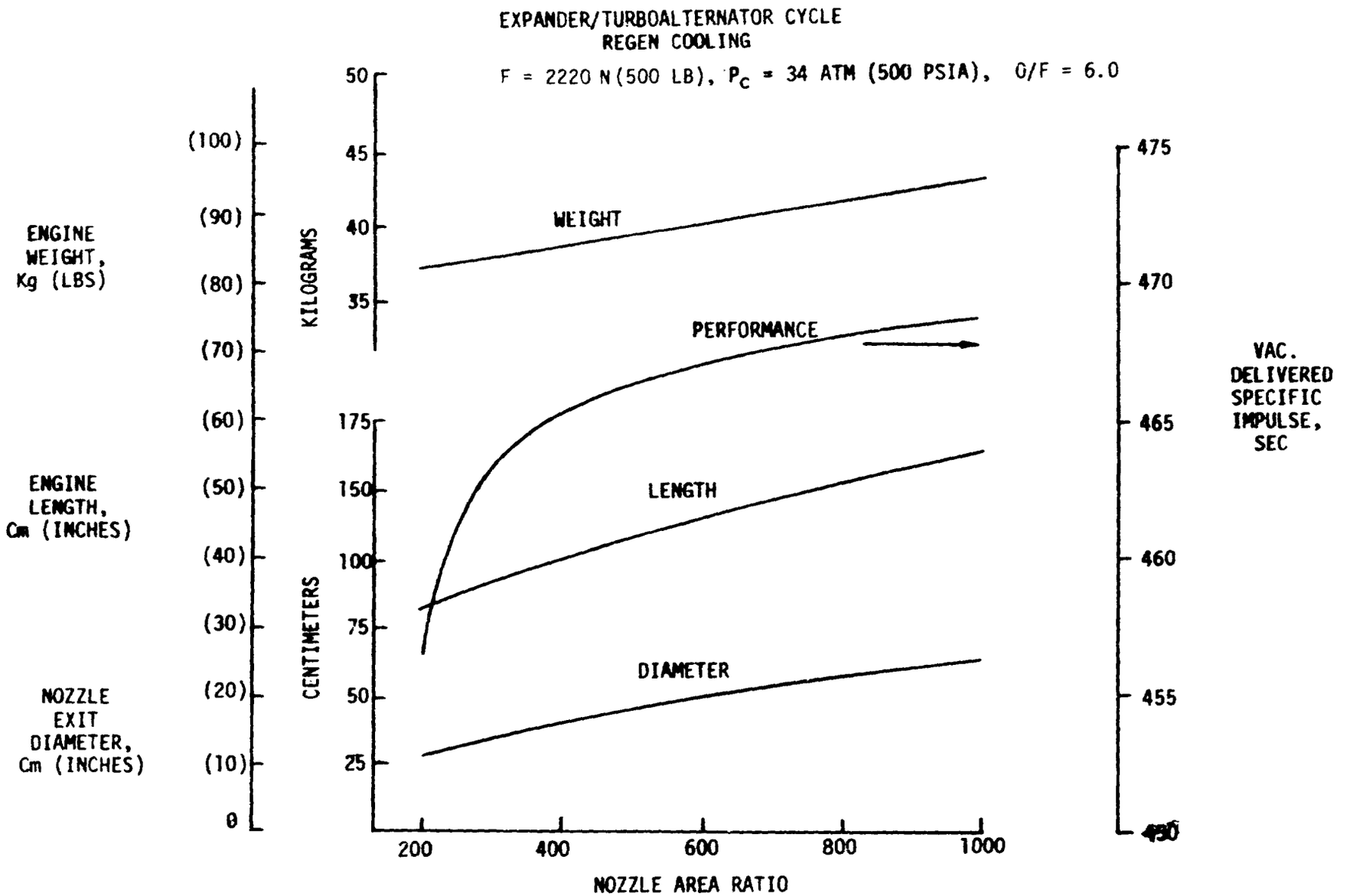

Figure 7. O_2/H_2 Engine Parametric Data Summary

I, B, Results and Conclusions (cont.)

5. Technology Items

Engine component technology programs should be undertaken to reduce the development risk, verify performance, and confirm the power balance of the low-thrust engine. The major technology areas are depicted in Figure 8. Specific items requiring technology are summarized below:

- Demonstrate the performance of high-speed, high-head rise, low-flow multistage, centrifugal pumps.
- Experimentally verify the performance of small, low-flow, partial-admission gas turbines.
- Experimentally evaluate the chamber coolant stability, verify the thermal predictions, and investigate thermally enhanced high heat flux chambers.
- Demonstrate high altitude ignition and restart.
- Optimize the engine thrust and mixture ratio control system.
- Experimentally verify high area ratio nozzle performance.

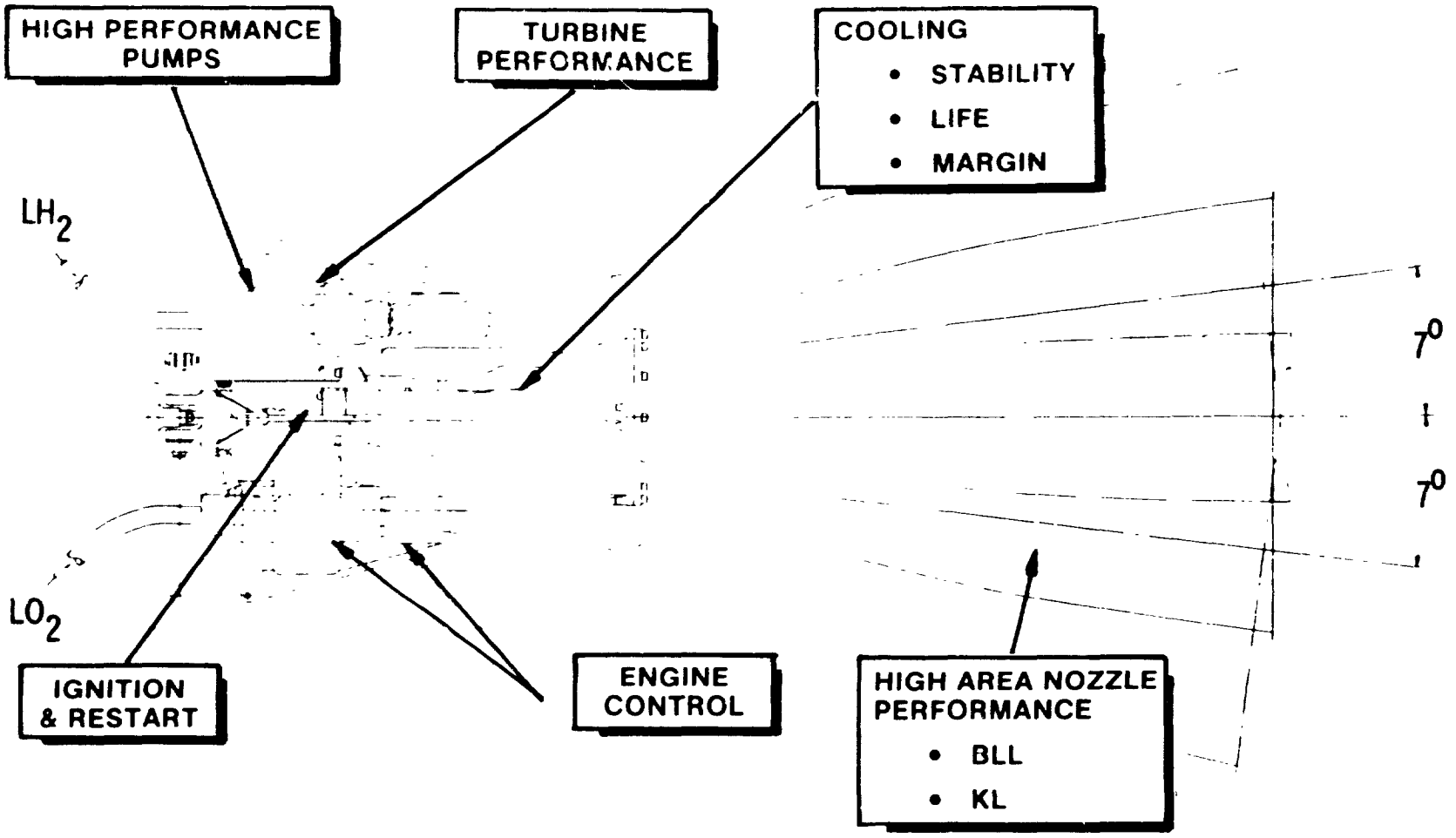

Figure 8. Technology Areas Summary

SECTION II

INTRODUCTION

A. BACKGROUND

A number of studies have forecast the need for large space structures such as microwave antennas and reflectors in geosynchronous equatorial orbit (GEO). These structures would be launched to low earth orbit (LEO) in a stowed condition by using the Space Shuttle and would subsequently be transferred to GEO by way of a high-energy space propulsion system. There are two options available for placement of these types of payloads in GEO. In the first option, the LEO-to-GEO transfer would be accomplished with the payload in the stowed condition, followed by manned or automated deployment and assembly in GEO. Either high or low thrust could be used for the transfer. In the second option, manned or automated deployment and assembly would be carried out in LEO, followed by a LEO-to-GEO transfer with the payload in the assembled condition. Here, low thrust would be required in order to preclude high inertia loading which would cause damage to the assembled payload.

Since the early 1970's, NASA and DoD have sponsored a number of studies which examined both vehicles and engine systems suitable for the high-thrust option noted above. Considerable effort has also been conducted on very low-thrust solar-electric propulsion systems which have application for missions in which extended LEO-to-GEO transfer times are acceptable. Chemical engine systems suitable for the low-thrust option have not received in-depth attention. It was the purpose of this work to provide the data necessary for orbit-transfer-vehicle studies utilizing low-thrust chemical propulsion.

B. ENGINE REQUIREMENTS

Engine requirements for the candidate low-thrust COTV engines used in this study are summarized in Table II.

The engine is planned to be used on a low-thrust orbit transfer vehicle and is expendable. To perform the mission, four perigee burns and one apogee burn were baselined for this study. The accumulated run time for these burns is shown as a function of thrust in Figure 9.

To conduct this study, currently achievable component performance levels and currently available materials were assumed.

C. STUDY APPROACH

The study effort was divided into four technical tasks plus a reporting task. In Task I, properties and/or theoretical performance of the subject propellants and propellant combinations over the low-thrust range of interest

TABLE II. - CANDIDATE LOW-THRUST ENGINE STUDY REQUIREMENTS

- Thrust, N (LB) — 445 to 13345 (100 to 3000)
- Propellants:

Oxidizer	Oxygen, O_2
Candidate Fuels	Hydrogen, H_2
	Methane, CH_4
	Kerosene, RP-1

- Engine Mixture Ratio:

O_2/H_2	O_2/CH_4	O_2/RP-1
6.0	3.7	3.0

- Propellant Inlet Temperatures, °K (°R):

O_2	H_2	CH_4	RP-1
90.4 (162.7)	21 (37.8)	112 (201)	298 (537)

- NPSH at Pump Inlet, M (FT)

O_2	H_2	CH_4	RP-1
0.61 (2)	4.57 (15)	1.68 (5.5)	13.7 (45)

- Service Life: Five Thermal Cycles Times a Safety Factor of 4 and an Accumulated Run Time Per Figure 9.
- Gimbal Angle: ±7° Square Pattern
- Engine Nozzle: 90° Contoured Bell
- Mission: Expendable Low-Thrust Orbit Transfer
- Meet Orbiter Safety and Environmental Criteria

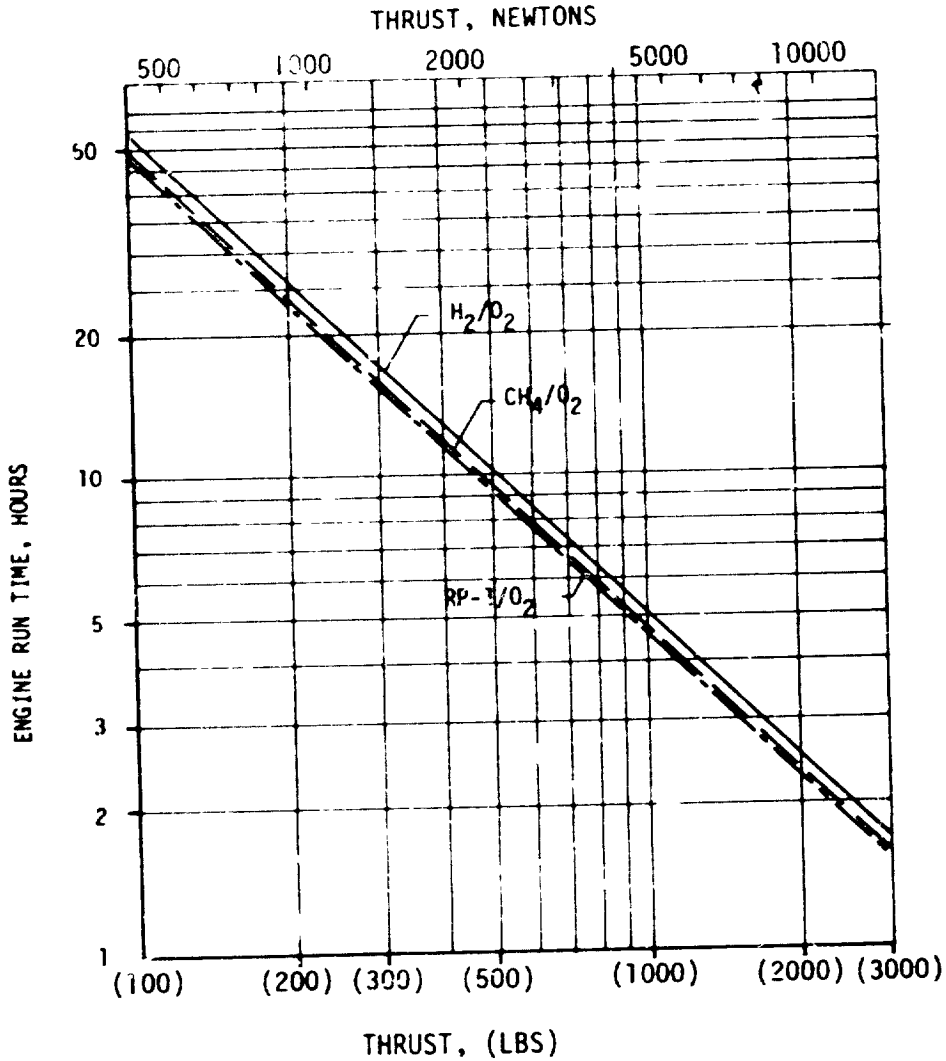

Figure 9. Low-Thrust Accumulated Run Time Guideline

II, C, Study Approach (cont.)

were determined. Task II involved analyses to establish the combined thrust level and chamber pressure range over which conventional film-cooled and regeneratively cooled low-thrust chamber designs are feasible. In Task III, engine system concepts were devised and evaluated over the thrust chamber film and regenerative cooling feasibility range to establish feasible design ranges if different from the cooling results. In addition, the effect of advancements in cooling technology upon the feasible design range was assessed as part of Task III. Two sets of parametric data were generated for the viable concepts. One set was based upon conventional (i.e., film and regenerative) cooling results; the other upon the advanced cooling predictions. These data were used to assist in the selection of a concept and design point for preliminary design. In Task IV, preliminary design was accomplished on the most attractive concept whereupon the parametric data for the selected concept were updated to reflect all study results.

SECTION III

PROPELLANT PROPERTIES AND PERFORMANCE

A. OBJECTIVES

The objectives of this task were to provide propellant and combustion gas property data and theoretical performance data for the propellants and propellant combinations under consideration in this study. These are listed in Table III.

B. DATA SUMMARY

The primary sources for the physical and thermal property data for the various propellants considered in this study are listed below:

- Oxygen - References 1, 2, 3, 4
- Hydrogen - Reference 5
- RP-1 - References 6, 7
- Methane - References 8, 9, 10,11

The propellant properties data summary is presented in Table IV.

The thermodynamic and transport property data for the combustion products were obtained from the One-Dimensional Equilibrium (ODE) Computer Program with Transport Properties (TRAN 72), described in Reference 12. This computer program was obtained from NASA/LeRC and includes ODE and frozen specific impulse and characteristic velocity data in addition to the extensive combustion gas transport property output. The thermodynamic and transport property data were tabulated over the mixture ratio and chamber pressure ranges shown in Table III and presented in Reference 13. This reference contains data on the following parameters:

Characteristic exhaust velocity

Combustion temperature (gas stagnation temperature)

Molecular weight

Thermal conductivity

Ratio of specific heats, equilibrium

Ratio of specific heats, frozen

Dynamic viscosity

Specific heat at constant pressure, equilibrium

Specific heat at constant pressure, frozen

Dittus-Bolelter factor

TABLE III. - PROPELLANTS AND PARAMETRIC RANGES

- Propellants - O_2, H_2, RP-1, CH_4
- Propellant Combinations

  O_2/H_2, O_2/RP-1, O_2/CH_4

- Parametric Ranges

  Chamber Pressure: 1.36 to 68 atm (20 to 1000 psia)

  Area Ratio: 1 to 1000

  Mixture Ratio:

  O_2/H_2: 4 to 7

  O_2/RP-1: 2.6 to 3.2

  O_2/CH_4: 3.4 to 4.0

TABLE IV. - PROPELLANT PROPERTIES DATA SUMMARY

	Oxygen	Hydrogen	RP-1	Methane
Formula	O_2	H_2	$(CH_2)_{12.37}$	CH_4
Molecular Weight	31.9988	2.01594	173.5151	16.043
Freezing Point, °K (°F)	54.372 (-361.818)	13.835 (-434.767)	224.8 (-51)	90.68 (-296.4)
Boiling Point, °K (°F)	90.188 (-297.346)	20.268 (-423.187)	~492.6 (~427)	111.64 (-258.7)
Critical Temperature, °K (°F)	154.581 (-181.433)	32.976 (-400.313)	679 (763)	190.6 (-116.7)
Critical Pressure, MN/m^2 (psia)	5.043 (731.4)	1.2928 (187.51)	2.344 (340)	4.60 (667)
Density, liquid at 298.15°K, kg/m^3 (at 77°F, lb/ft^3)	1140.8[a] (71.23)	70.78[a] (4.419)	800 (49.94)	422.6[a] (26.38)
Heat Capacity, liquid at 298.15°K, J/g-°K) (at 77°F, Btu/lb-°F)	1.696[a] (.405)	9.690[a] (2.316)	1.98 (.474)	3.50[a] (0.835)
Viscosity, liquid at 298.15°K, mN-sec/m^2) (at 77°F, lb_m/ft-sec)	.1958[a] (1.316×10^{-4})	.0132[a] ($.887 \times 10^{-5}$)	1.53 (1.04×10^{-3})	0.1155[a] (7.76×10^{-5})
Thermal Conductivity, liq. at 298.15°K, k/m-°K (at 77°F, Btu/ft-sec-°F)	.1515[a] (2.433×10^{-5})	.0989[a] (1.589×10^{-5})	.137 (2.2×10^{-5})	.193[a] (3.10×10^{-5})
Heat of Formation, liquid at 298.15°K, kcal/mol (at 77°F, Btu/lb)	-3.093[a] (-174.0)	-2.134[a] (-1905)	-6.2[b] (-796)	-21.37[a] (-2400)

[a]At NBP

[b]kcal/mole CH_2 Unit

III, B, Data Summary (cont.)

Main chamber theoretical performance data were also generated with the previously referenced TRAN 72 Computer Program. The ODE performance portion of the program is equivalent to the JANNAF One-Dimensional Equilibrium Program. The ODE vacuum specific impulse was calculated over the same chamber pressure and mixture ratio ranges as the combustion gas property data. Performance was obtained for expansion area ratios ranging from 1:1 to 1000:1. The data were plotted for four chamber pressures at 1.36, 6.8, 34.0, and 68.0 atm (20,100, 500 and 1000 psia). A summary of these data, also presented in Reference 13, is given in Table V.

TABLE V. - THEORETICAL ODE SPECIFIC IMPULSE DATA SUMMARY

NOZZLE AREA RATIO = 400

PROPELLANT COMBINATION	MIXTURE RATIO	CHAMBER PRESSURE ATM (PSIA)	ODE I_{s_v}, SEC
O_2/H_2	6.0	1.36 (20)	482.0
O_2/CH_4	3.7	1.36 (20)	396.0
O_2/RP-1	3.0	1.36 (20)	385.0
O_2/H_2	6.0	68.0 (1000)	485.0
O_2/CH_4	3.7	68.0 (1000)	404.0
O_2/RP-1	3.0	68.0 (1000)	393.5

SECTION IV

THRUST CHAMBER COOLING ANALYSIS

A. OBJECTIVES AND GUIDELINES

The primary objectives of this task were as follows:

- Determine the combined thrust level and chamber pressure range over which low-thrust chamber designs are feasible using conventional cooling methods and design criteria.
- Evaluate advanced cooling concepts and schemes to extend the feasible operating regimes.
- Provide heat transfer and hydraulic parametric data for use in engine system analysis and preliminary design efforts.

It should be noted that the engines considered in this study were either regeneratively cooled or film cooled. Combined regen/film cooling, transpiration cooling, or trans-regen cooling were not considered in this study.

The guidelines used to conduct the analysis and the criteria used to establish the maximum and minimum chamber pressure levels are shown in Tables VI and VII respectively. Except where noted, these study guidelines and criteria were specified by NASA/LeRC in the contract statement of work. They were used primarily to assess the capability of each coolant through application of conventional cooling methods and design criteria. Advanced cooling scheme evaluations included the following assessments: 1) the effect of the carbon deposition assumption upon the results; 2) the use of a purified RP-1 that is similar to JP-5; 3) the use of thermal barriers with O_2/RP-1 and O_2/CH_4 systems; 4) oxygen cooling; and 5) a relaxation of the channel dimensional limit criteria.

Other guidelines were established during the performance of the study. These included 1) material recommendations; 2) radiation-cooled nozzle attachment area ratio criteria; 3) flow stability criteria; and 4) thrust chamber geometry definitions. These are discussed briefly herein.

The materials of construction that were selected by ALRC and the temperature limits that were used to conduct the coolant analysis are presented in Table VIII and Figures 10 through 13. Figure 10 was used in conjuction with Figure 9 to establish the radiation-cooled nozzle wall temperature limit at the attachment point as a function of thrust. The lower limit temperature line of Figure 10 was used to construct Figure 11. The chamber and tube bundle nozzle wall temperature limits set by the cycle life and accumulated run time criteria are shown in Figures 12 and 13, respectively.

TABLE VI. - COOLING ANALYSIS GUIDELINES

- 90% Bell Nozzles (ϵ = 400:1)
- Coolant Inlet Temperature

  H_2 = 21°K (37.8°R)

  RP-1 = 298°K (537°R)

  CH_4 = 112°K (201°R)
- Possible benefit of carbon deposition on hot gas-side wall shall be neglected for conventionally cooled systems.
- Coking limit

  RP-1 = 561°K (1010°R), normal; 700°K (1260°R)* purified

  CH_4 = 978°K (1760°R)
- Dimensional Limits

  Tubular construction

  Minimum wall thickness = .0254 cm (.010 in.)

  Nontubular construction

  Minimum slot width = .0762 cm (.03 in.)

  Maximum slot depth/width= 4 to 1

  Minimum web thickness = .0762 cm (.03 in.)

  Minimum wall thickness = .0635 cm (.025 in.)

  Minimum channel depth = .0889 cm (.035 in.)*
- Service Life

  Five thermal cycles times a safety factor of four.

  Engine run time as shown by Figure 9.

*ALRC recommendation

TABLE VII. - COOLANT EVALUATION CRITERIA

MAXIMUM Pc CRITERIA:

- Regeneratively Cooled Cases

  1. Maximum Velocity of Gaseous Coolant Equal to Mach 0.3.
  2. Maximum Velocity of Liquid Coolant Equal to 61 m/sec (200 feet/second)
  3. RP-1 or CH_4 Coolant-Side Wall Temperature Equal to Their Respective Coking Temperature.

- Film-Cooled Cases

  Coolant weight flow is at a magnitude which degrades specific impulse by 10% when compared to an uncooled case.

MINIMUM Pc CRITERIA:

- Regeneratively Cooled Cases

  1. Coolant state at the jacket discharge must be single phase.
  2. Coolant flow through the jacket must be stable.

- Film-Cooled Cases

  Coolant weight flow is at a magnitude which degrades specific impulse by 3% when compared to an uncooled case.

TABLE VIII. - MATERIAL RECOMMENDATIONS

- Regen Chambers (all Propellants)
  - Zirconium Copper, aged at 867°K (1100°F)
  - Electroformed Nickel Closeout
- Film-Cooled Chambers
  - H_2 Coolant: Haynes 188; Temp. Limit = 1256°K (1800°F) based upon strength degradation.
  - CH_4 and RP-1 Coolants; FS-85 with a Silicide Coating; Temp. Limit = 1583 to 1939°K (2390 to 3030°F) depending upon coating life and thrust level*.
- Tube Bundle Nozzle
  - Nitronic 40 (21-6-9)
- Radiation-Cooled Nozzle
  - FS-85 Columbium with R512 Silicide Coating (see Figure 10 for Temperature Limit)

*Same as radiation-cooled nozzle extension

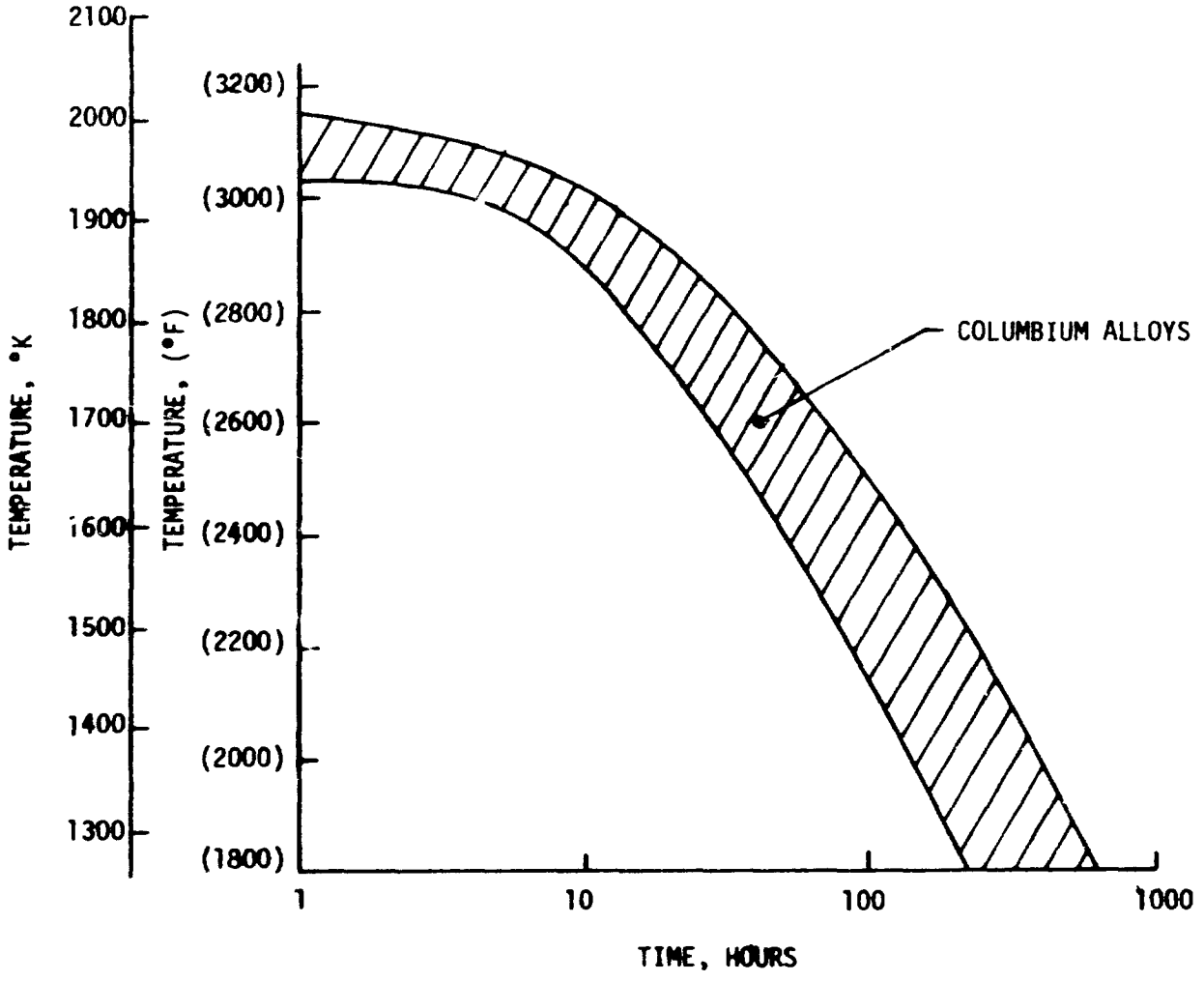

Figure 10. R512 Silicide Coating Oxidation Protection in Hours

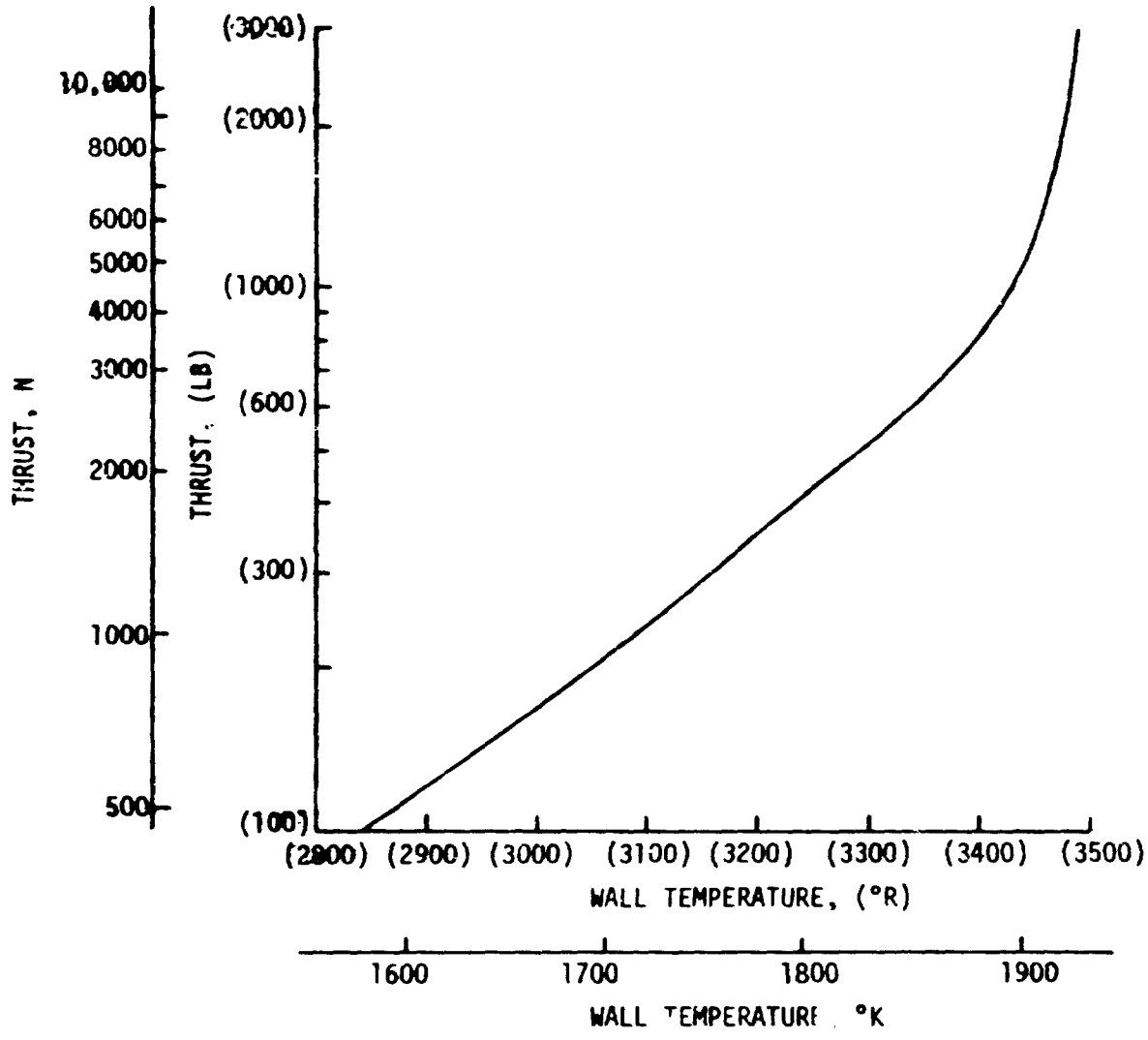

Figure 11. Wall Temperatures for Radiation-Cooled Nozzle Attachment Point

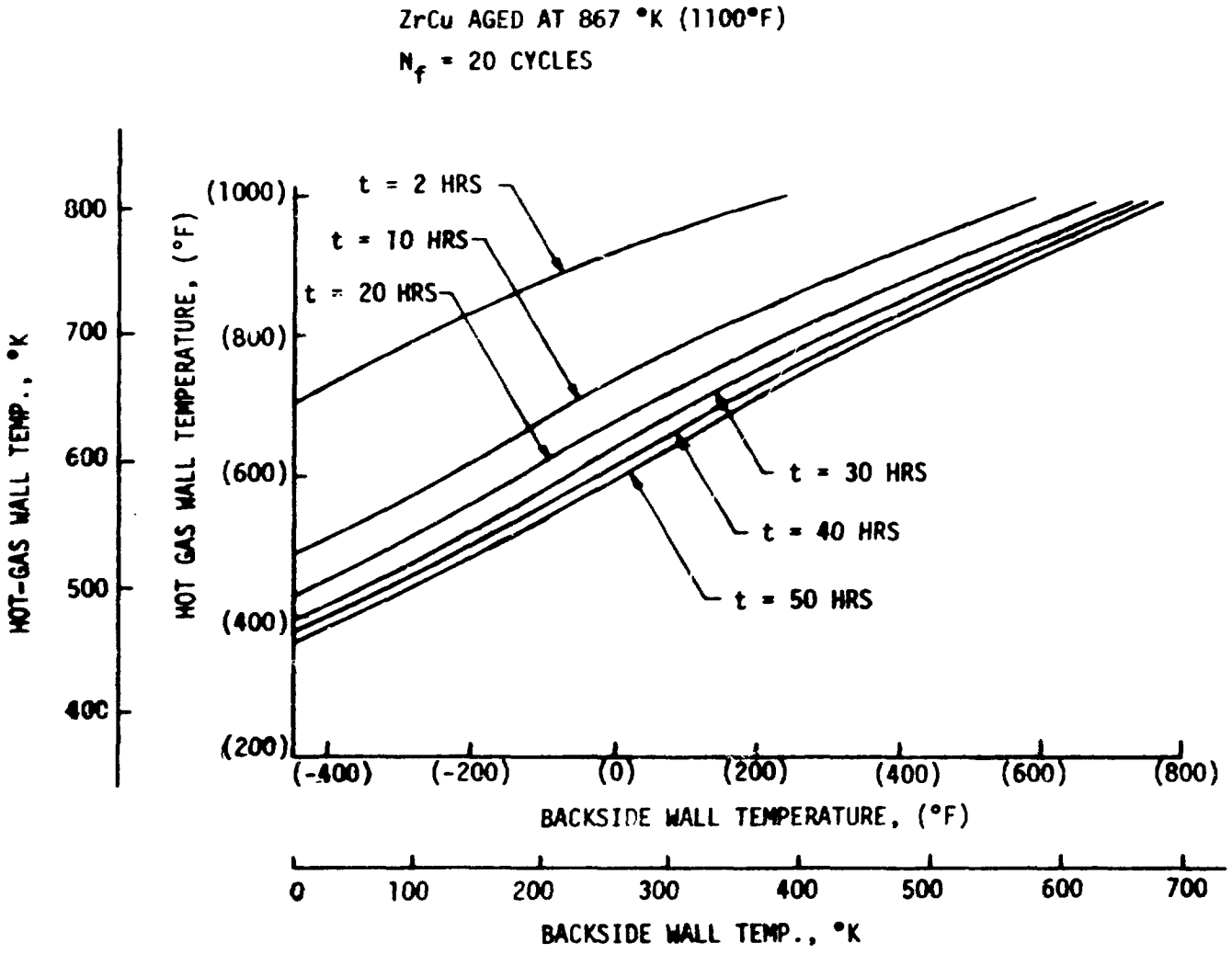

Figure 12. Allowable Hot Gas-Side Wall Temperature for Zirconium Copper

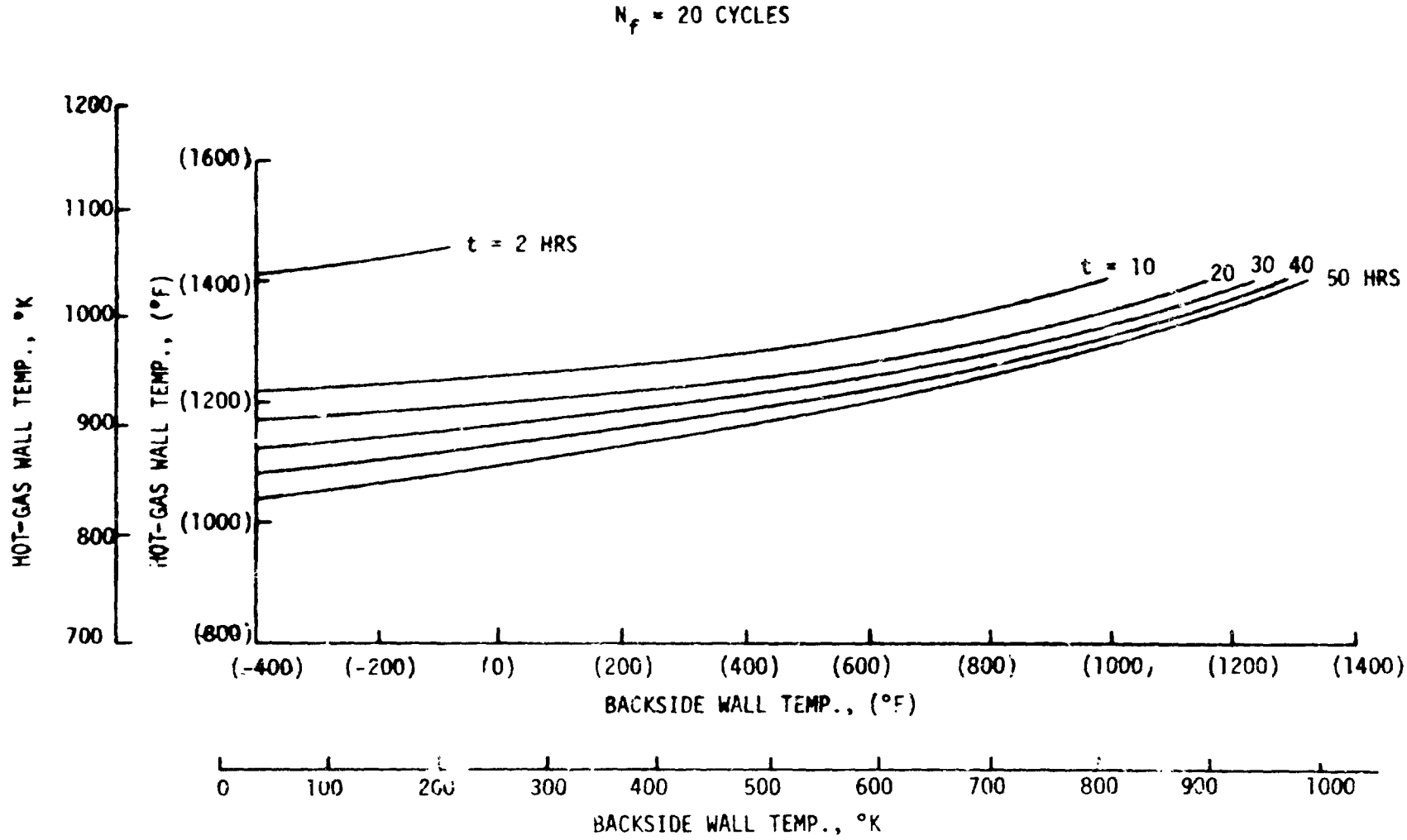

Figure 13. Hot-Gas Wall Temperature vs Backside Wall Temperature for Nitronic (21-6-9) Tubes

The approximate analytical criterion of Friedly et al., (References 14 and 15) was used as the basis for the prediction of coolant flow oscillations. This criterion represents an extension of Zuber's analysis (Reference 16) to include the dynamics of the heat transfer from the wall. Thurston (References 17 and 18) has shown that Zuber's model is in excellent qualitative agreement with empirical data for the onset of flow instability. The approximate criterion of Friedly, et al. (References 14 and 15) has been shown to be in reasonable quantitative agreement with oxygen and hydrogen data. Both criteria (i.e., Zuber's and Friedly's, et al.) can be written in the form of Rogers' empirical correlation (Reference 19) which Thurston (Reference 18) has shown to be in agreement with hydrogen, nitrogen, and oxygen data. However, both analyses indicate a dependence on additional system parameters not included in the simple empirical correlation. In addition, the Rogers-Thurston criteria requires the use of pseudo two-phase properties which have not been developed for methane. For these reasons, and to provide a better basis for including the effects of axial variations in cooling jacket parameters, the analytical model of Friedly, et al was used in preference to the Rogers-Thurston empirical correlation.

Chamber geometry definitions consisted primarily of establishing length and construction ratio scaling equations for the parametric cooling analysis. Short chamber lengths alleviate the cooling problem but may not meet performance criteria (i.e., 98% energy release efficiency). Minimum chamber lengths were established for both state-of-the-art and advanced chamber/injector designs. The conventional state-of-the-art scaling is based upon the Integrated Thruster Assembly (ITA) design (Reference 20) as follows:

- Minimum Chamber Lengths (L') for Conventional Designs:
  - O_2/H_2 and O_2/CH_4 based upon scaling ITA design

    L' (cm) = $6.35 \times \sqrt{23.1/Pc} + 9.9$ (Pc in atm)

    L' (in.) = $2.50 \times \sqrt{340/Pc} + 3.9$ (Pc in psia)
  - O_2/RP-1 based upon vaporization limited performance calculations

    L' (cm) = $6.68 \times \sqrt{20.4/Pc} + 30.5$ (Pc in atm)

    L' (in.) = $2.63 \times \sqrt{300/Pc} + 12.0$ (Pc in psia)
- Contraction Ratio:

  3.3:1 for both regen and film cooling based upon ITA

For the advanced cooling evaluations, the contraction ratio was fixed at 3.3:1, but the minimum chamber lengths were reduced. The reduction was based upon an analysis of historical thrust chamber length data, correlated as a function of thrust and pressure for each propellant combination. The correlation was derived to fit the lower boundary of the historical data as this correlation is felt to be more representative of recent or advanced technology. The advanced technology chamber length (L') correlations are:

Propellants	L' Units(1)	Advanced Design L' Correlation
O_2/RP-1	cm	$L' = 5.50 \times (F/Pc)^{0.23}$
	in.	$L' = 5.66 \times (F/Pc)^{0.23}$
O_2/CH_4	cm	$L' = 4.22 \times (F/Pc)^{0.23}$
	in.	$L' = 4.35 \times (F/Pc)^{0.23}$
O_2/H_2	cm	$L' = 3.24 \times (F/Pc)^{0.23}$
	in.	$L' = 3.34 \times (F/Pc)^{0.23}$

(1) When L' is in cm, F is in newtons and Pc is in atmospheres.
When L' is in inches, F is in lbF and Pc is in psia.

B. REGENERATIVE COOLING ANALYSIS

1. RP-1 Regenerative Cooling

Standard RP-1 was evaluated initially as a regenerative coolant by applying conventional guidelines and design criteria. The coolant jacket designs analyzed were cooled in two passes from the injector end to an area ratio of 6:1 and back to the injector. The results obtained showed that cooling with RP-1 was not feasible because the RP-1 bulk temperature exceeds the study coking temperature limit of 561°K (1010°R) for standard RP-1. As shown by Figure 14, results were obtained over the entire thrust and chamber pressure ranges of interest. The figure also shows that even with purified RP-1 (i.e., a coking temperature limit of 700°K (1260°R)), the feasible operating regime would be limited to high thrust and low chamber pressure operation.

Because of the results obtained in the initial evaluations, it became necessary to investigate the incorporation of design features that would minimize the enthalpy rise of the RP-1 coolant. As a result, a thermal barrier was included in the chamber barrel section, shorter chamber lengths (L') were used, and benefits from gas-side carbon deposition were considered.

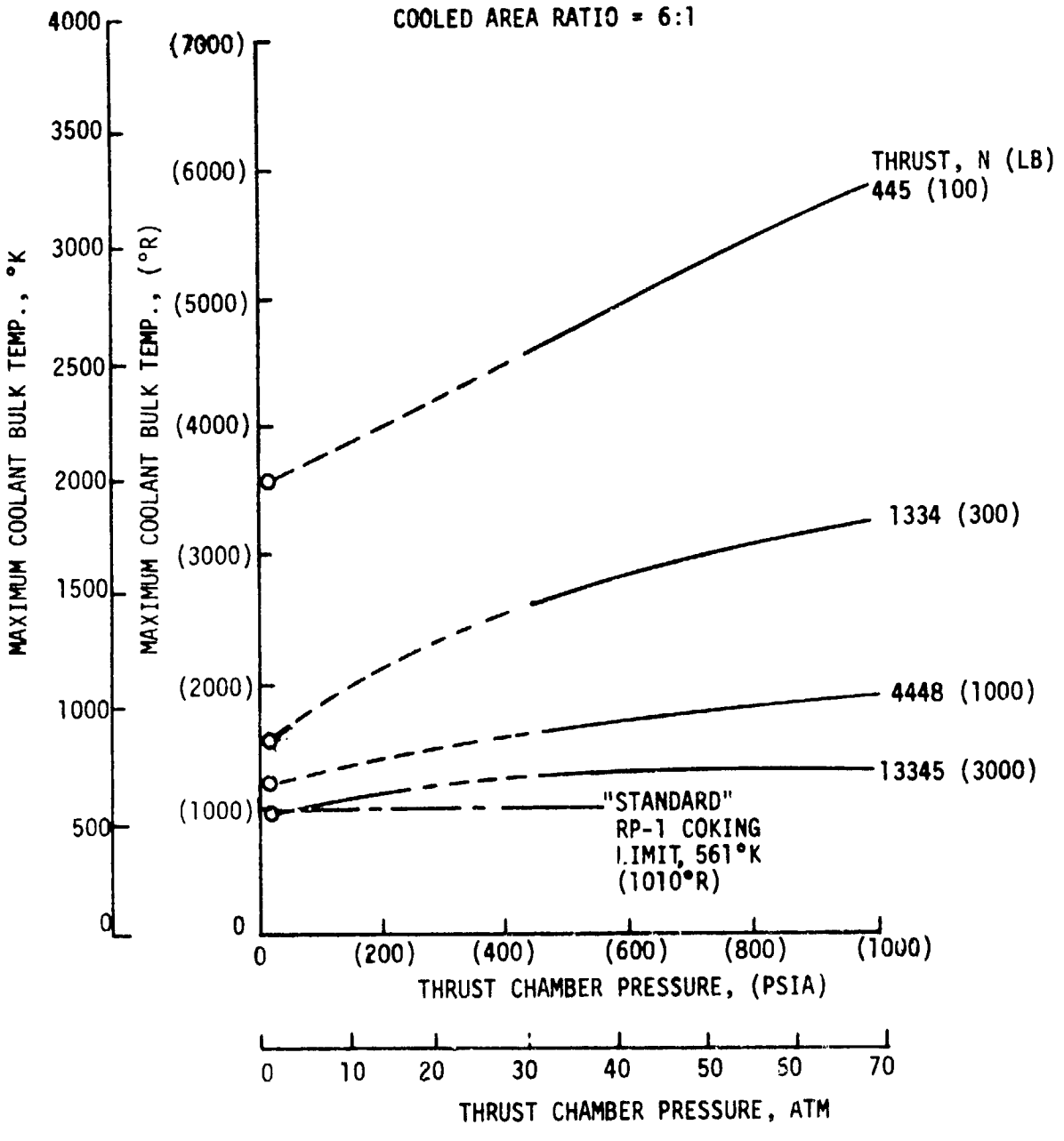

Figure 14. RP-1 Conventional Regenerative Cooling Results

IV, B, Regenerative Cooling Analysis (cont.)

The thickness of the thermal liner was assumed to be 0.1 times the chamber radius, and the thermal conductivity was assumed to be equivalent to a graphite at 39.8 watts/m°K (23 BTU/hr-ft-°F). The advanced design chamber length equation was assumed, and the carbon deposition correlation reported in Reference 21 was used.

When all three of the new features were incorporated, the entire thrust and chamber pressure operating map appeared to be feasible with an RP-1 coking temperature limit of 700°K (1260°R). Only the very low thrust and chamber pressure region resulted in coolant outlet bulk temperatures exceeding the nominal coking limit of 561°K (1010°R) for "standard" RP-1. The carbon layer was the major factor that influenced these results. A comparison of the coolant bulk outlet temperatures with and without the carbon layer is shown in Figure 15. This figure shows that the coolant bulk temperature is increased significantly without the carbon layer but that a reasonable operating range appears to be feasible from the standpoint of the coolant enthalpy rise. Coolant bulk outlet temperatures of 700°K (1260°R) or less result at thrusts of 1334 N (300 lb) or greater. A coking limit of 561°K (1010°R) excludes operation at thrust below 4448 N (100 lb) and at chamber pressures above 6.8 atm (100 psia).

Recent experimental findings do not support the carbon deposition correlations found in the literature. Tests were conducted under Contract NAS 3-21030 to determine the combustion and heat transfer characteristics of LOX/RP-1 propellants in the 68 to 136 atm (1000 to 2000 psia) chamber pressure range. Although the calorimeter chamber used in these tests was blackened by the testing, the heat transfer data, combined with the very light to nonexistent sooting near the injector, gave no indication of the existence of a soot thermal barrier (Ref. 22).

Because of uncertainties in the experimental data base and the considerations of clean engine starts and carbon layer spalling, it was considered prudent not to base the design studies on the dependence of a carbon layer. Any benefit from the carbon deposit would provide a further design safety margin. It is believed that further technology effort is required in this area before a high-confidence design that depends upon the carbon layer buildup can be recommended.

Using a combination of a thermal barrier (e.g., graphite) and a minimum chamber length design (i.e., highly efficient injection and combustion), feasible designs were calculated for RP-1 as the coolant over the boundary shown in Figure 16. The feasibility boundary runs from F = 13345 N (3000 lbF), Pc = 47.6 atm (700 psia) to F = 1344N (300 lbF), Pc = 1.36 atm (20 psia). Intercooling (i.e., to cool down RP-1 after the first coolant pass) is necessary to achieve the high thrust and chamber pressure corner of the feasibility map.

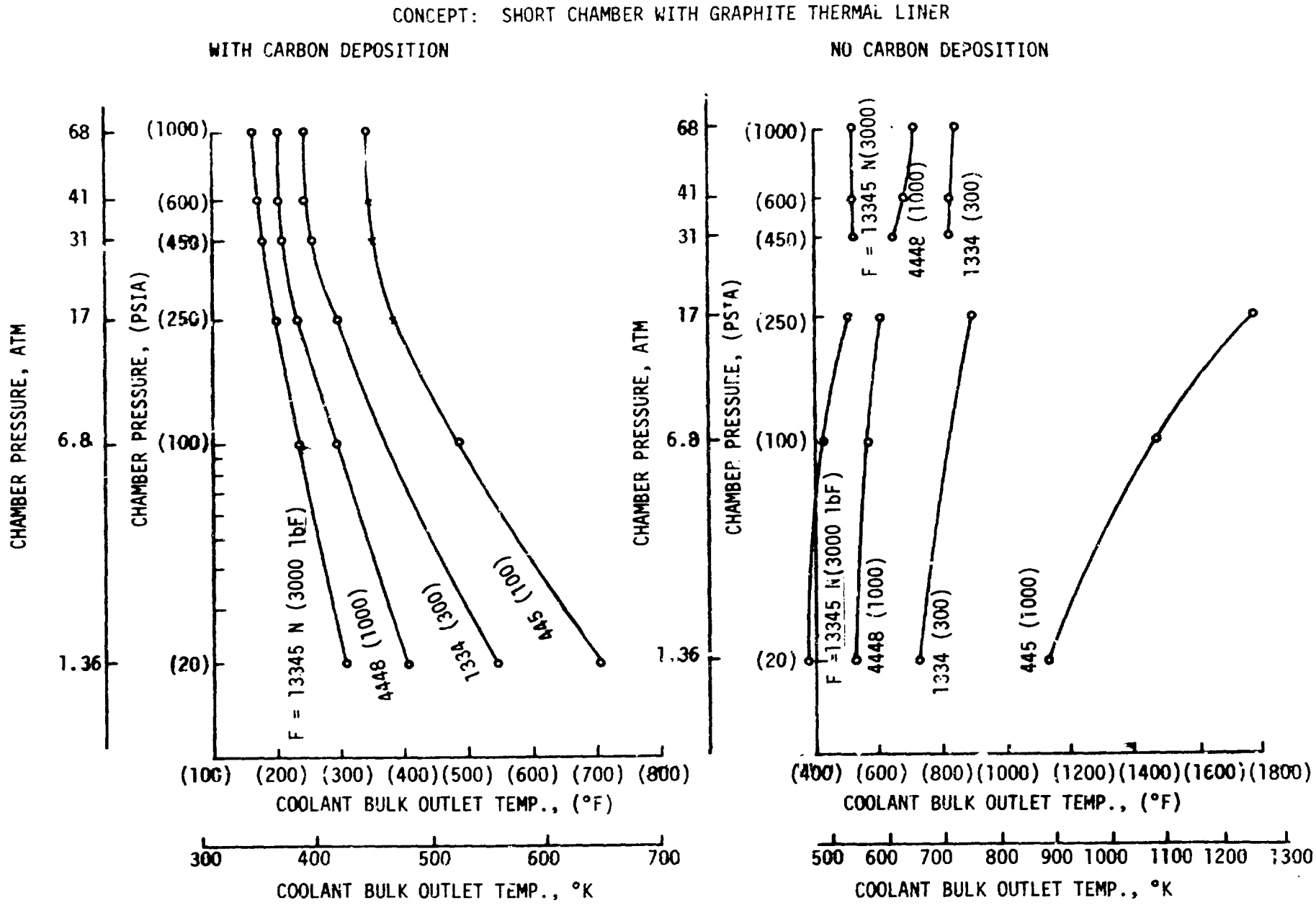

Figure 15. Influence of Carbon Deposition Upon RP-1 Coolant Bulk Outlet Temperature

ASSUMPTIONS:

(1) PURIFIED RP-1
(2) MINIMUM CHAMBER L'
(3) THERMAL BARRIER
(4) NO BENEFIT FROM CARBON DEPOSITION

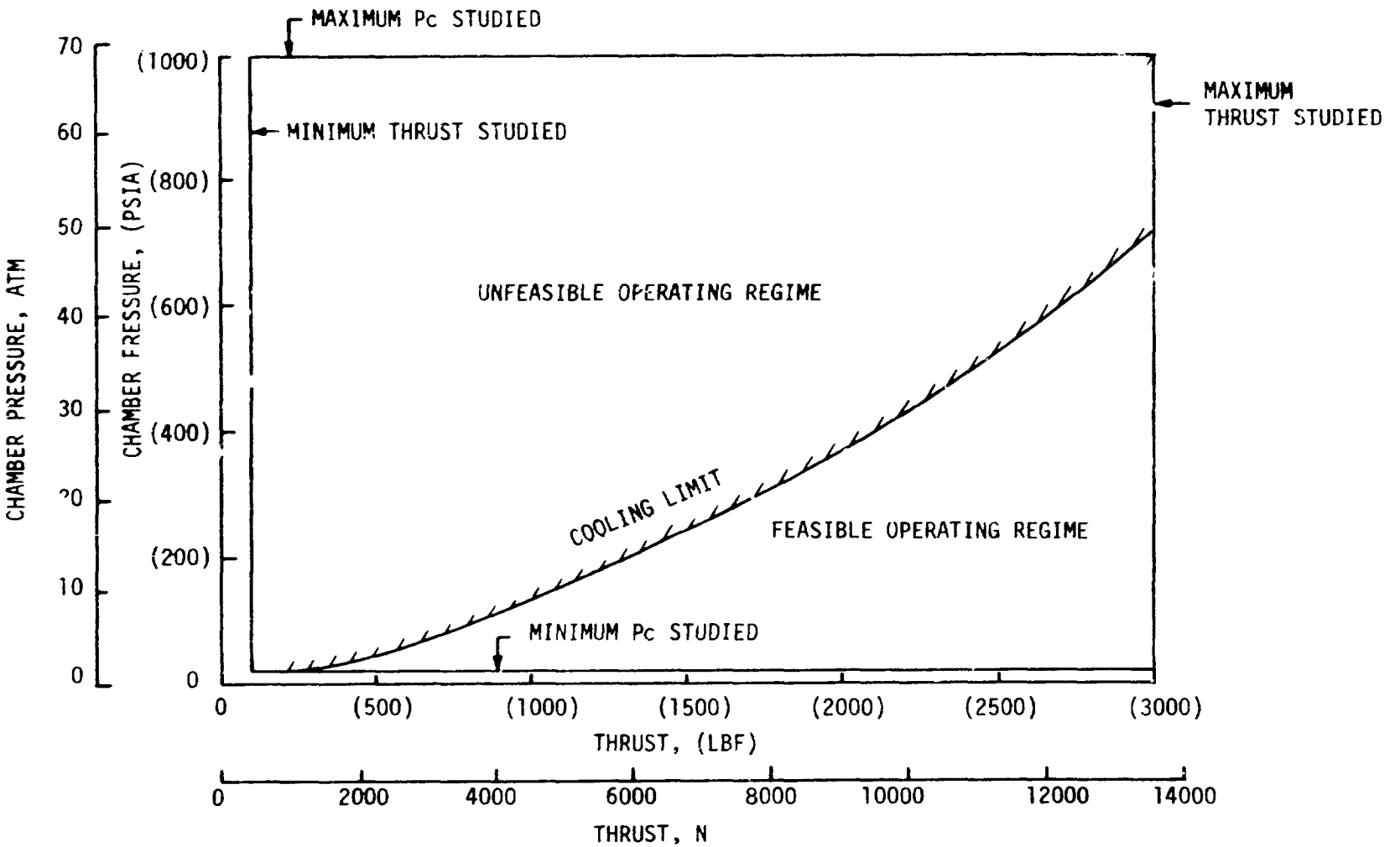

Figure 16. RP-1 Advanced Regenerative Cooling Results

IV, B, Regenerative Cooling Analysis (cont.)

2. Oxygen Regenerative Cooling

A cursory analysis to assess the feasibility of oxygen cooling for the O_2/RP-1 engines was also performed by using a graphite liner and short L' chambers. A feasible design was accomplished only when a carbon layer was assumed. A number of attempts to design for a thrust of 13345 N (3000 lb) at chamber pressures of 61 atm (900 psia) and 30.6 atm (450 psia) were made by applying conventional channel design criteria and assuming no carbon layer. Pressure drops were excessive in all cases. The convergent section of the nozzle was invariably the point of computational failure, suggesting that optimization of the barrel-nozzle radius of curvature effects on the coolant-side coefficient or consideration of unique channel concepts might result in feasible designs. However, further investigations in this area were beyond the scope of this study.

3. Methane Regenerative Cooling

During the initial phases of this study, a review of available design correlations indicated that the ALRC correlation for oxygen at supercritical pressure (Reference 23) was most applicable for use with supercritical methane. This correlation was used to conduct the thermal analysis of methane as a regenerative coolant in the conventional designs. After this initial work was completed, a heated tube study of the heat transfer characteristics of propane at supercritical pressures was performed on Contract NAS 9-15958 by ALRC. The resultant correlation is reported in Reference 24.

An analysis was conducted to determine if the use of the propane correlation would result in significant differences in the study results. As shown below, the results were comparable, indicating only a small ΔP reduction.

	Oxygen Correlation	Propane Correlation
Thrust, N (lbF)	13345 (3000)	13345 (3000)
Chamber Pressure, atm (psia)	68 (1000)	68 (1000)
Channel ΔP, atm (psia)	5 (72.8)	4.6 (67.4)
Max. Mach No.	0.20	0.19
Min. Channel Depth, cm (in.)	0.196 (0.077)	0.198 (0.078)

Because methane and propane are the two lowest molecular weight members of the saturated aliphatic homologous series, it was decided that the propane correlation would be more applicable to methane than the oxygen correlation used in the initial work. Therefore, all further thermal analyses with methane in the advanced cooling concept study were performed by using the propane correlation.

The initial studies of methane (CH_4) as a regenerative coolant were conducted by applying conventional guidelines and design criteria. Chambers were cooled in two passes, with the coolant flowing from the injector to the radiation-cooled nozzle attachment point and back to the injector. The cases analyzed and the limiting criteria are presented in Figure 17. Operation is limited to a high thrust, high chamber pressure region primarily due to the Mach number criteria. Feasible designs could not be obtained with CH_4 below its critical pressure of 45.4 atm (667 psia). Therefore, further work was conducted by always keeping the coolant jacket outlet pressure above the critical pressure of CH_4. This, of course, places the burden upon the engine pumping system and rules out regeneratively cooled pressure-fed engine options because tank weights get too heavy. For all cases, the methane coolant bulk outlet temperature never exceeded the coking limit of 978°K (1760°R) and thus is not a concern as it was for RP-1.

Further analyses using methane as a regenerative coolant were conducted to determine if the feasible design range could be enlarged. Emphasis was placed upon an evaluation of lower thrust levels than were obtained with the conventional schemes. Thermal barriers and shorter chambers were incorporated into the designs, but carbon deposition was not because of the RP-1 thermal results. A propellant intercooler was included as necessary to obtain a solution. Intercooling consisted of reducing the coolant bulk temperature to its initial value before the return pass in the two-pass cooling scheme. The results are summarized in Table IX.

The results of the initial analysis at 4448 N (1000 lbF) and 47.6 atm (700 psia) are included on the table for comparison. This point was previously determined to be Mach number limited. For the new design, the Mach number slightly exceeds the design criterion of 0.3, but the channel pressure drop is satisfactory and the minimum channel depth is well above the desired conventional fabrication minimum of 0.089 cm (0.035 in.). A thrust of 2669 N (600 lbF) and 68 atm (1000 psia) chamber pressure resulted in an excessive Mach number and pressure drop. When an intercooler is used at this point, only the channel depth fails to meet the conventional criteria.

Based upon these results, it was estimated that the lower thrust limit previously determined could be decreased to 355 N (800 lb). The estimated feasible operating regimes for both the conventional and advanced cooling schemes are presented in Figure 18.

4. Hydrogen Regenerative Cooling

The coolant-side heat transfer correlation used for hydrogen was that formulated by Hess and Kunz (Reference 25). While this correlation was developed for hydrogen at supercritical pressures, it also gives good results at subcritical pressures at high degrees of superheat. The coolant circuits

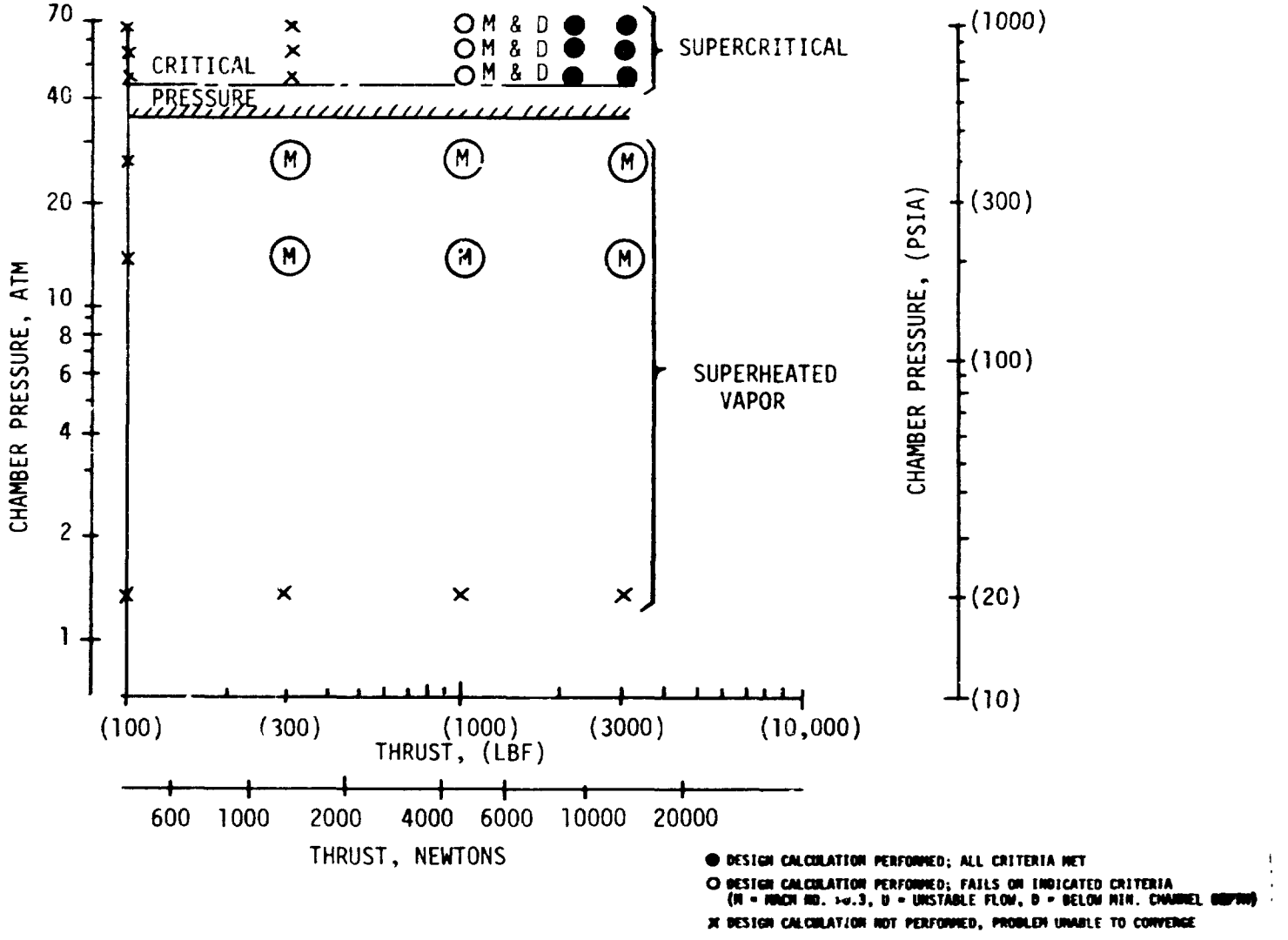

Figure 17. CH_4 Regen Cooling Matrix, Conventional Designs

TABLE IX. - METHANE ADVANCED REGEN COOLING SCHEME THERMAL DATA SUMMARY

CONCEPT: SHORT CHAMBER WITH GRAPHITE THERMAL LINER

Thrust, N (lbF)	Chamber Pressure atm (psia)	Channel ΔP atm (psi)	Coolant Outlet Temp. °K (°R)	Max. Mach No.	Min Channel Depth (2 pass) cm (in.)	No. of Channels	Inter-Cooler
4448 (1000)	68 (1000)	9.7 (142)	229 (412)	0.13	0.081 (0.032)	22	Yes
4448 (1000)(1)	47.6 (700)	15.8 (232)	567 (1020)	0.40	0.081 (0.032)	25	No
4448 (1000)	47.6 (700)	8.4 (123)	397 (715)	0.38	0.178 (0.070)	26	No
2669 (600)(2)	68 (1000)	44.4 (652)	356 (641)	0.96	0.081 (0.032)	17	No
2669 (600)	68 (1000)	18.4 (270)	279 (503)	0.29	0.056 (0.022)	17	Yes
2669 (600)	47.6 (700)	7.6 (112)	237 (427)	0.16	0.061 (0.024)	21	Yes

(1) Conventional long L' design without thermal liner

(2) Impractical Design: last data point calculated; computer convergence failure at ϵ = -1.07 on second pass

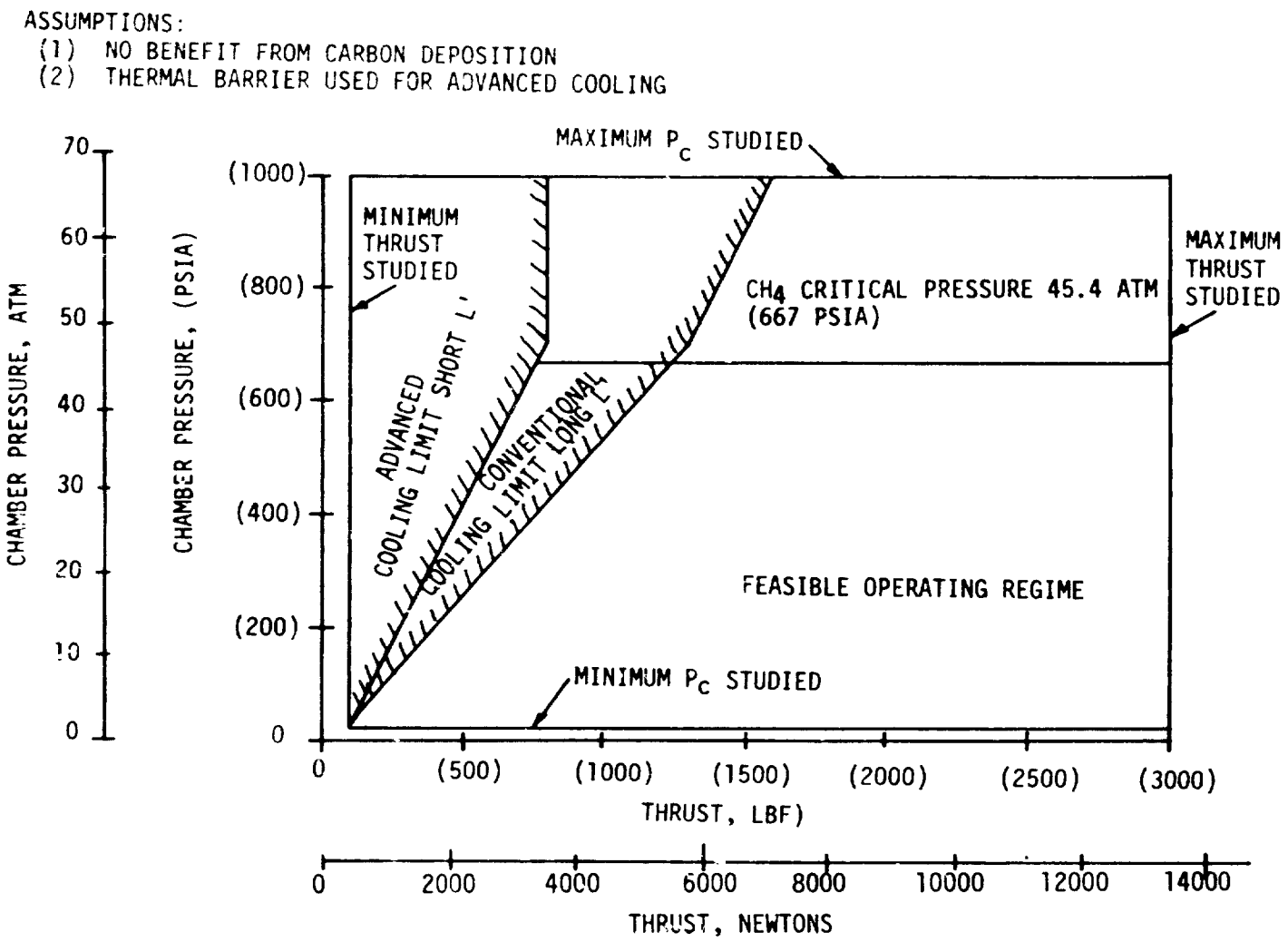

Figure 18. CH_4 Regenerative Cooling Results

analyzed were primarily single pass, with the hydrogen flowing from the radiation-cooled nozzle attachment point to the injector. A few two-pass cases were investigated in an attempt to obtain a design solution.

The heat transfer studies considered both conventional long L' chambers and short chambers. The long chambers are desirable for engine cycles which use heated hydrogen as a turbine drive fluid because the hydrogen bulk outlet temperature increases with chamber length. However, the long chambers reach the cooling limits more quickly than the short L' chambers. Hence, short chambers result in a larger feasible cooling regime. Thermal liners were not included in these analyses as they would penalize the engine power balance.

The cases that were analyzed by using the conventional chamber L' equation are shown in Figure 19, along with the limiting conventional design criteria. A summary of the thermal results is presented in Table X. The table and figure show that conventional channel Mach number and channel depth limits constrain operation at low thrust-high Pc and high thrust-low Pc combinations. The feasible cooling map with hydrogen covers both the supercritical and subcritical pressure regimes. The critical pressure of hydrogen is 12.8 atm (188 psia), and the coolant jacket exit pressure was always held above this value to obtain practical design solutions. This penalizes pressure-fed systems with regeneratively cooled engines because high hydrogen tank pressures would be required. Data also show that relaxing the channel depth criteria results in enlarging the feasible operating regime. Based upon these results, the feasible hydrogen regenerative cooling map as shown in Figure 20 was established.

C. FILM COOLING ANALYSIS

Both gas and liquid film cooling models were used to perform the design analysis of thin-walled chambers with adiabatic external surfaces. The gas film cooling model was developed during contractual work performed in the past by ALRC for NASA/LeRC. (References 26, 27, and 28). The liquid model is similar to the gas model downstream of a liquid film. Effects of boundary layer shear forces on the liquid film are based upon Reference 29.

Figure 21 shows the results of the film cooling studies to establish the upper chamber pressure limit, based upon a 10% performance degradation, for the three fuels. This performance degradation is based upon a performance comparison with an engine requiring no film cooling.

Hydrogen and RP-1 cannot be used as film coolants at thrusts below about 4448 N (1000 lbF), and their chamber pressure ranges are very limited. Hydrogen is penalized by the low wall temperature, 1255°K (1800°F) obtainable with compatible materials, and RP-1 is penalized by the long chamber lengths required to achieve a minimum study-specified energy release efficiency of

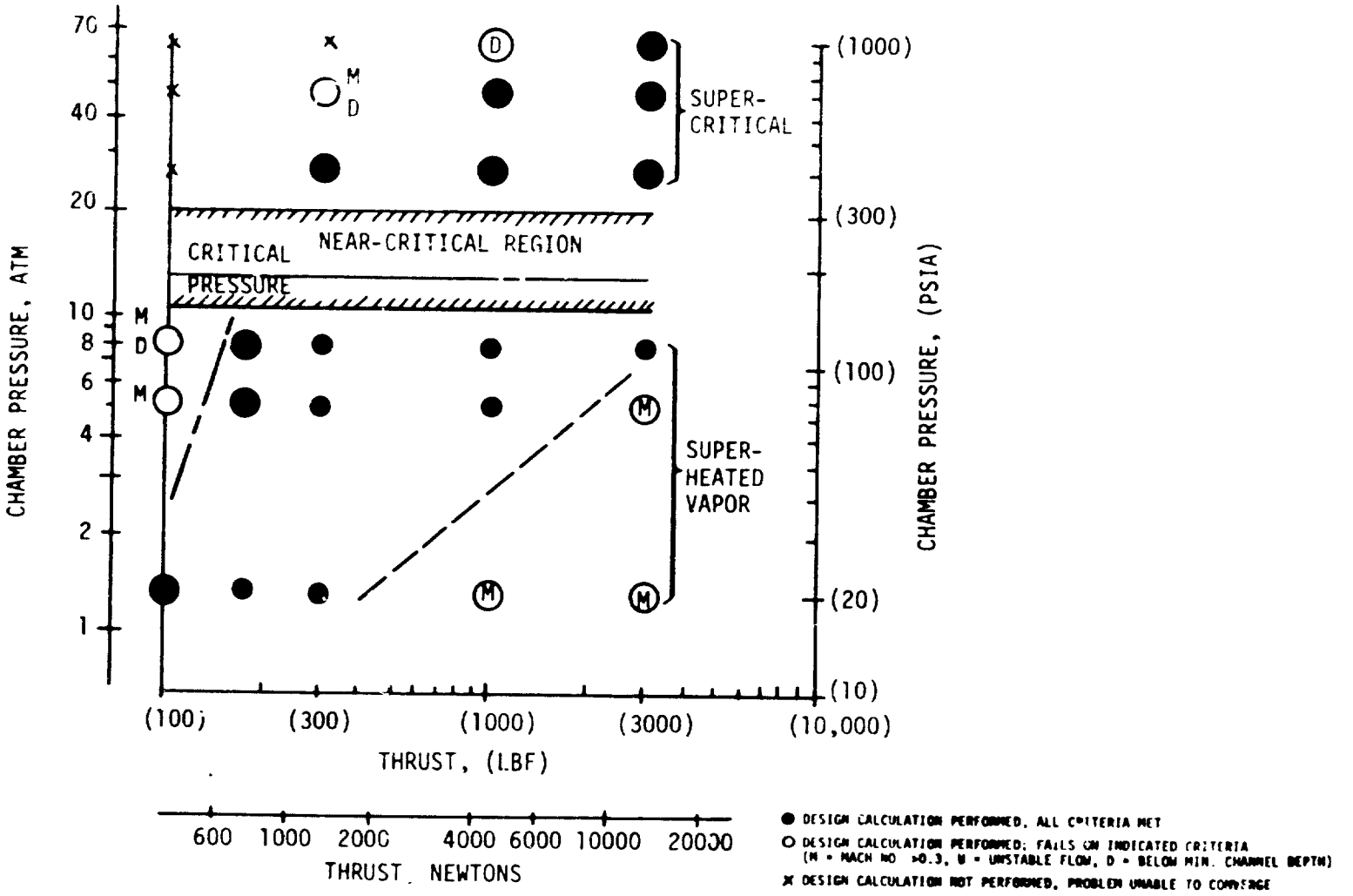

Figure 19. H_2 Regen Cooling Matrix, Conventional Designs

TABLE X. - HYDROGEN REGENERATIVE COOLING THERMAL DATA SUMMARY

NOTE: Conventional L' Equation Except Where Noted

THRUST N (LBF)	CHAMBER PRESSURE ATM (PSIA)	CHANNEL ΔP ATM (PSI)	COOLANT OUTLET TEMP. °K (°R)	MACH NO.	MIN. CHANNEL DEPTH (1 PASS) CM (IN.)	
13345 (3000)	68 (1000)	1.42 (20.9)	172 (310)	.09	0.211	(.083)
	47.6 (700)	0.71 (10.5)	158 (285)	.10	0.330	(.130)
	27.2 (400)	0.60 (8.8)	137 (246)	.10	0.330	(.130)
	7.8 (115)	0.95 (14.0)	124 (223)	.29	0.330	(.130)
	5.1 (75)	1.20 (17.6)	122 (219)	.37	0.330	(.130)
	1.36 (20)	1.36 (20.0)	121 (218)	.57	0.330	(.130)
4448 (1000)	68 (1000)	5.77 (84.8)	279 (503)	.18	0.079	(.031)
	47.6 (700)	1.77 (26.0)	234 (421)	.11	0.104	(.041)
	27.2 (400)	0.31 (4.6)	189 (340)	.05	0.173	(.068)
	68 (1000)(1)	14.8 (218)	441 (794)	.25	0.122	(0.48)
	7.8 (115)	0.27 (3.9)	189 (341)	.16	0.330	(.130)
	5.1 (75)	0.33 (4.8)	186 (334)	.21	0.330	(.130)
	1.36 (20)	0.60 (8.8)	182 (328)	.45	0.330	(.130)
1334 (300)	68 (1000)	*	*	*	*	
	47.6 (700)	10.5 (154.3)	431 (775)	.73	0.053	(.021) (2-PASS)
	27.2 (400)	1.61 (23.7)	375 (675)	.27	0.099	(.039) (2-PASS)
	7.8 (115)	0.10 (1.4)	341 (613)	.09	0.330	(.130)
	5.1 (75)	0.11 (1.6)	329 (592)	.12	0.330	(.130)
	1.36 (20)	0.15 (2.2)	313 (567)	.21	0.330	(.130)
778 (175)	7.8 (115)	0.38 (5.6)	454 (821)	.07	0.710	(.028)
	5.1 (75)	0.10 (1.4)	439 (790)	.09	0.330	(.130)
	1.36 (20)	0.11 (1.6)	416 (748)	.19	0.330	(.130)
445 (100)	68 (1000)	*	*	*	*	
	47.6 (700)	*	*	*	*	
	27.2 (400)	*	*	*	*	
	7.8 (115)	5.55 (81.6)	621 (1117)	.68	0.051	(.020)
	5.1 (75)	1.58 (23.2)	596 (1072)	.46	0.089	(.035)
	1.36 (20)	0.07 (1.1)	559 (1006)	.17	0.330	(.130)

*Design Solution Not Achieved

(1) L' Increased From 13.7 cm (5.4 in.) to 23.6 cm (9.3 in.)

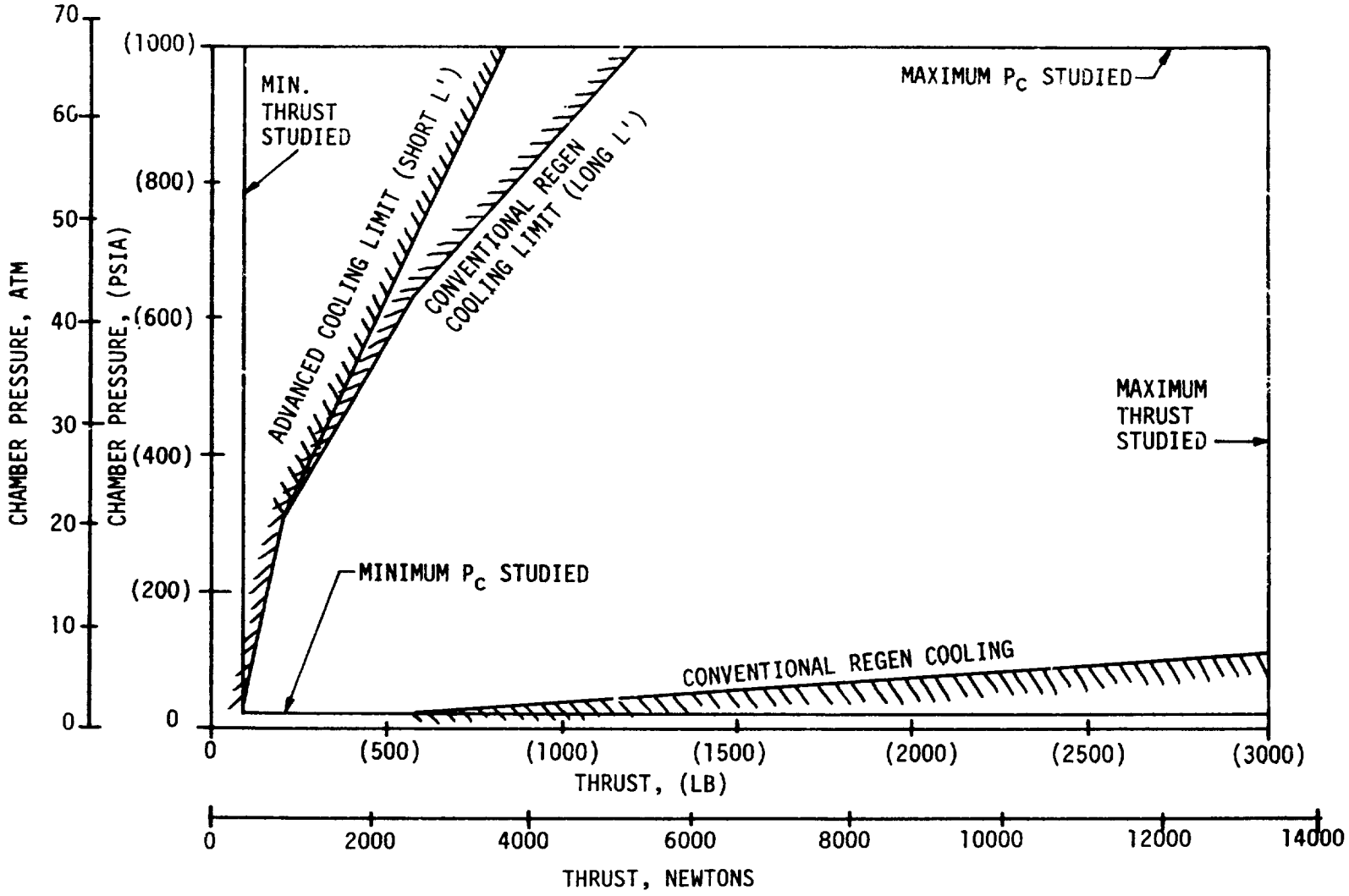

Figure 20. H_2 Regenerative Cooling Results

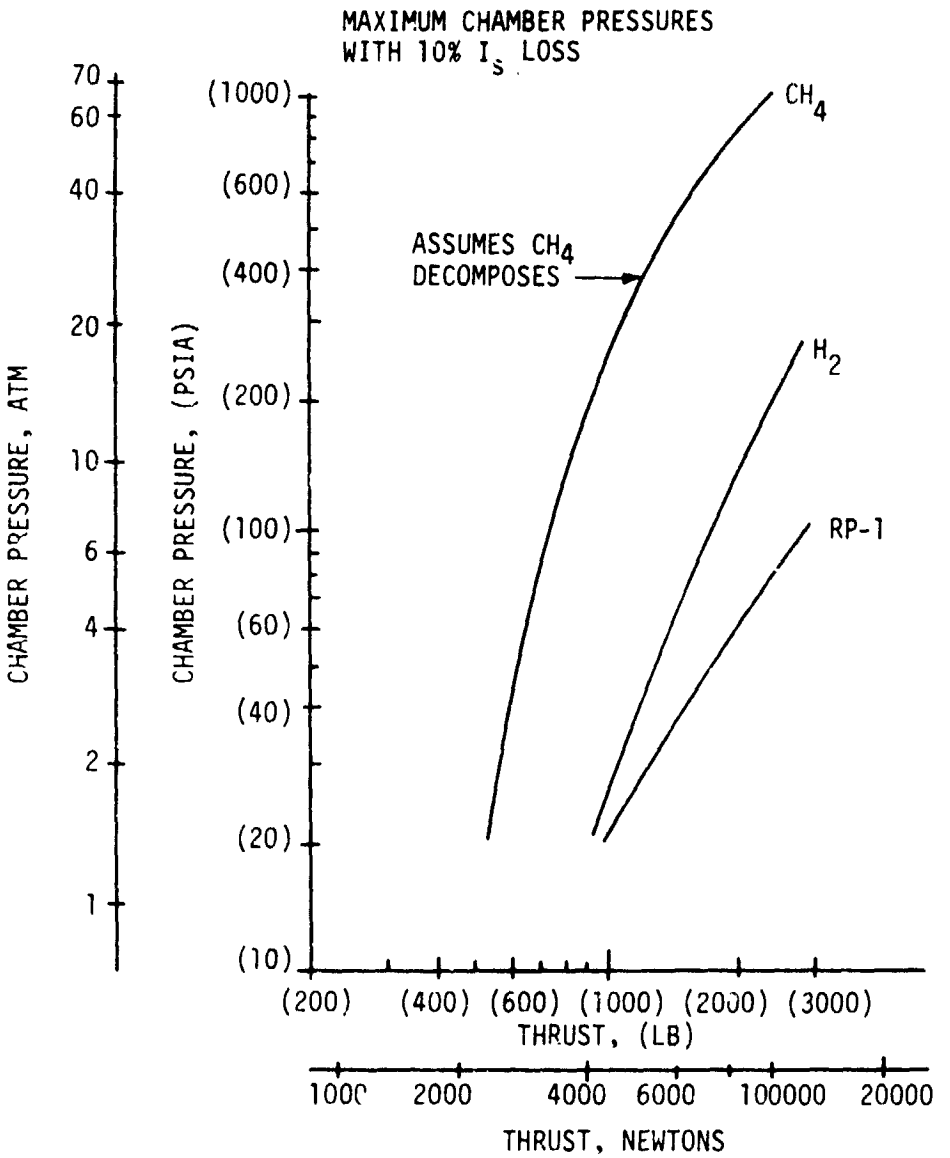

Figure 21. Film Cooling Analyses Results

98%. RP-1 film-cooled engines were dropped from further study because of the small operating range. Lower-limit chamber pressures corresponding to a 3% performance degradation were found to be approximately at or below the specified minimum chamber pressure of 1.36 atm (20 psia).

The feasibility of methane film cooling is highly dependent upon the kinetics of the methane decomposition. This analysis was beyond the scope of the current effort, but the sensitivity of the results to the chemistry model assumption was assessed. If methane decomposes as assumed in Figure 21, it provides the largest operating range. However, assuming no CH_4 decomposition and, thus, no coolant reaction with the entrained core gases, the coolant requirement exceeds 50% of the fuel and the performance loss exceeds 20%. With the complete decomposition assumption, the required coolant flow is about 33% of the fuel flow and the performance loss is 10%. Because of this uncertainty, CH_4 film-cooled engines were not analyzed further in the study. Data are required to verify the models.

D. COOLING ANALYSES CONCLUSIONS AND RECOMMENDATIONS

Based upon the results presented herein, the following conclusions were reached:

- Viable concepts with conventional cooling methods:
  - O_2/H_2, H_2 Regen-Cooled
  - O_2/H_2, H_2 Film-Cooled
  - O_2/CH_4, CH_4 Regen-Cooled
- Advanced coolant schemes and concepts are required for O_2/RP-1, RP-1 cooled engines.
- CH_4 coolant jacket outlet pressure must be held above critical.
- LOX cooling of O_2/RP-1 engine is impractical in a conventional chamber design.
- Carbon deposition assumption creates a major impact on the study results.
- O_2/H_2, H_2 cooled engines have the largest thrust and Pc cooling feasibility ranges.
- RP-1 film cooling thrust and Pc feasibility range is very small.
- CH_4 film cooling thrust and Pc feasibility range is dependent upon decomposition assumption.

IV, D, Cooling Analyses Conclusions and Recommendations (cont.)

In addition, the following decisions and recommendations were made for continuing the study in the conceptual design and parametric phase.

- RP-1 and film-cooled concepts were dropped from further study.
- Pressure-fed CH_4 regen-cooled concepts are impractical.
- Concepts requiring further conceptual study are:

Propellant Combination	Cooling Method	Coolant	Cooling Scheme
O_2/RP-1	Regen	RP-1	Advanced
O_2/H_2	Regen	H_2	Conventional and advanced
O_2/H_2	Film	H_2	Conventional
O_2/CH_4	Regen	CH_4	Conventional and advanced

SECTION V

ENGINE SYSTEM CONCEPTUAL DESIGN AND PARAMETRIC ANALYSES

A. OBJECTIVES AND GUIDELINES

The objectives of this phase of the study were:

- Assess the feasibility of various design approaches defined in Section V, B.
- Establish feasible design ranges if different from the cooling results.
- Prepare parametric performance, weight, and envelope data for the applicable concepts over the feasible design ranges.
- Determine advantages and disadvantages of concepts.
- Assess technology requirements.

The parametric data were generated over the entire study thrust and chamber pressure ranges, but the feasible cooling and/or cycle power balance limits were superimposed on the figures displaying the data.

All analyses were conducted at the nominal propellant mixture ratios and a nozzle area ratio of 400:1.

The conceptual design analysis was conducted using guidelines both specified by the contract and established during the course of this study. These guidelines are summarized in Table XI.

B. PROPULSION SYSTEM CANDIDATES

The propulsion system candidates were screened to identify those most promising for the COTV application. Seven concepts were evaluated: two pressure-fed and five pump-fed. These concepts are described briefly herein.

The pressure-fed system concepts evaluated are shown in Figures 22 and 23.

The conventional pressure-fed system concept is shown in Figure 22. In this concept, the engine run tanks are pressurized to the required pressure levels by a regulated helium source. The concept is applicable with both regeneratively and film-cooled engines. A parallel pressurized tank concept

TABLE XI. - ENGINE SYSTEM STUDY GUIDELINES

- Pressure Drop Criteria
  - Injectors:
    - Liquid[1] - 15% of Upstream Pressure
    - Gas[1] - 8% of Upstream Pressure
  - Valves
    - Liquid Control[1] - 5% of Upstream Pressure
    - Gas Control[1] - 10% of Upstream Pressure
    - Shutoff[1] - 1% of Upstream Pressure
    - Check Valve[2] - 2% of Upstream Pressure
    - Orifice[2] - 1% of Upstream Pressure
    - Pulsation Damper[2] - 2% of Upstream Pressure
    - Liquid Regulator[2] - 5% of Downstream Pressure
- Minimum Bearing Diameter[2]: 10mm

	LH_2	LO_2	CH_4	RP-1
Maximum Bearing DN,[1] (RPM) (mm)	2×10^6	1.5×10^6	1.9×10^6	1.8×10^6
Minimum NPSH,[1] m(ft)	4.57 (15.0)	0.16 (2.0)	1.68 (5.5)	1.37 (45.0)
Maximum Suction Specific Speed,[2] $(rpm)(m^3/sec)^{1/2}/(m)^{3/4}$ $[(rpm)\ (gpm)^{1/2}(ft)^{3/4}]$	775 [40,000]	581 [30,000]	620 [32,000]	503 [26,000]
$(NPSH)\ (2g)/C_m^2$ [2]	1.3	2.3	2.08	3.0

[1] Specified by the Contract Statement Of Work

[2] ALRC Derived Guideline

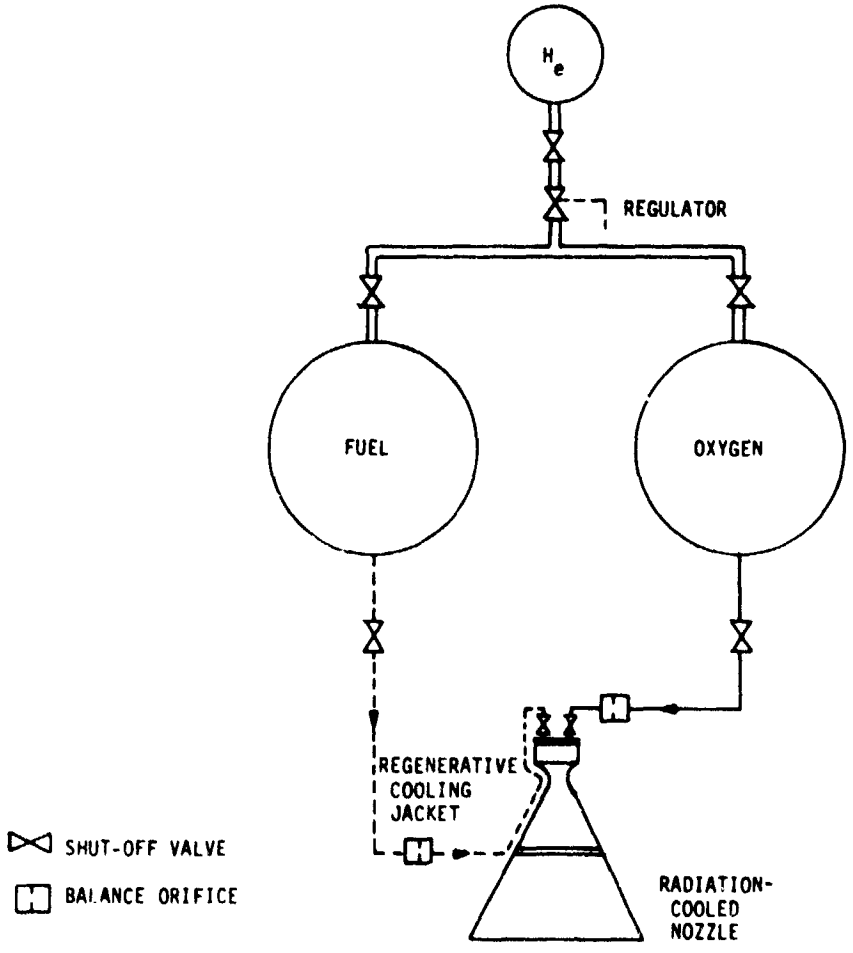

Figure 22. Conventional Pressure-Fed Concept

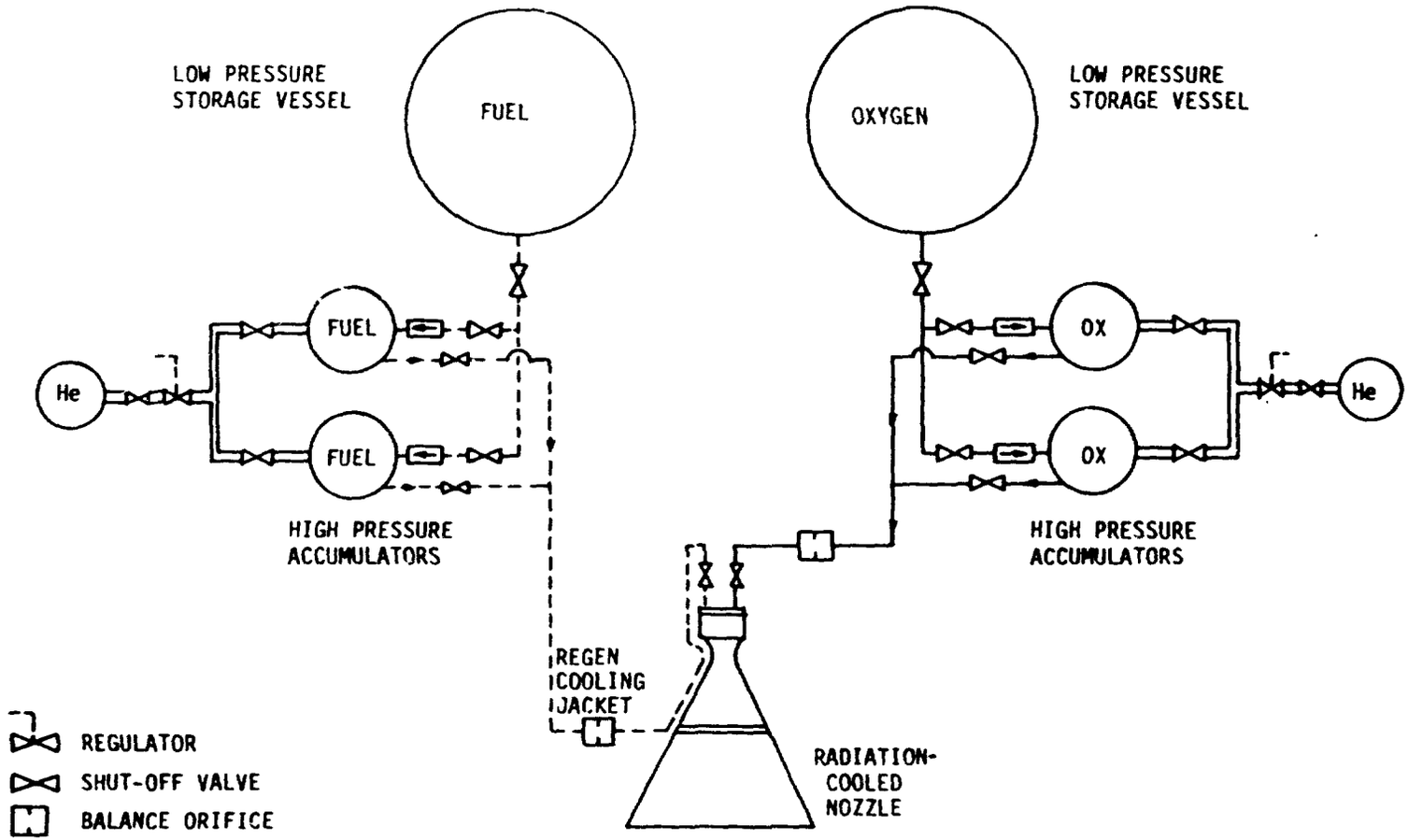

Figure 23. Parallel Accumulator Concept

is shown in Fig. 23. In this concept, both the fuel and oxygen are stored in low-pressure main propellant tanks. Two small parallel accumulators in each propellant feed system are located downstream of these main propellant tanks. These accumulators are alternately filled from the main propellant tank and pressurized to provide the engine propellant supply. When the propellant is expelled, the tank is vented and then refilled from the main tank. While one tank is being filled, the engine runs off the parallel tank. The advantage of this system over the basic pressure-fed concept is a reduction in the high pressure tankage weight. The accumulators are sized to provide the apogee burn. Again, the engine can be either regen or film-cooled.

Figure 24 shows a pump-fed concept in which the pumps are driven by electric motors with fuel cells as the power source. Analysis has indicated that the weight of batteries is prohibitive. Of course, in comparison to gas turbine-driven pumping systems, the weight of the fuel cells and electric motors is also a concept disadvantage. The concept schematic shown has a pulsation damper (very small accumulator) downstream of the pumps. This component would have been required if positive displacement pumps had been selected in component screening analysis. However, the results obtained under Contract NAS 3-21960, Low-Thrust Chemical Propulsion System Pump Technology, for NASA/LeRC showed that centrifugal pumps were the best choice. Therefore, the pulsation dampers were eliminated in the final system evaluations.

Figure 25 shows a pump-fed concept with an electric motor drive using a turboalternator as the power source. This concept has potential application with heated hydrogen or methane as the turbine drive fluid. A small amount of the heated fuel bypasses the turbine. This bypass flow provides the power control. Cycle power balances were performed to determine if the maximum operating chamber pressure of this system differs from the cooling limits. This is discussed in the next section. This concept is relatively lightweight, provided that the horsepower of the pumps is low enough to keep the weight of the electrical components down.

An expander cycle pump-fed concept is shown in Figure 26. This concept is also applicable with heated hydrogen or methane as the drive fluid for the turbines. A series turbine cycle arrangement was selected because the full-flow oxygen turbine is much more efficient than the extremely low-flow oxygen turbine in a parallel arrangement. The fuel turbine bypass valve shown on the figure is used to provide mixture ratio control, whereas the valve bypassing flow around both turbines is for power control. In addition to proving the lightest-weight pump-fed system, this is also the simplest because it does not require any additional components.

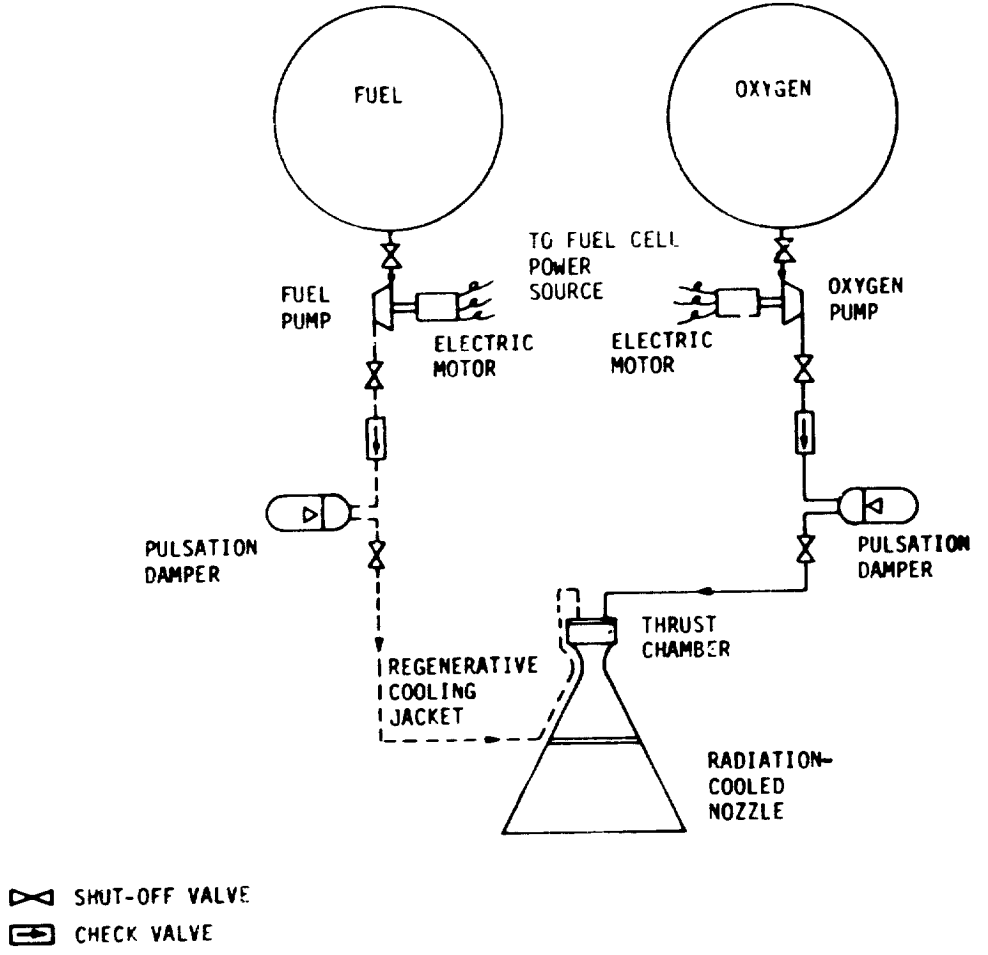

Figure 24. Auxiliary Power Source (Fuel-Cells) Concept

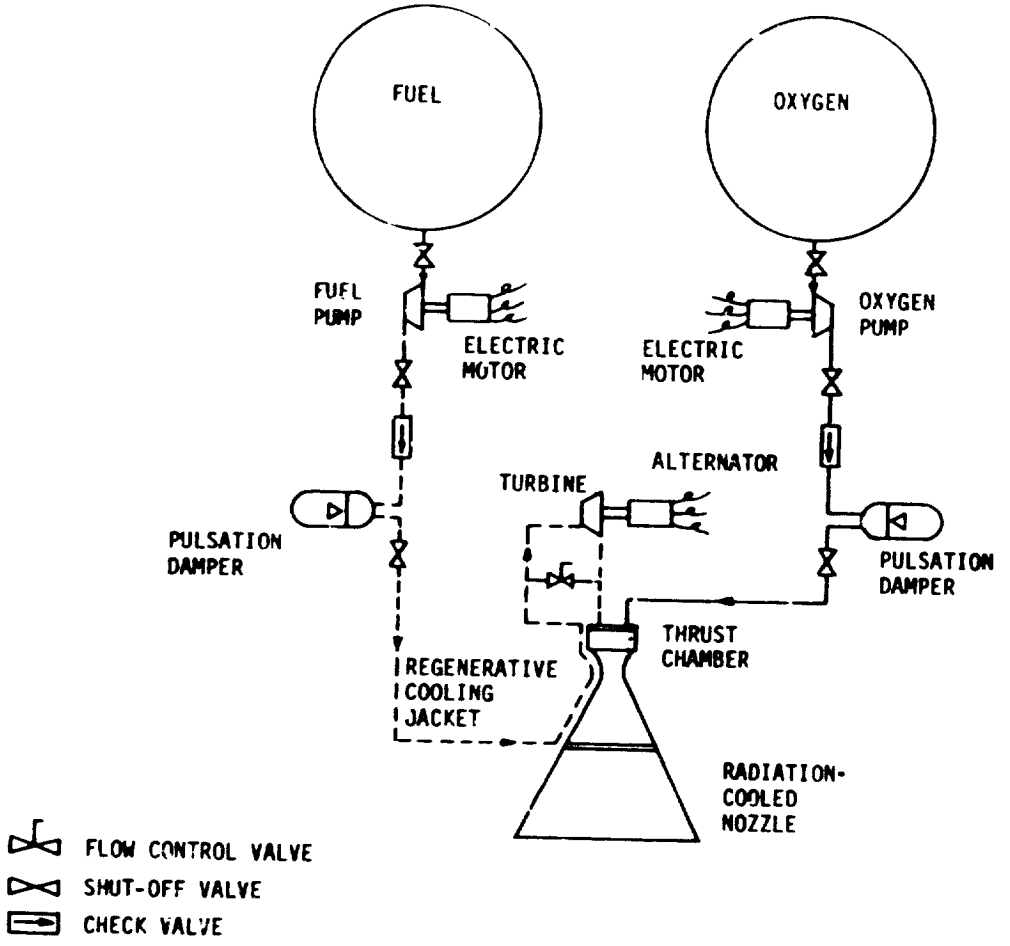

Figure 25. Turboalternator Concept

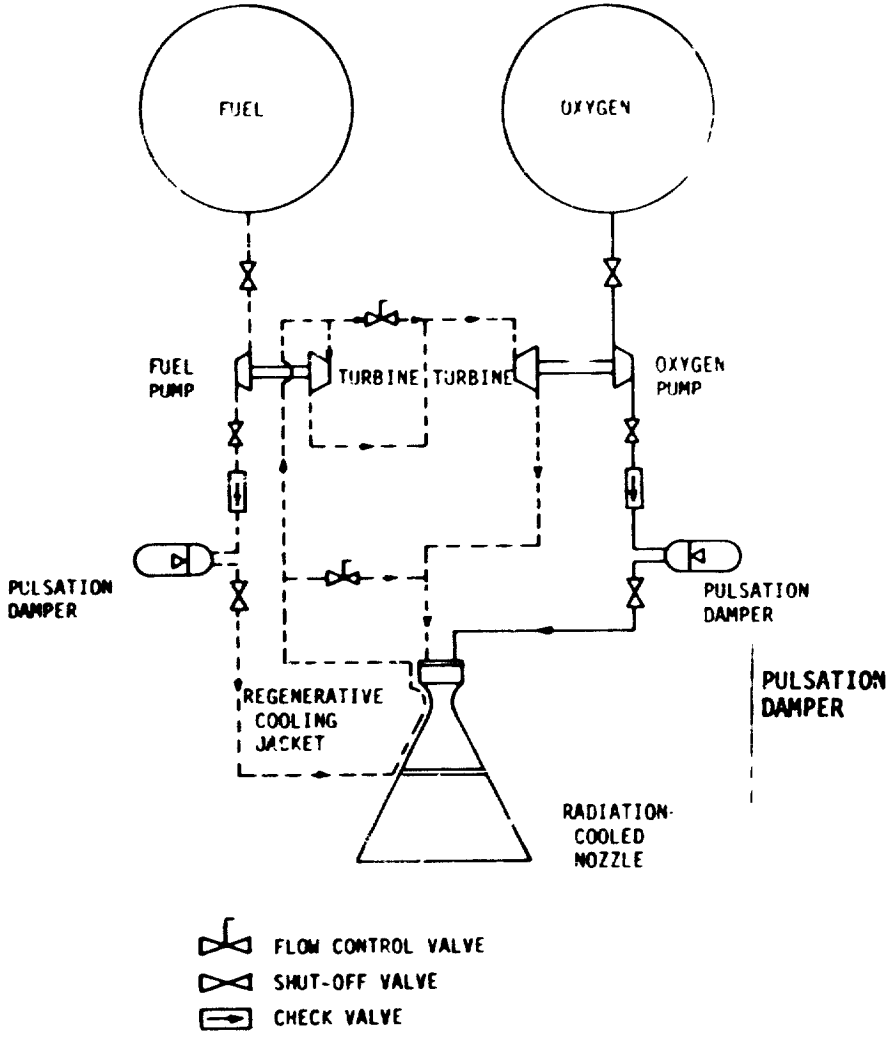

Figure 26. Expander Cycle Concept

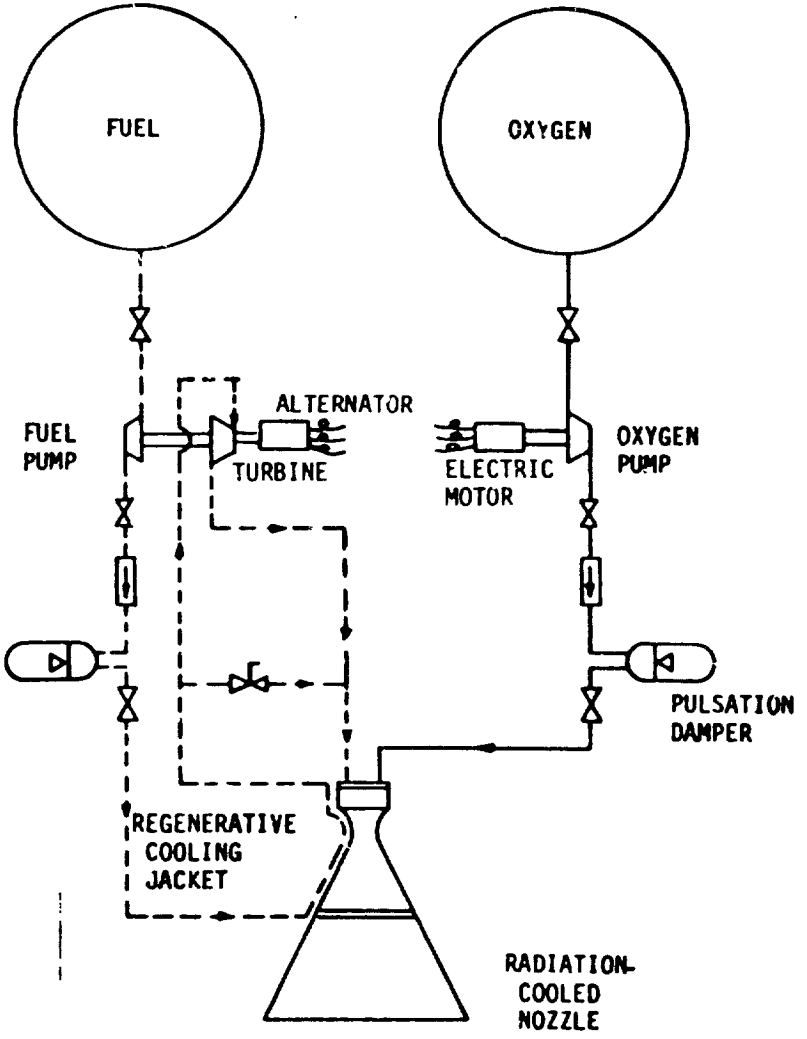

Figure 26a. Expander/Turboalternator Concepts

A mixed expander/turboalternator concept is shown in Figure 26a. This concept incorporates some of the best features of the expander and turboalternator cycles. The hydrogen turbopump is driven in the expander mode which eliminates the electric motor required for the turboalternator cycle. The lower horsepower oxygen pump is driven by an electric motor with the advantage over an expander cycle being the elimination of a hot gas bipropellant seal. The potential disadvantage is the weight of the electrical components.

Figure 27 shows a pump-filled feed tank concept. In this concept, the engine run tanks are filled by pumps from the low-pressure main vessels during mission coast periods. The possible advantage of this concept is that the pump flows can be much higher than the engine flows; this may provide a more suitable operating regime for the pumps (i.e., the pump design is not restricted by the engine thrust level). The disadvantage would be the additional weight of the high-pressure accumulators. A regulator is shown downstream of the engine run tanks to maintain constant engine pressures. Without this regulator, the chamber pressure and engine thrust would decay as the propellant is expelled. This system is applicable with both regeneratively or film-cooled engines.

C. SYSTEM EVALUATIONS AND PARAMETRIC DATA SUMMARY

1. O_2/RP-1 System Evaluations

Based upon the cooling analyses results, only the regeneratively cooled concepts were analyzed for the O_2/RP-1 systems. Two pressure-fed and two pump-fed engine concepts are applicable with O_2/RP-1. They are:

- Conventional Pressure-Fed
- Parallel Accumulator
- Auxiliary Power Source
- Pump-Filled Feed Tank

Engine performance and envelope data applicable for all concepts although specific operating points may vary (i.e., pressure-fed concepts applicable in the 1.36 to 13.6 atm (20 to 200 psia) range and pump-fed systems more applicable to chamber pressures greater than 6.8 atm (100 psia). The parametric performance and envelope data at an area ratio of 400:1 are shown in Figures 28 and 29, respectively. As can be seen, the very low-pressure engines are extremely large and have low performance levels. Performance numbers above and to the left of the cooling limit line represent impractical engine designs. Similarly, the impractical systems are below and to the left of the cooling limit on the envelope plot.

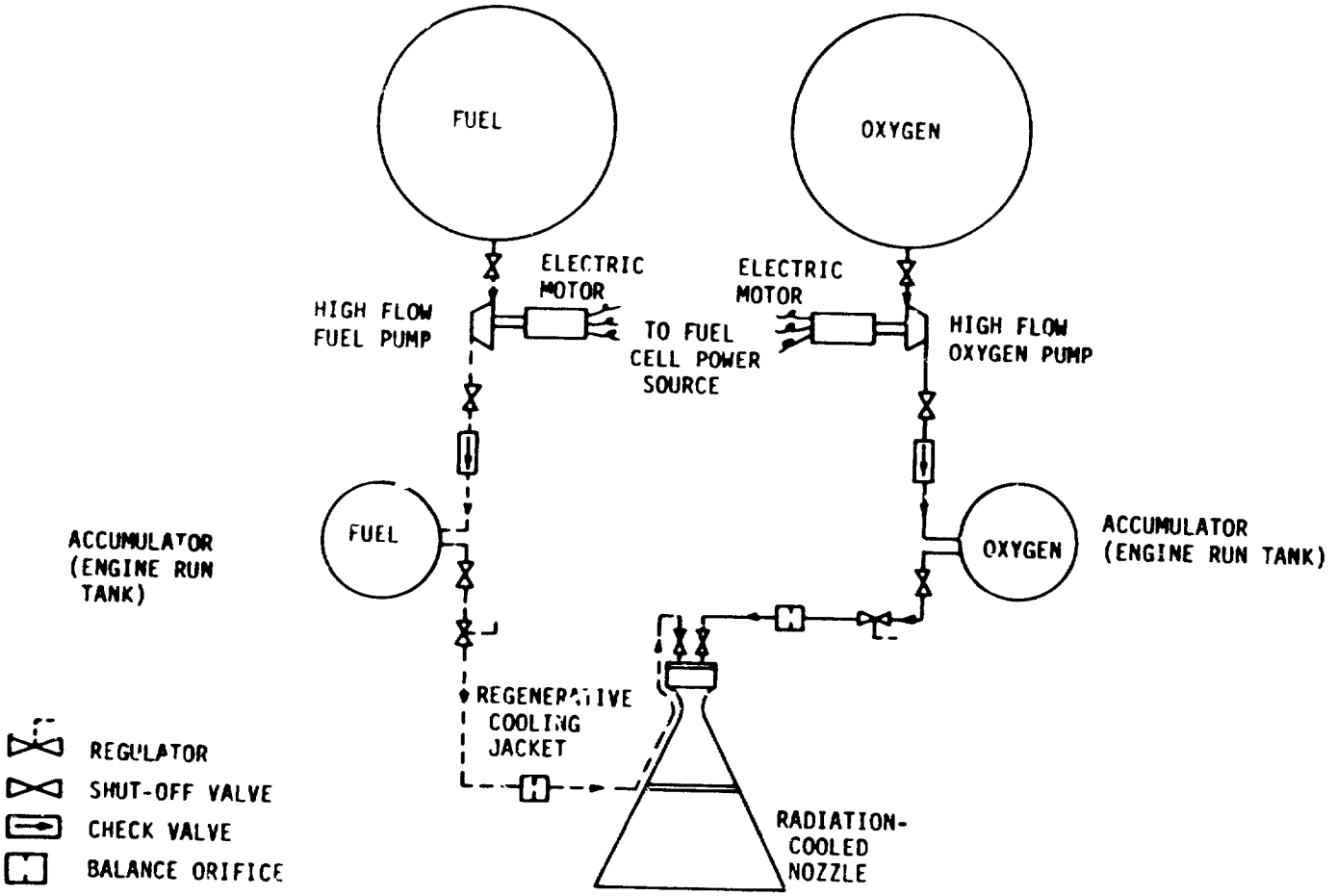

Figure 27. Pump-Filled Feed System Tank Concept

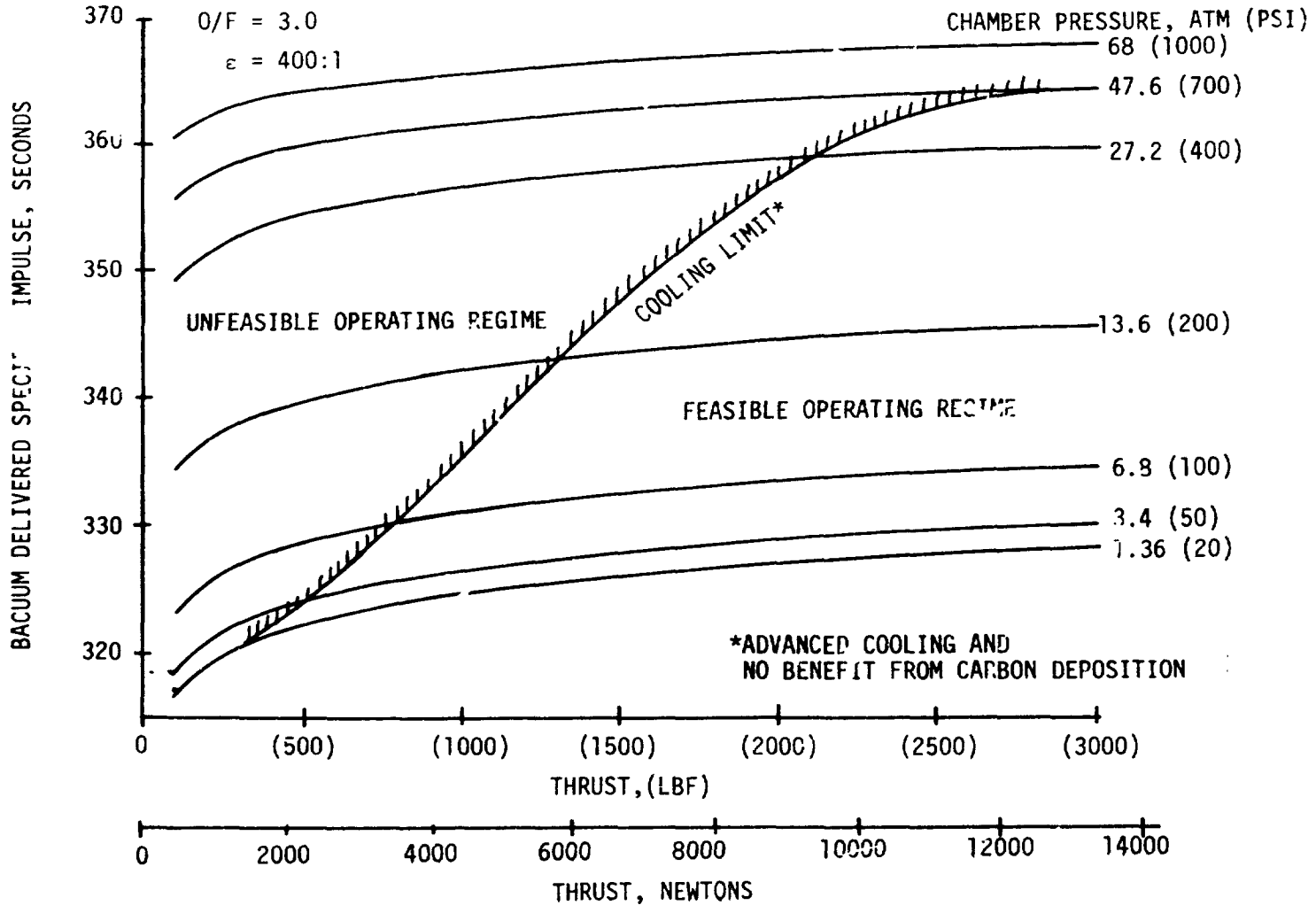

Figure 28. Delivered I_s For All O_2/RP-1 Regen-Cooled Concepts

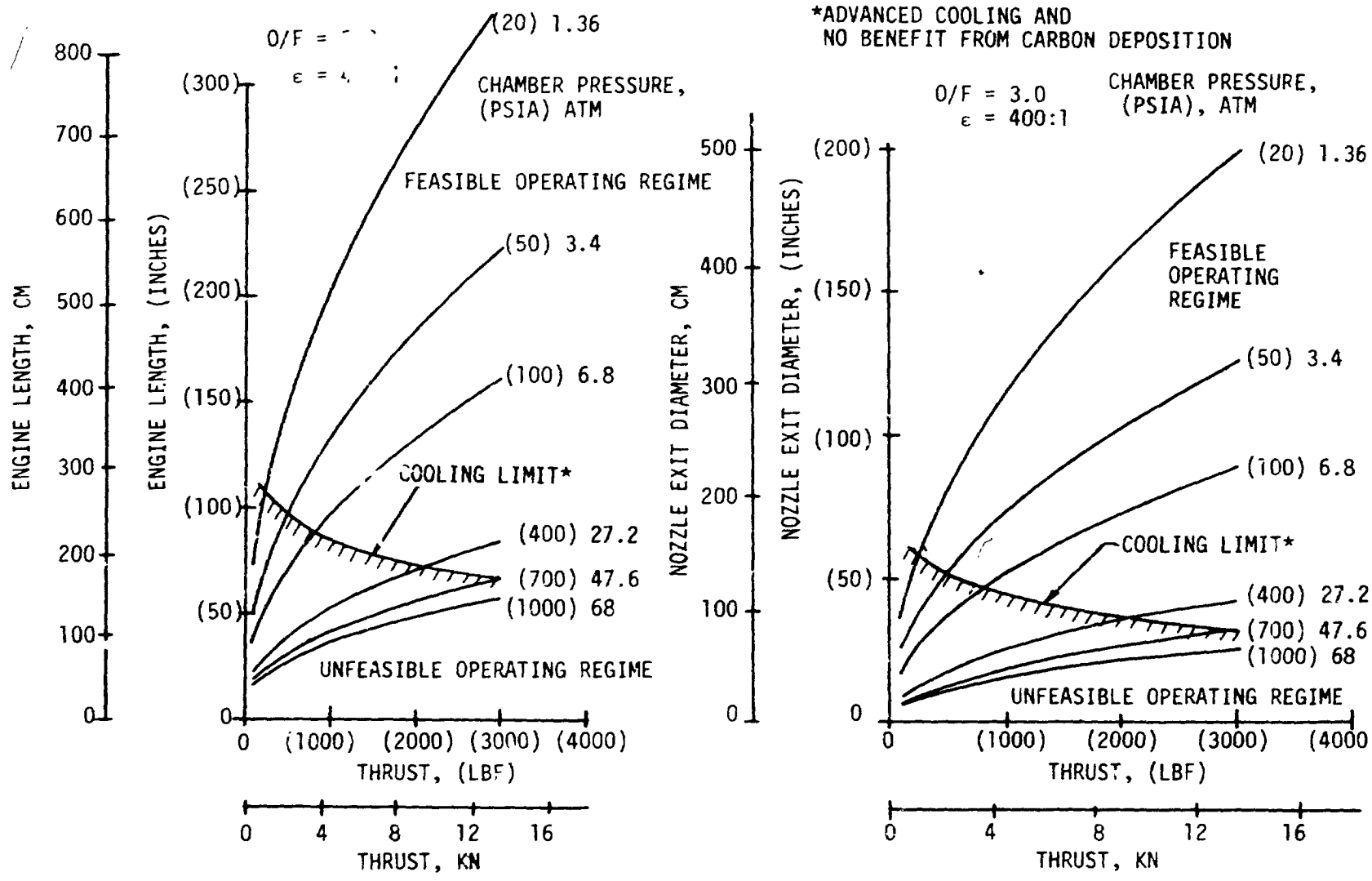

Figure 29. O_2/RP-1 Engine Envelope Data For All Concepts

The relative weights of the various concepts are compared at a thrust chamber pressure of 10.2 atm (150 psia) on Figure 30. The relative weights include the weights of the tanks, accumulators, pressurization system, and the engine and electrical components. The data show that pump-fed systems are lighter than pressure-fed concepts. This occurs because the weight of the fuel cells, pumps, and electrical components are lighter than the additional tank and pressurization system weights of the pressure-fed system. The auxiliary power source concept is the best O_2/RP-1 candidate. Parametric weight data for this concept is shown in Figure 31. The weight of the engine includes all electrical components. The additional fuel cell weight requirements that can be charged to the engine system are also shown on the figure. The auxiliary power source concept results in the highest performance, smallest engine envelope, and lightest system weight with O_2/RP-1 propellants.

2. O_2/CH_4 System Evaluations

Only regeneratively cooled engine concepts were determined to be practical. In addition, the high critical pressure of CH_4 ruled out pressure-fed systems. Three pump-fed systems were evaluated with O_2/CH_4. They are:

- Auxiliary Power Source
- Turboalternator
- Expander

Engine cycle power balance calculations were performed for the turboalternator and expander cycles to determine if the feasible design ranges were limited further by the power considerations. Pump discharge pressure requirements as a function of chamber pressure are summarized in Figure 32. The maximum pressure obtainable is approximately 47.6 atm (700 psia), and good design practice would dictate the selection of a chamber pressure in the 34 to 37.4 atm (500 to 550 psia) range to avoid large system sensitivities to minor component variations. The power balance upper limit was combined with the cooling limits, as shown in Figure 33. The auxiliary power source concept could operate over the total feasible cooling ranges and is applicable with the short chamber L' because it does not depend upon the heat input into the CH_4 to derive cycle power.

Delivered performance and engine envelope data at an area ratio of 400.1 for all three O_2/CH_4 concepts are shown in Figures 34 and 35, respectively. At the same low thrust design point, the delivered performance of the O_2/CH_4 engine is much greater than that of the O_2/RP-1 engine; also, the envelope is much smaller because a higher operating chamber pressure is feasible with O_2/CH_4. For example:

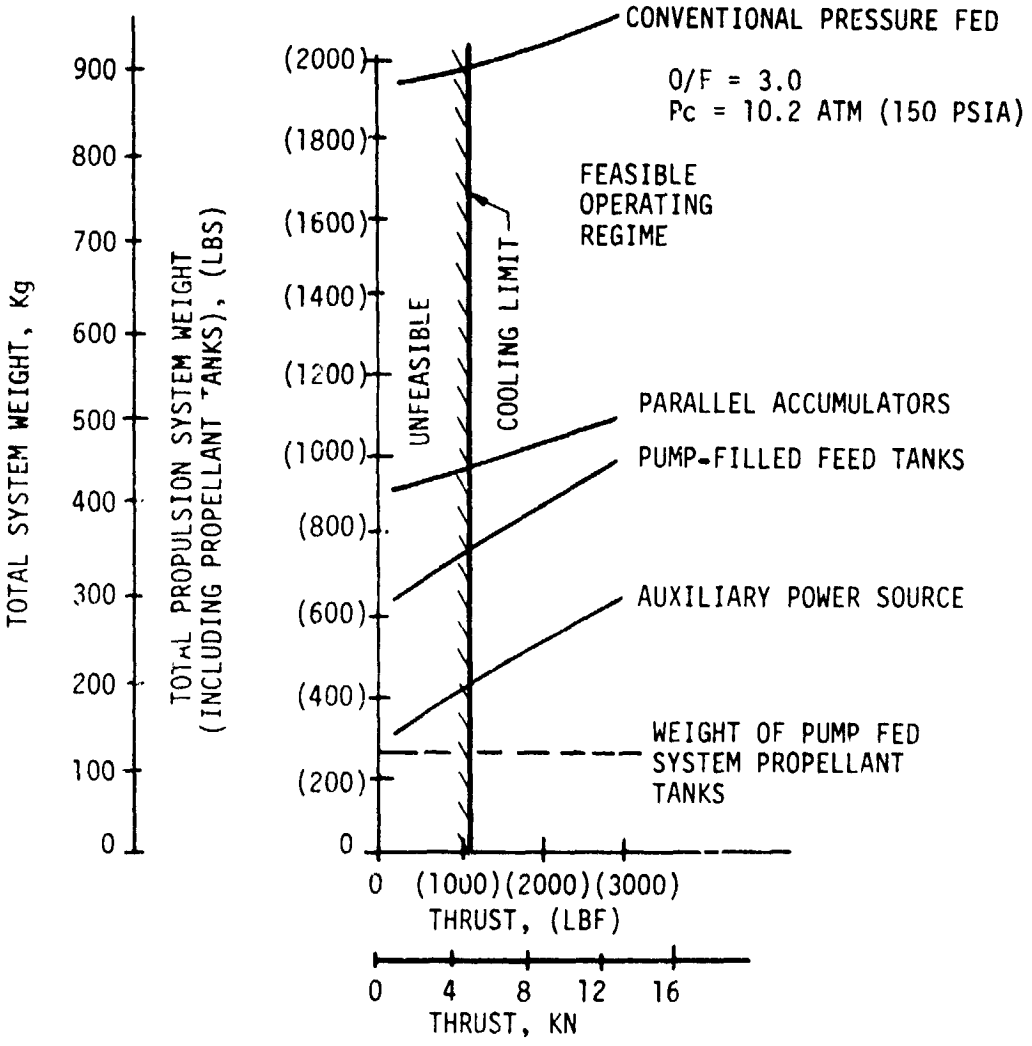

Figure 30. O_2/RP-1 Propulsion System Weight Data

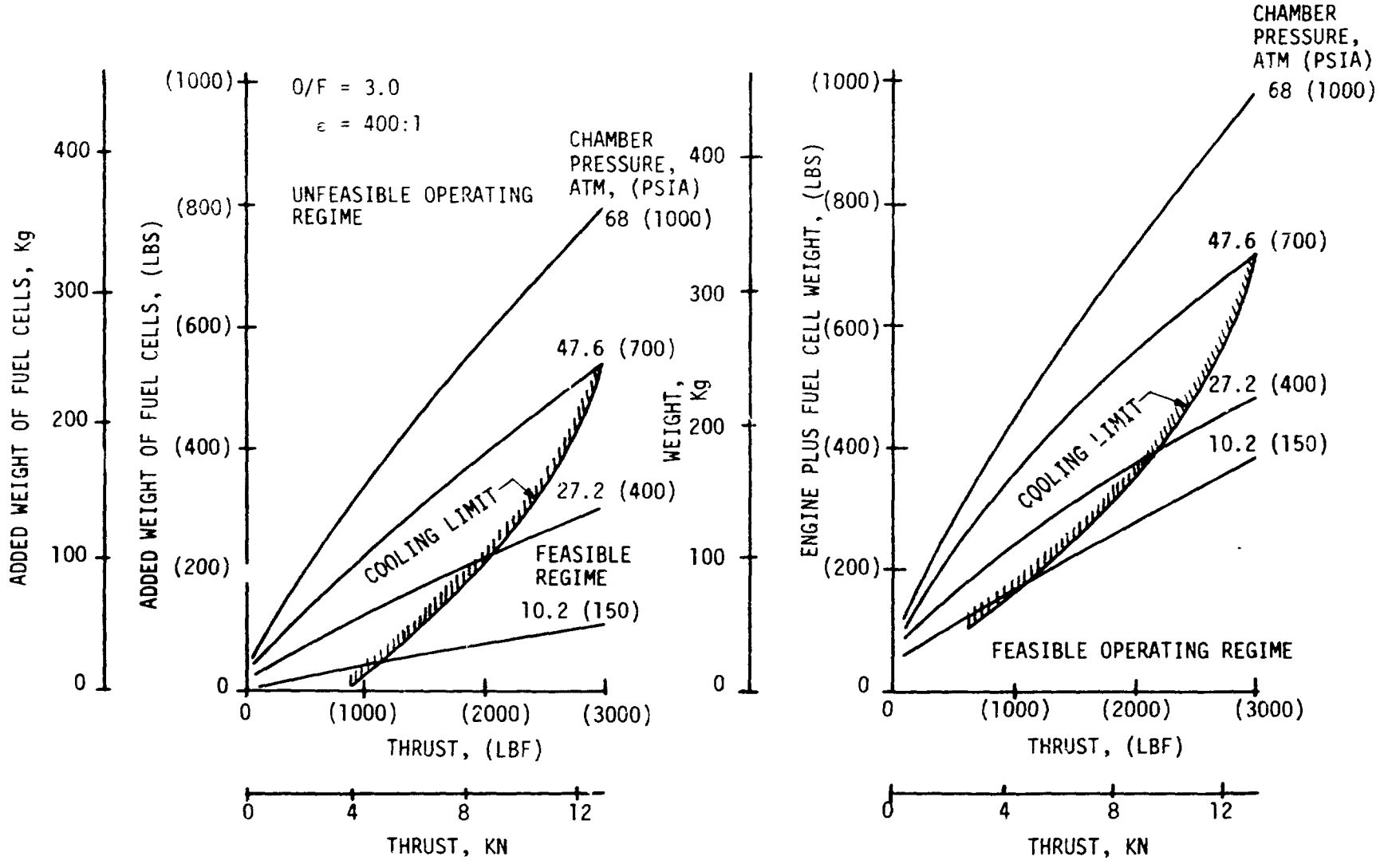

Figure 31. O_2/RP-1 Auxiliary Power Source, Regen-Cooled Engine Concept Weight Data

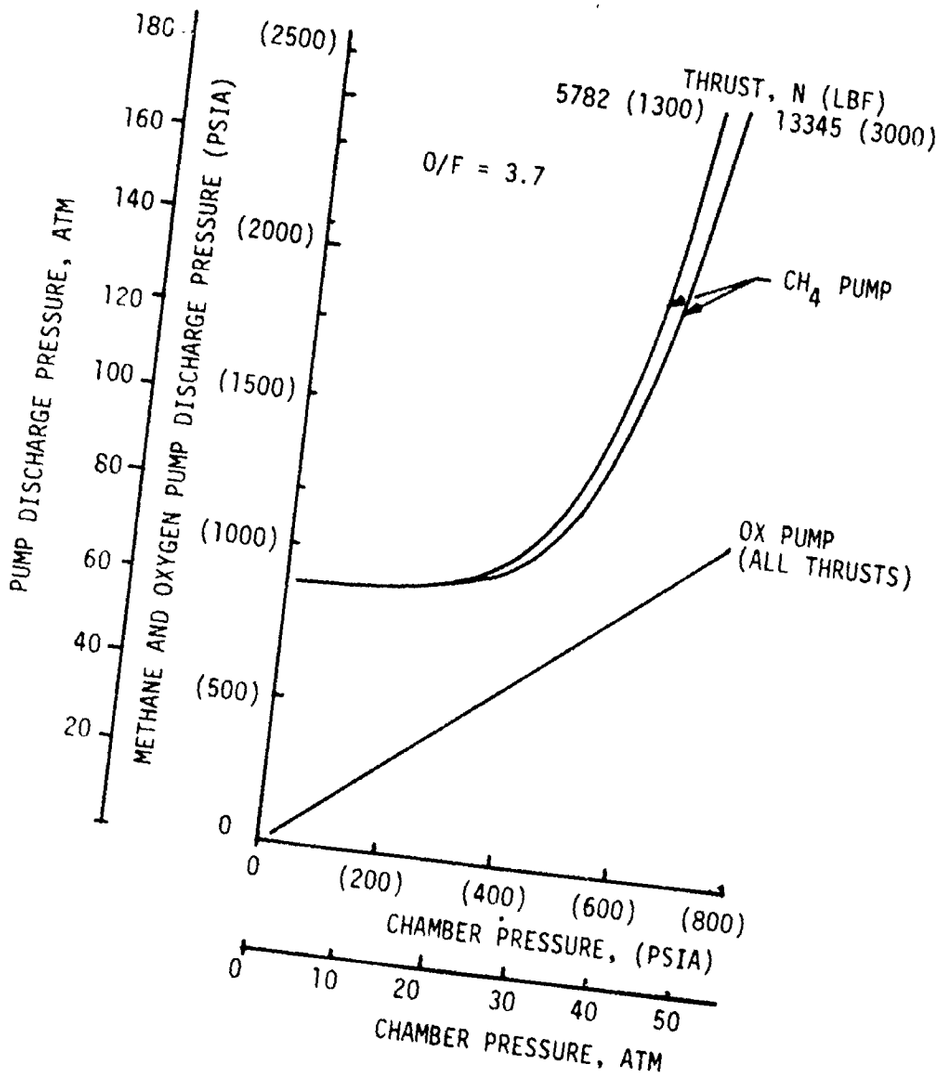

Figure 32. O_2/CH_4 Turboalternator and Expander Cycle Power Balance Data

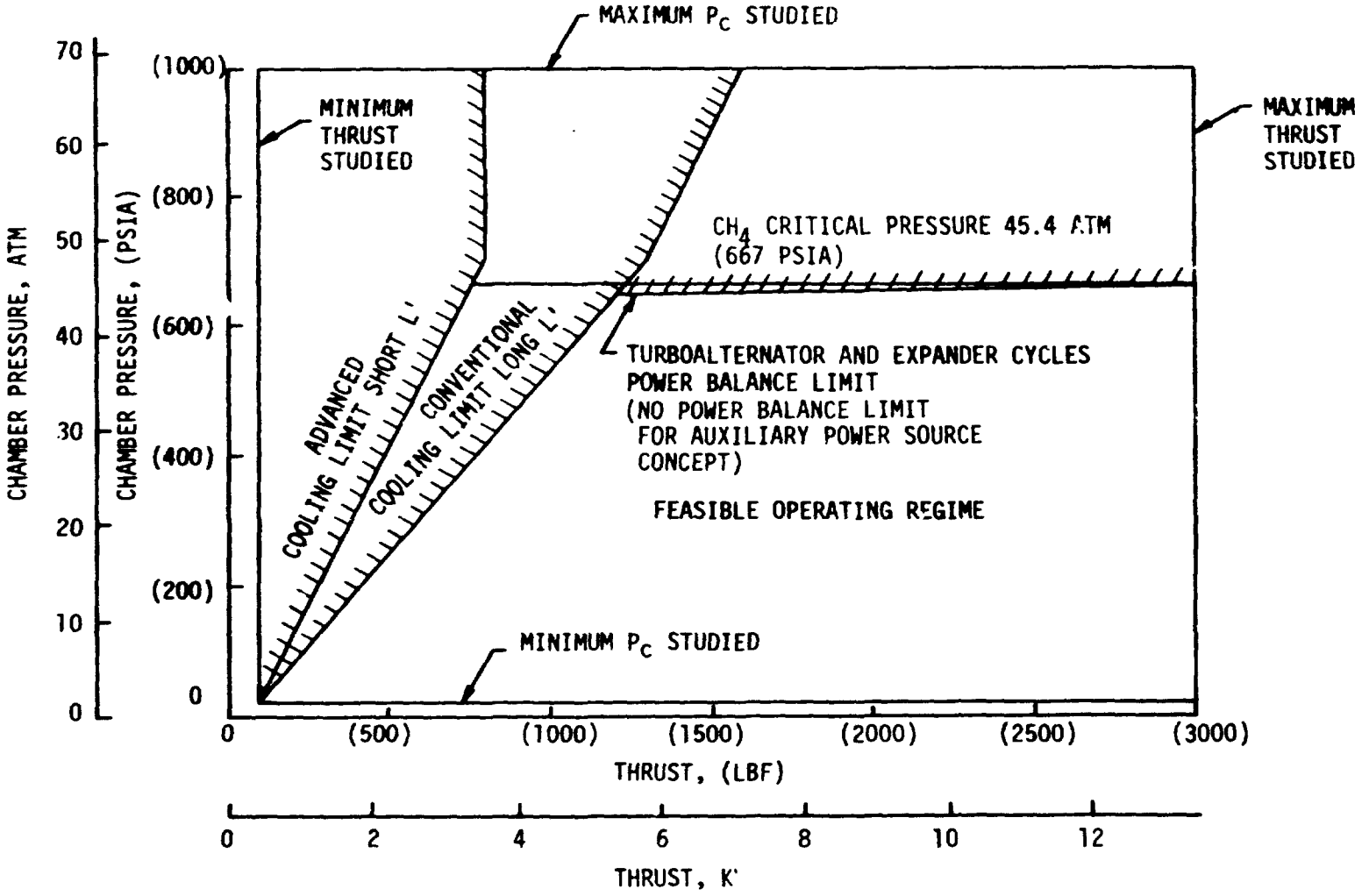

Figure 33. O_2/CH_4 Regen-Cooled Engine Operating Limits

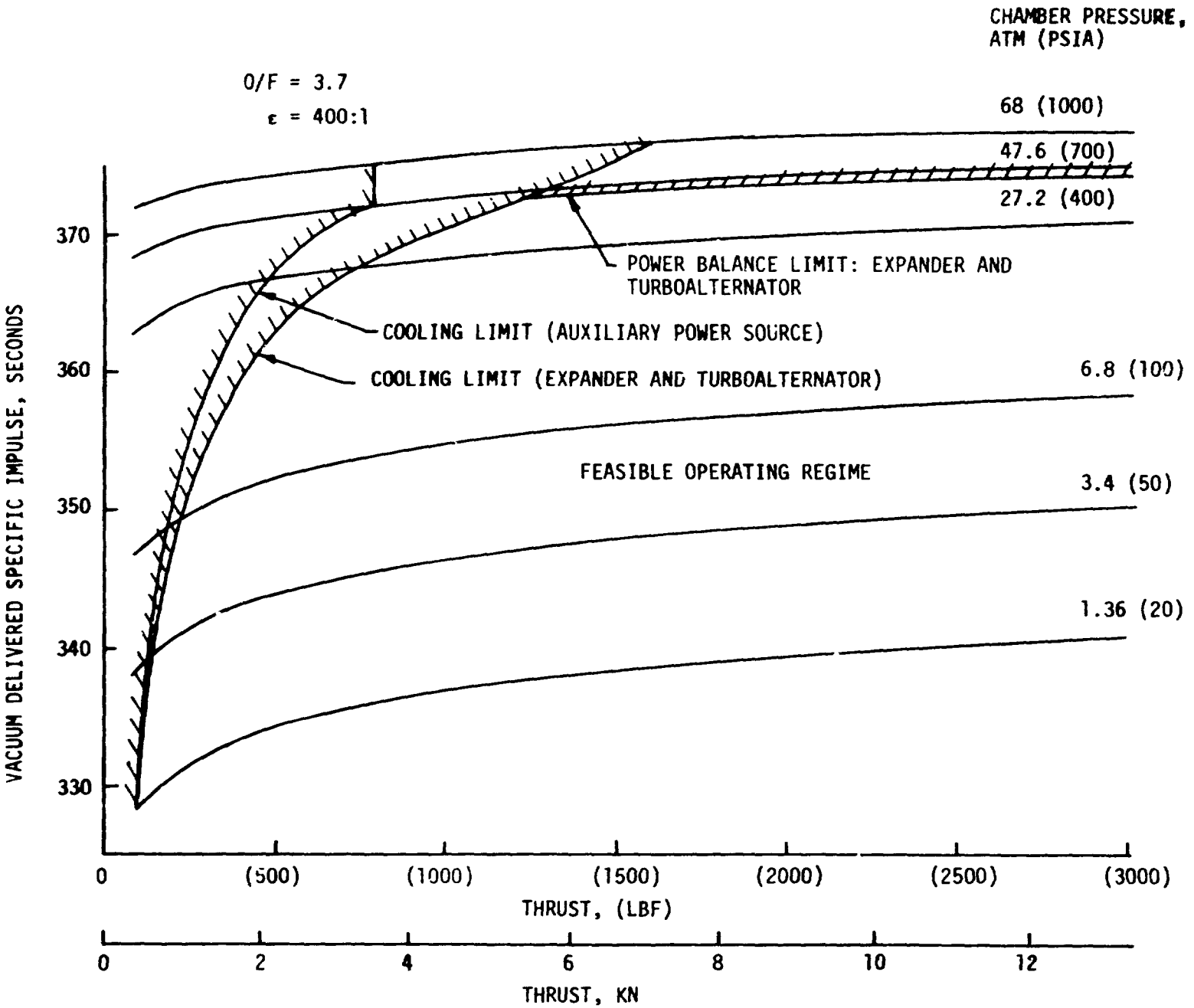

Figure 34. Delivered I_s For All O_2/CH_4 Regen-Cooled Concepts

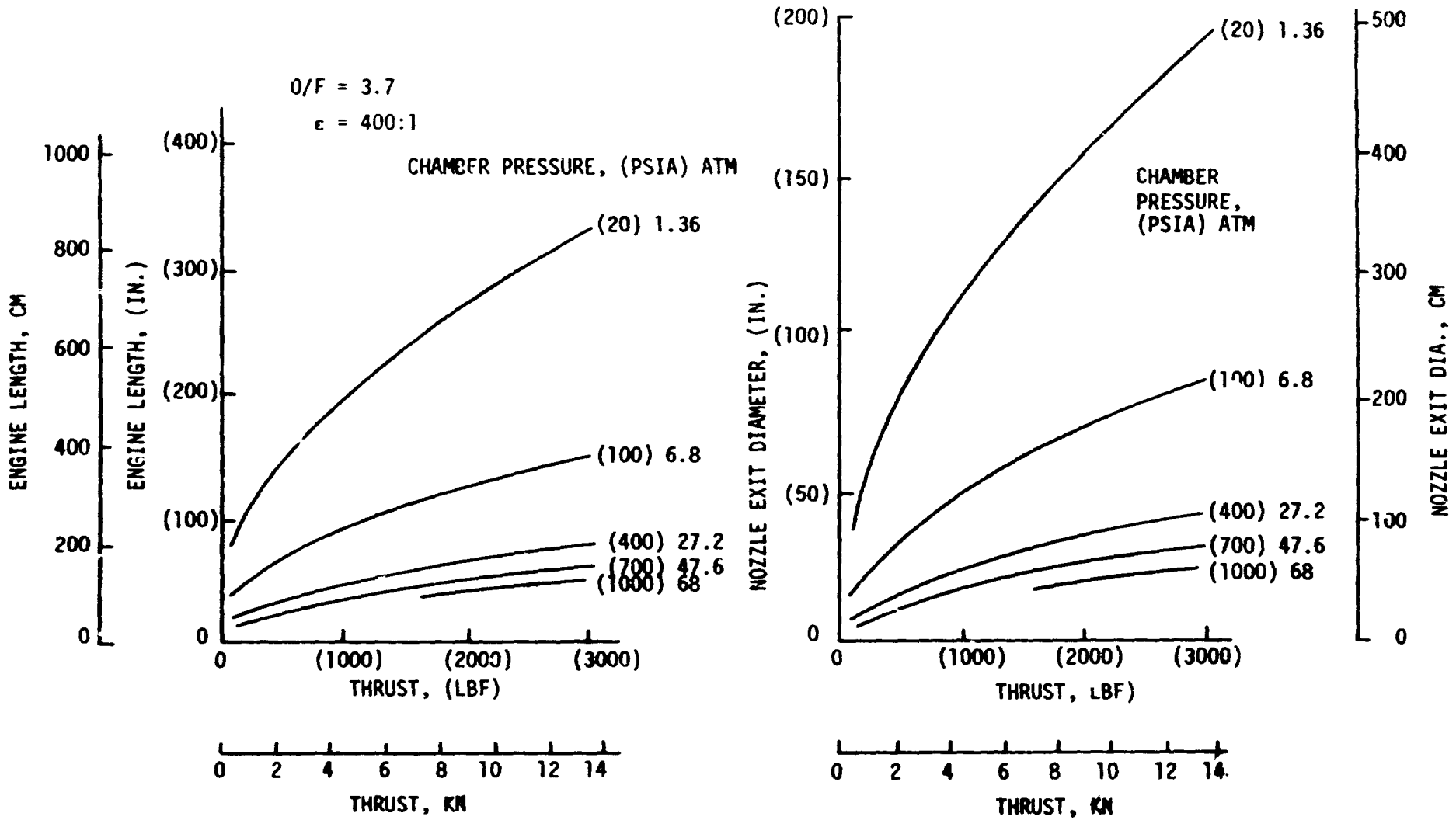

Figure 35. O_2/CH_4 Regen-Cooled Concepts Engine Envelope Parameters

Propellant Combination	Thrust KN (lb)	Chamber Pressure atm, psia	Delivered Is, sec	Engine Length, cm (in.)
O_2/RP-1	4.45(1000)	10.2(150)	335	218(86)
O_2/CH_4	4.45(1000)	27.2(400)	369	132(52)

The weight of the basic engine (including the additional components attributable to the engine) is shown in Figure 36 at a thrust level of 4448 N (1000 lbF). Weight comparisons of O_2/CH_4 regen-cooled engine concepts in the figure show that an expander cycle results in the lowest engine weight because it has the fewest components. The weight of the expander cycle decreases with increasing pressure because the physical size of the engine decreases. The electrical components and fuel cell weights become the dominant factors at chamber pressures above 20.4 and 13.6 atm (300 and 200 psia) for the turboalternator and auxiliary power source concepts, respectively. Below these pressures, the engine weight is dominated by the large 400:1 nozzle.

3. O_2/H_2 System Evaluations

Both regeneratively cooled and film-cooled concepts were evaluated in the system analysis. Parametric data were established for the following cases:

Concept	Cooling Scheme
Conventional Pressure-Fed	Film and Regen
Parallel Accumulator	Film and Regen
Auxiliary Power Source	Film and Regen
Turboalternator	Regen
Expander	Regen
Pump-Filled Feed Tank	Regen
Mixed Expander/Turboalternator	Regen

The parametric data which were submitted to NASA/LeRC as part of an informal data dump are summarized in this section.

Engine cycle power balance calculations were performed to establish the power limits for the expander and turboalternator cycles. The results of the power balance calculations are summarized in Figure 37 and combined with the cooling limits in Figure 38. Again, the power limit is the maximum upper value, and design points at about 34 atm (500 psia) chamber pressure are recommended to achieve reasonable power balance margins. The O_2/H_2 film-cooled engine operating regime analyzed was established by the cooling analysis and presented as Figure 39.

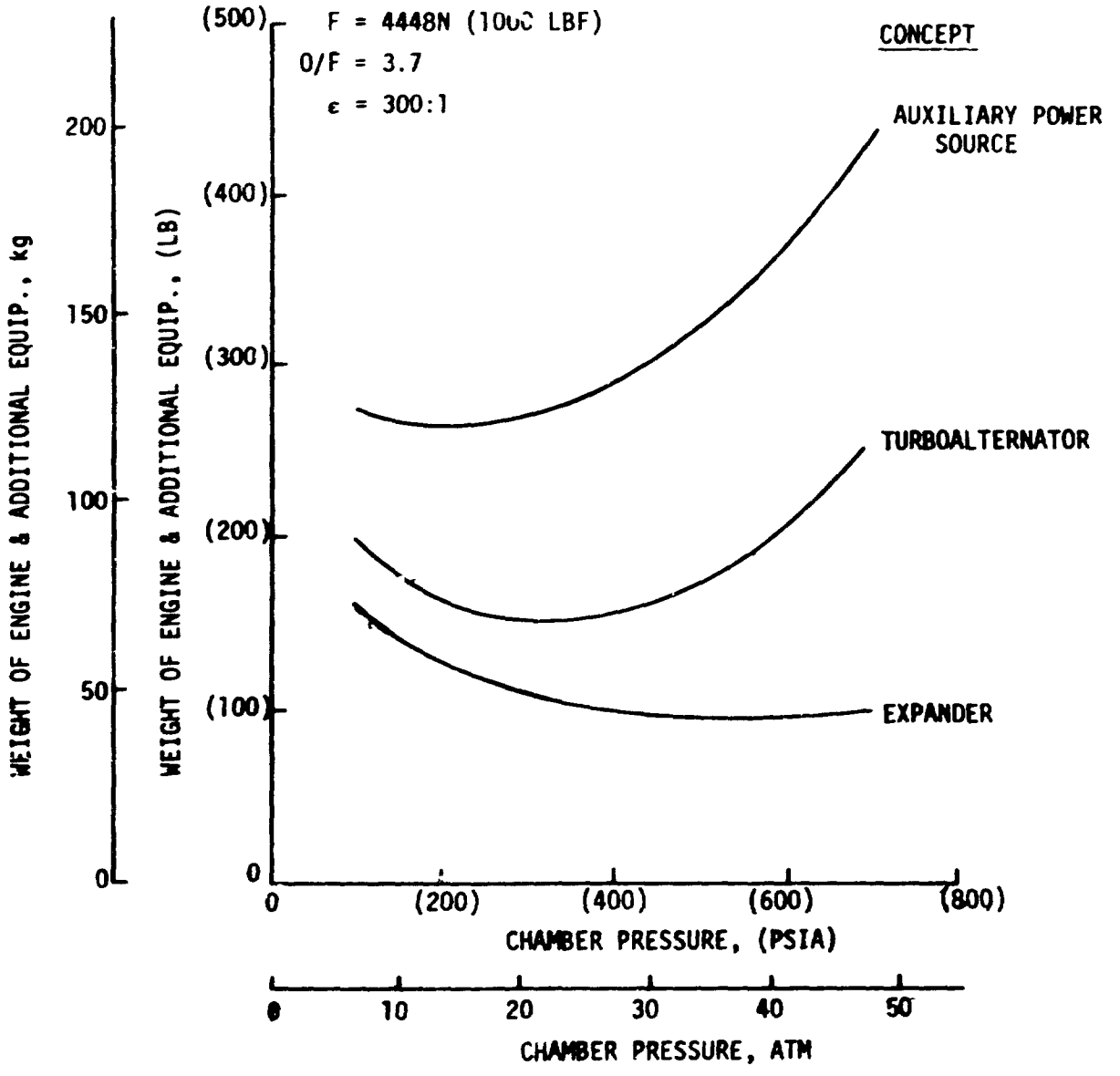

Figure 36. O_2/CH_4 Regen-Cooled Engine Concept Weight Comparisons

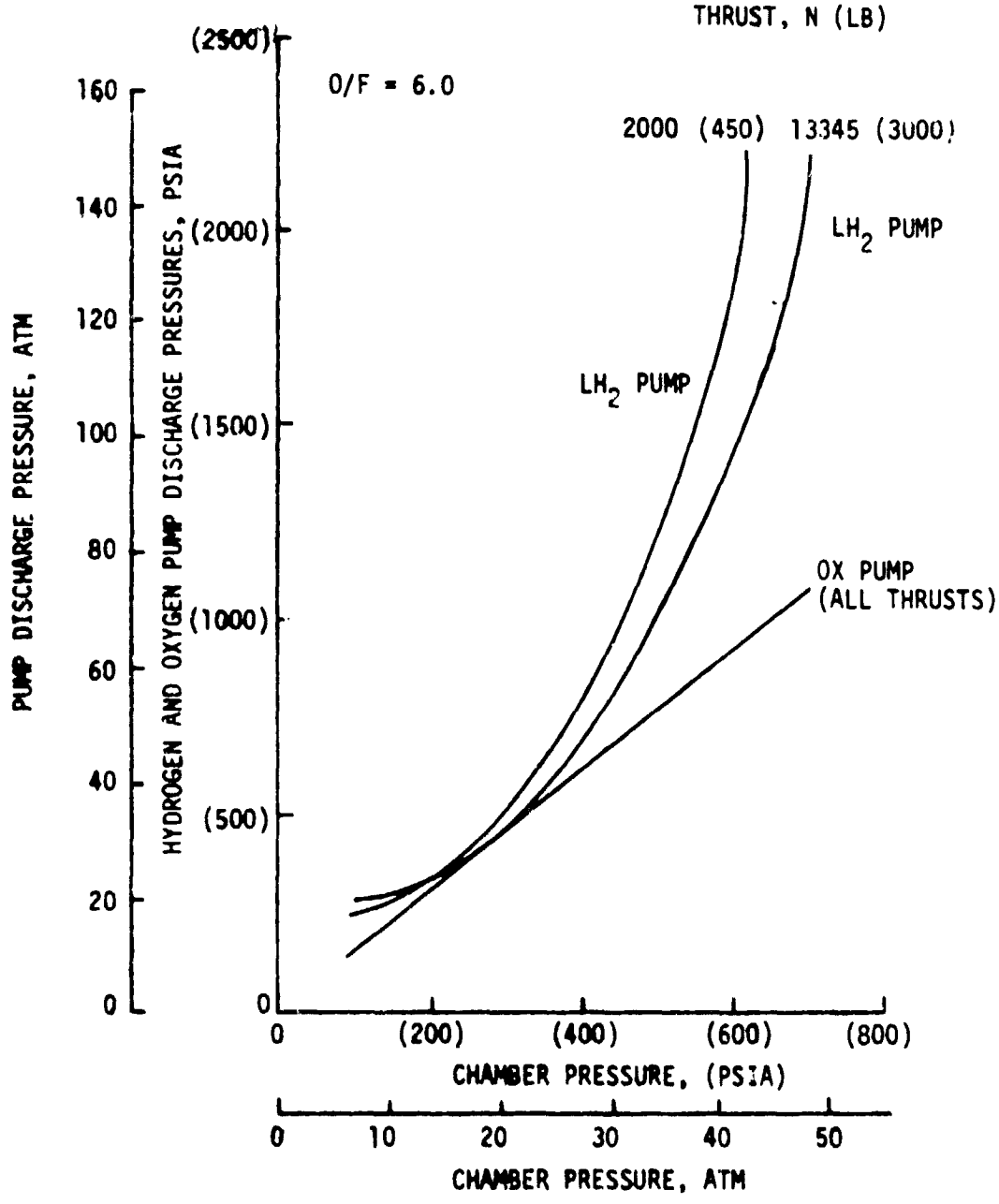

Figure 37. O_2/H_2 Turboalternator and Expander Cycle Power Balance Data

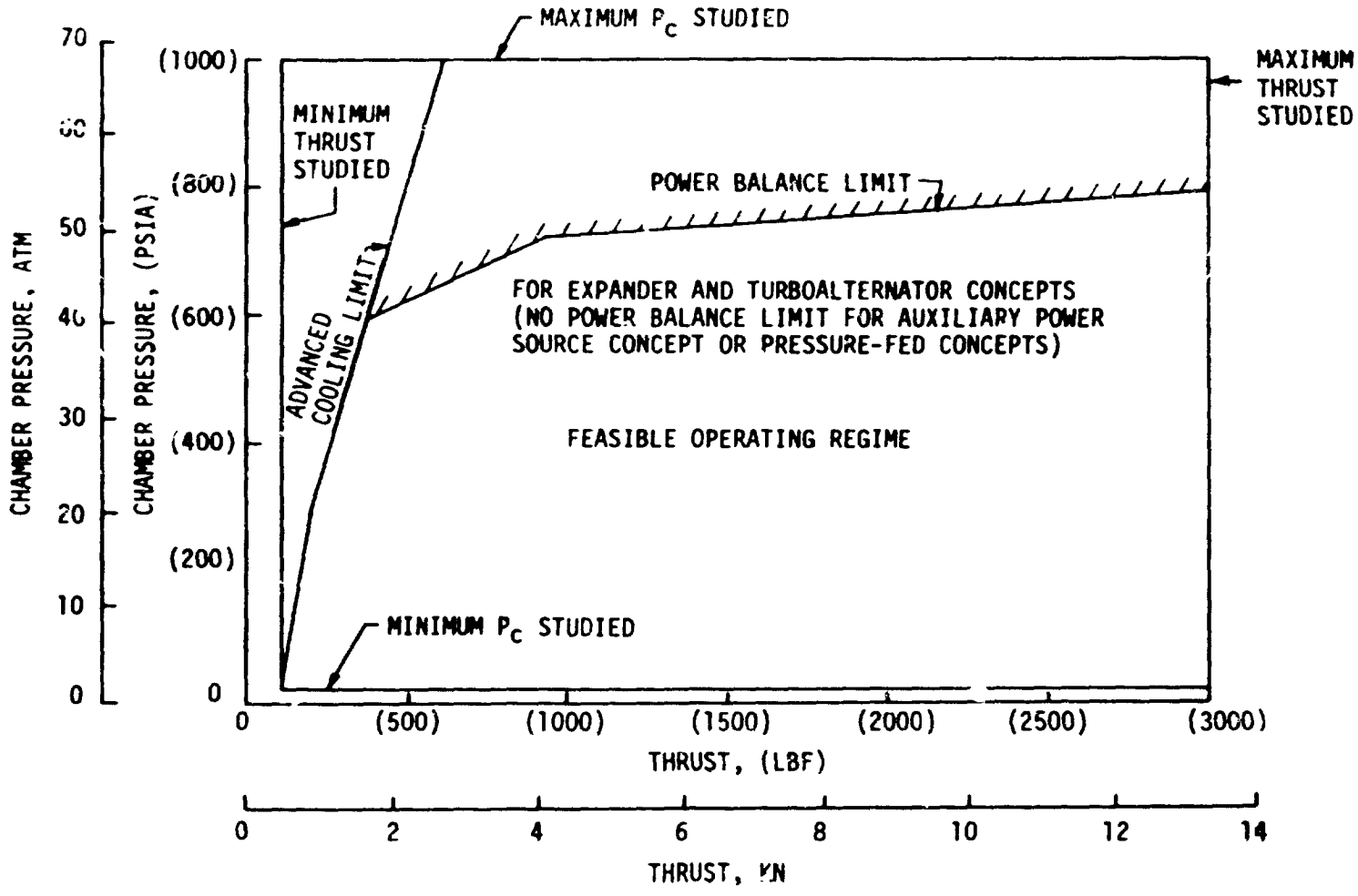

Figure 38. O_2/H_2 Regen-Cooled Engine Operating Limits

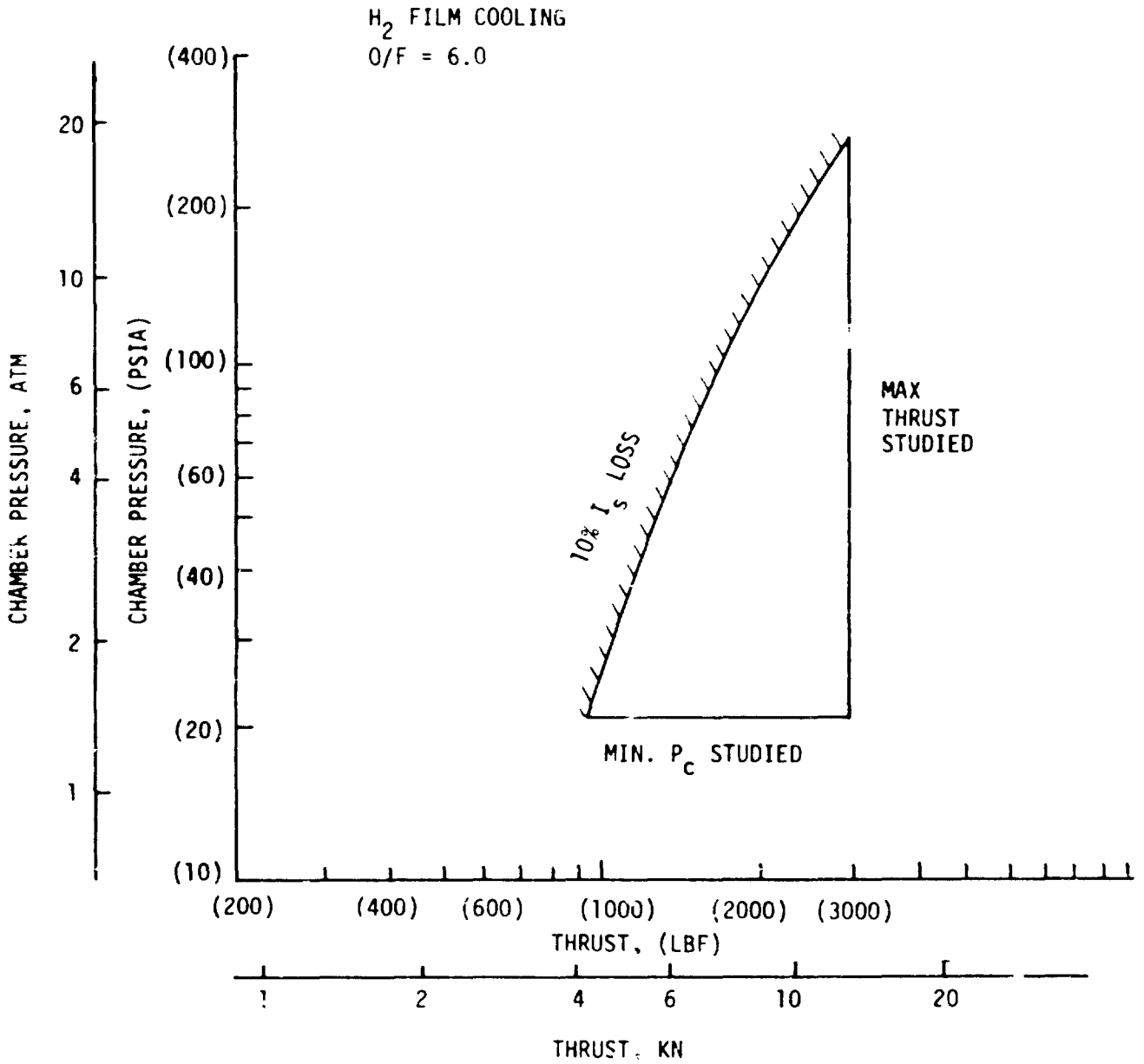

Figure 39. O_2/H_2 Film-Cooled Engine Operating Region

O_2/H_2 engine performance parametric data at an area ratio of 400:1 are presented on Figures 40 and 41 for the regeneratively and film-cooled engine cases, respectively. For the regen systems, performance drops off as thrust and chamber pressure decrease because of increased kinetic losses. Film-cooled engines were not found to be feasible below a thrust level of about 4.45 KN (1000 lb). Above approximately 6.8 atm (100 psia) chamber pressure, the performance of the film-cooled engine decreases with increasing chamber pressure because of the film-cooling losses. Performance also drops off at low chamber pressures because of the increased kinetic losses. Therefore, the film-cooled engines have a chamber pressure at which performance is maximized, as shown by the figure. The performance of the regen-cooled engine is 85 secs higher (i.e., 465 vs 380 secs) than that of the film-cooled engine at a thrust level of 4.45 KN (1000 lb) if it is assumed that the regen-cooled engine is capable of operating at a chamber pressure of 34 atm (500 psia). Compared to the data presented for the O_2/CH_4 and O_2/RP-1 systems in the previous section, the 465-sec delivered performance value of the O_2/H_2 engine is 96 and 130 sec higher than that of the O_2/CH_4 and O_2/RP-1, engines, respectively.

O_2/H_2 engine envelope parametric data are shown in Figure 42 as functions of thrust and chamber pressure. A comparison of these data with those for the O_2/RP-1 and O_2/CH_4 systems shows that the envelope does not vary significantly with propellant combination.

The relative system weights of the various O_2/H_2 concepts are compared in Figure 43 at a thrust level of 4.45 KN (1000 lb). The relative weight includes the weight of the engine, the difference in propellant tank and pressurization system weights, and any additional equipment such as accumulators, fuel cells, electric motors, and alternators. The data show that pump-fed systems are significantly lighter than the pressure-fed cases. The pump-fed system weight advantage is even greater than that shown with O_2/RP-1 propellants because the hydrogen tank is so large.

The weights of the pump-fed systems are compared on an expanded scale in Figure 44. The expander cycle is the lightest-weight engine because it has the fewest components, although the mixed expander/turboalternator cycle described in Figure 27 weighs only 4.5 to 9 kg (10 to 20 lb) more. The reasons for the data trends are the same as those explained for the O_2/CH_4 pump-fed systems in Figure 36.

D. CONCEPTUAL ANALYSIS CONCLUSIONS AND RECOMMENDATIONS

The conceptual design and parametric analyses showed that a hydrogen regeneratively cooled, pump-fed O_2/H_2 engine has the following advantages:

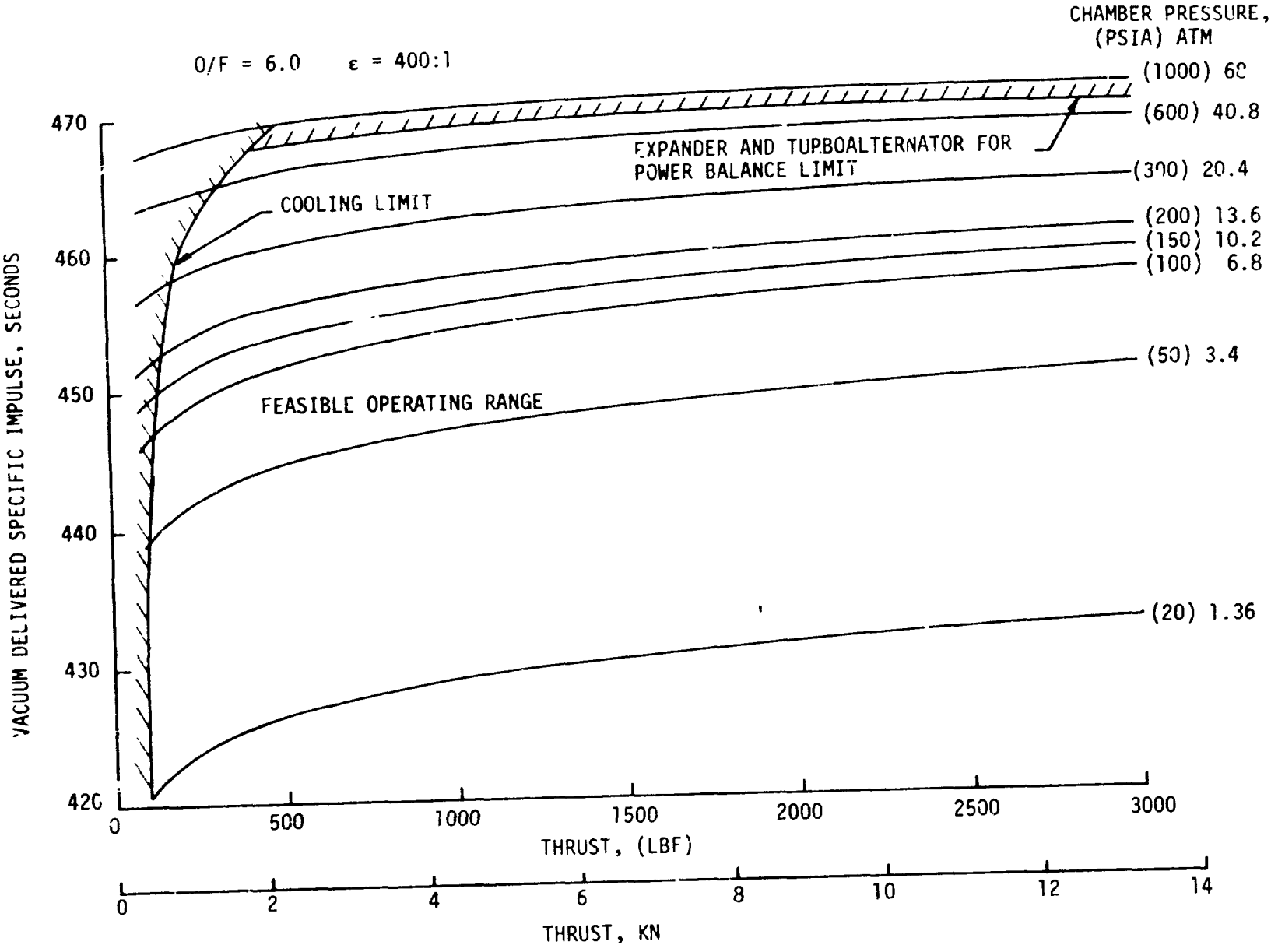

Figure 40. Delivered I_s For All O_2/H_2 Regen-Cooled Concepts

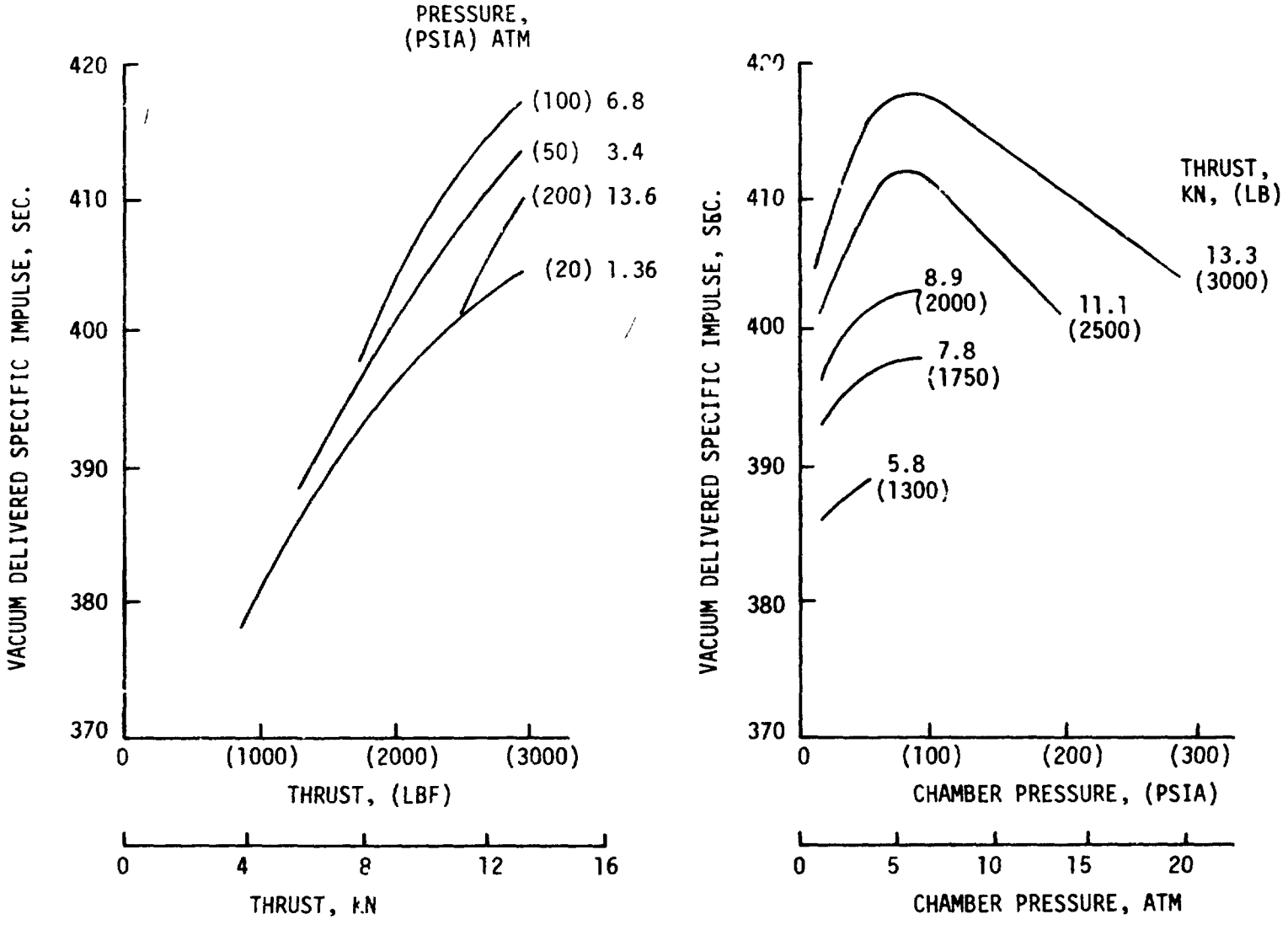

Figure 41. O_2/H_2 Pressure-Fed, Film-Cooled Engine Concept Performance Parametrics

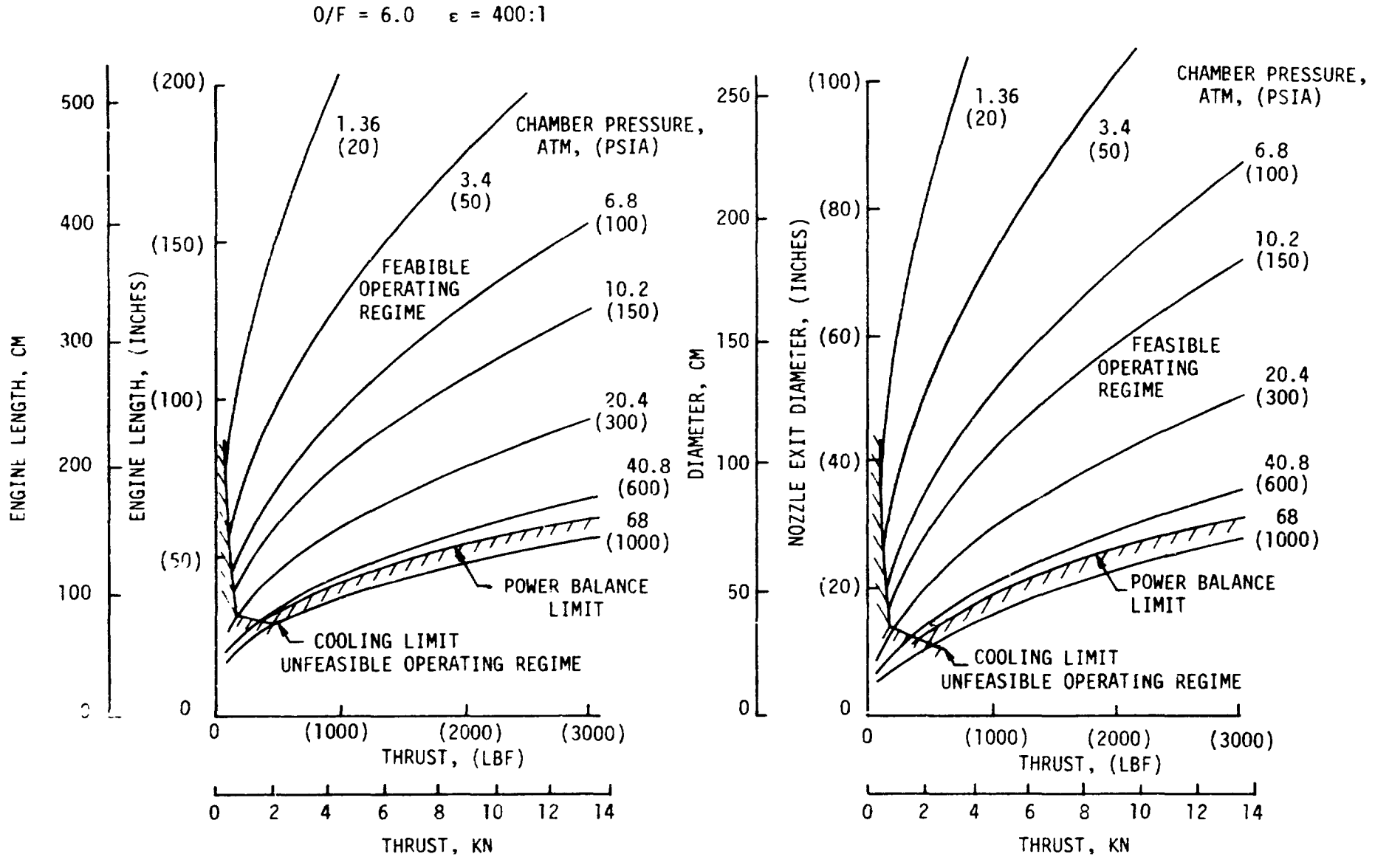

Figure 42. O_2/H_2 Engine Envelope Data For All Concepts

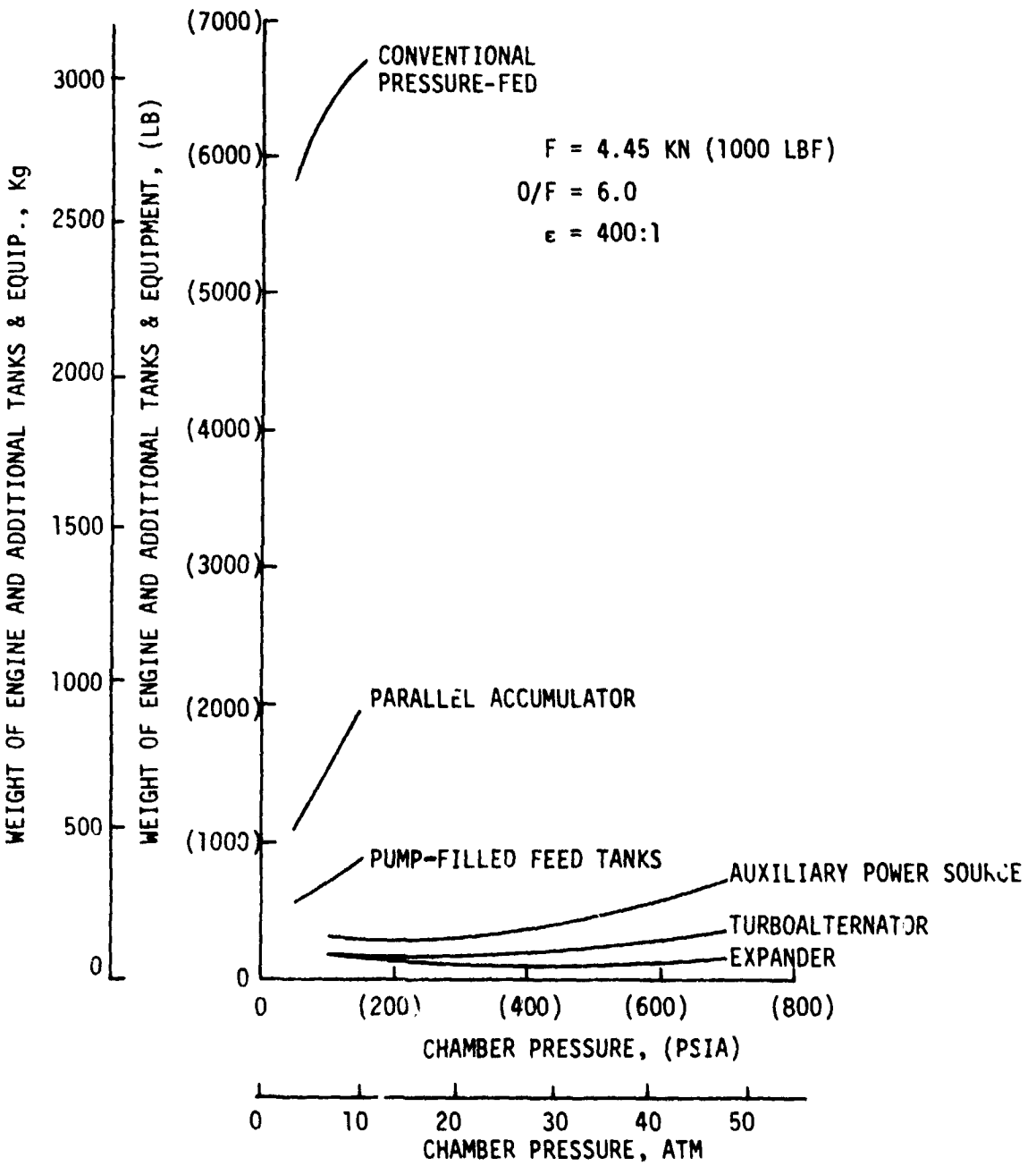

Figure 43. O_2/H_2 Regen-Cooled Engine Concept Propulsion System Relative Weight Comparisons

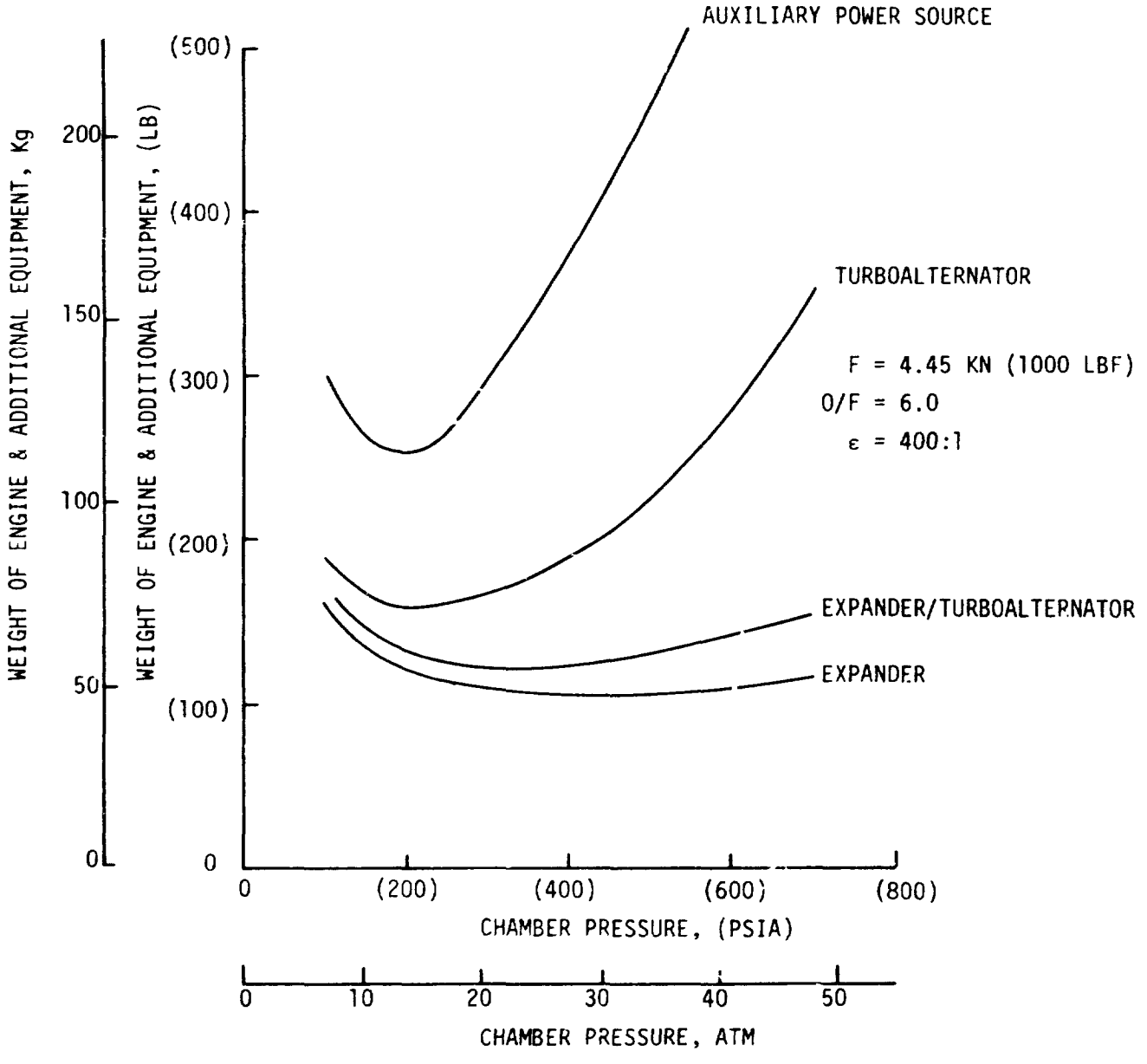

Figure 44. O_2/H_2 Regen-Cooled, Pump-Fed Engine Concept Weight Comparisons

V, D, Conceptual Analysis Conclusions and Recommendations (cont.)

- Highest Performance
- Lowest Thrust and Highest Pc Capability
- Lightweight Expander or Turboalternator Cycle Feasibility
- Small Engine Envelope

A comparison of regen-cooled engine data at the same thrust level (4.45 KN (1000 lbF)) shows:

Propellant Combination	Design Chamber Pressure atm (psia)	Delivered Is, sec	Engine Length, cm (in.)	Weight kg (lb)
O_2/RP-1	10.2(150)(1)	335	218(86)	77.1(170)(3)
O_2/CH_4	27.2(400)(2)	369	132(52)	43.1(95)(4)
O_2/H_2	34(500)(2)	465	122(48)	(41.7)(92)(4)

(1) Based upon cooling limit
(2) Based upon power balance considerations
(3) Auxiliary power source
(4) Expander cycle

Based upon the cooling and conceptual analyses results, an O_2/H_2 pump-fed, regeneratively cooled engine was recommended and approved by NASA/LeRC for preliminary design.

SECTION VI

ENGINE SYSTEM PRELIMINARY DESIGN

A. OBJECTIVES AND GUIDELINES

The objectives of this part of the study were to provide preliminary design information on one engine concept and to update the parametric performance, weight, and envelope data on the basis of the preliminary design evaluations.

The engine design point was selected on the basis of the obtained thrust chamber cooling data and engine system conceptual design and parametric analyses results. The design point selected is shown in Table XII. The thrust level was selected in concert with NASA/LeRC. It is on the low side of the system study recommendations, but does provide a reasonable point of departure for future technological optimization. The chamber pressure was selected on the basis of obtained cooling and power balance results and allows for some design margin.

The engine requirements as defined by the statement of work (SOW) are listed below:

- Propellant Inlet Temperature °K (°R)
  - Hydrogen Pump 21 (37.8)
  - Oxygen Pump 90.4 (162.7)
- NPSH at Engine Inlet, m (ft)
  - Hydrogen 4.57 (15.0)
  - Oxygen 0.61 (2.0)
- Service Life 5 thermal cycles (times safeyy factory of 4) and 11 hrs accumulated run time (derived from Figure 9)
- Gimbal Angle (Square Pattern), degrees ± 7

The preliminary design parameters include:

- Engine assembly and system layout drawings.
- Engine assembly weight and center of gravity.

TABLE XII.- ENGINE DESIGN POINT

° Propellant Combination	O_2/H_2
° Engine Vacuum Thrust, N (LB)	2224 (500)
° Thrust Chamber Pressure, atm (psia)	34 (500)
° Engine Mixture Ratio	6.0
° Nozzle Area Ratio	400:1
° Thrust Chamber Coolant	H_2
° Cooling Method	Regen
° Engine Cycle	Mixed Expander & Turboalternator

- Engine performance and power balance data at design thrust and design MR, as well as at ±10% design MR.
- Description of engine operation and control.
- Thrust chamber, injector, and nozzle layout drawings.
- External views of turbopumps and valves.
- Design and off-design analyses of pumps and drives.

The parametric data were updated for the selected engine concept as a function of thrust and chamber pressure over a nozzle expansion area ratio range from 200 to 1000:1.

B. ENGINE SYSTEM DESIGN

1. Engine System Description

The engine cycle selected for preliminary design is a pump-fed mixed expander and turboalternator cycle. The expander/turboalternator concept is shown in Figure 45. This concept incorporates the best features of the expander and turboalternator cycles. The hydrogen turbopump is driven in the expander mode, and the oxidizer turbopump is driven in the turboalternator mode. This eliminates one large electric motor, thus reducing the size of the alternator required for the pure turboalternator cycle. Only the lower horsepower oxygen pump is driven by an electric motor. The advantage of the mixed expander/turboalternator cycle over an expander cycle is the elimination of a hot-gas bipropellant seal. A minor weight penalty for the alternator and electric motor is involved, but this weight penalty is insignificant when the total system weight is considered.

The hydrogen is pumped to the required discharge pressure for delivery to the thrust chamber. Series-redundant shutoff valves are shown downstream of the turbopumps to meet the safety and environmental criteria of the Orbiter payload bay (i.e., no propellant leakage into the payload bay). The hydrogen enters the thrust chamber coolant jacket at an area ratio of 23:1 and flows forward through the slotted copper chamber to the injector head end. Eighty percent of the hydrogen flow is used to drive the LH_2 TPA turbine and alternator assembly. The remaining heated hydrogen bypasses the turbine assembly and provides the cycle power balance margin and engine thrust control. The large bypass flow was selected because of the uncertainty of meeting component nominal performance values (i.e., efficiencies, pressure drops, and coolant temperature rises) at these low-thrust levels.

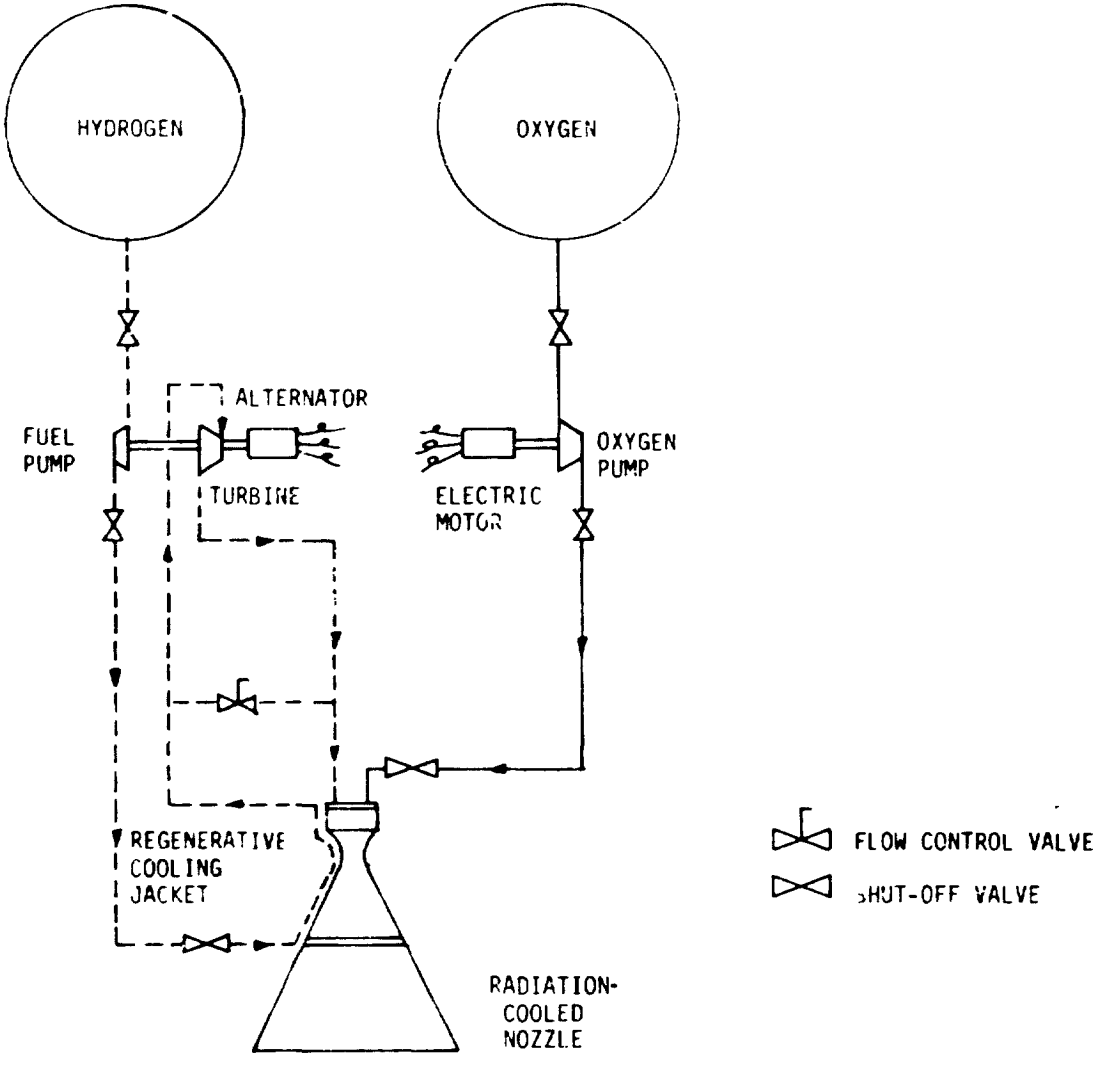

Figure 45. Baseline Mixed Expander and Turboalternator Cycle

The oxygen is pumped to its required discharge pressure and delivered directly to the thrust chamber injector in the liquid state to be mixed and burned with the gaseous hydrogen.

The nozzle is radiation-cooled from an area ratio of 23:1 to the exit (ϵ = 400:1). FS-85 columbium with a silicide coating was preliminarily selected as the nozzle extension material because of its high temperature capability. ALRC has obtained considerable experience in the design and manufacturing of radiation-cooled nozzles on the Transtage, Apollo, and OMS engine programs.

The cooling circuit scheme described has been selected because of its simplicity. The regeneratively cooled section has only one inlet manifold and one outlet manifold. Regeneratively cooling a tube bundle nozzle from an area ratio of 23:1 to 200:1 would increase the hydrogen temperature slightly and help the cycle power balance. However, it would increase the mechanical design complexity and add tube bundle inlet and outlet manifolds.

The engine assembly layout is shown in Figures 46 and 47. The engine features side-mounted pump and drive systems which are located in opposite quadrants. The series-redundant shut-off valves are mounted inline and approximately 45° away from the pumps. The engine controller is also side-mounted on the engine. The controller requirements (i.e., size, power, weight) were estimated to be one third of those required for a 66.7 KN (15,000 lb) thrust OTV engine (described in Reference 30). The low-thrust engine controller requirements are estimated as follows:

CONTROLLER REQUIREMENTS

Weight, Kg (lb)	5.44 (12)
Power, watts	96
Volume, m^3 ($in.^3$)	7.34×10^{-3} (448)

The above estimate does not include the power supply. With the power supply, the weight would approximately double.

The engine is 101.6 cm (40 in.) long and has a 40.6 cm (16 in.) nozzle exit diameter. To accommodate a $\pm 7°$ gimbal requirement, the diameter is 65.5 cm (25.8 in.).

The engine center of gravity in the axial direction was calculated to be 30 cm (11.8 in.) from the gimbal center. Referring to Figure 47, the center of gravity location in the Y and Z axes is +2.21 cm (0.87 in.) and +2.29 (0.90 in.), respectively.

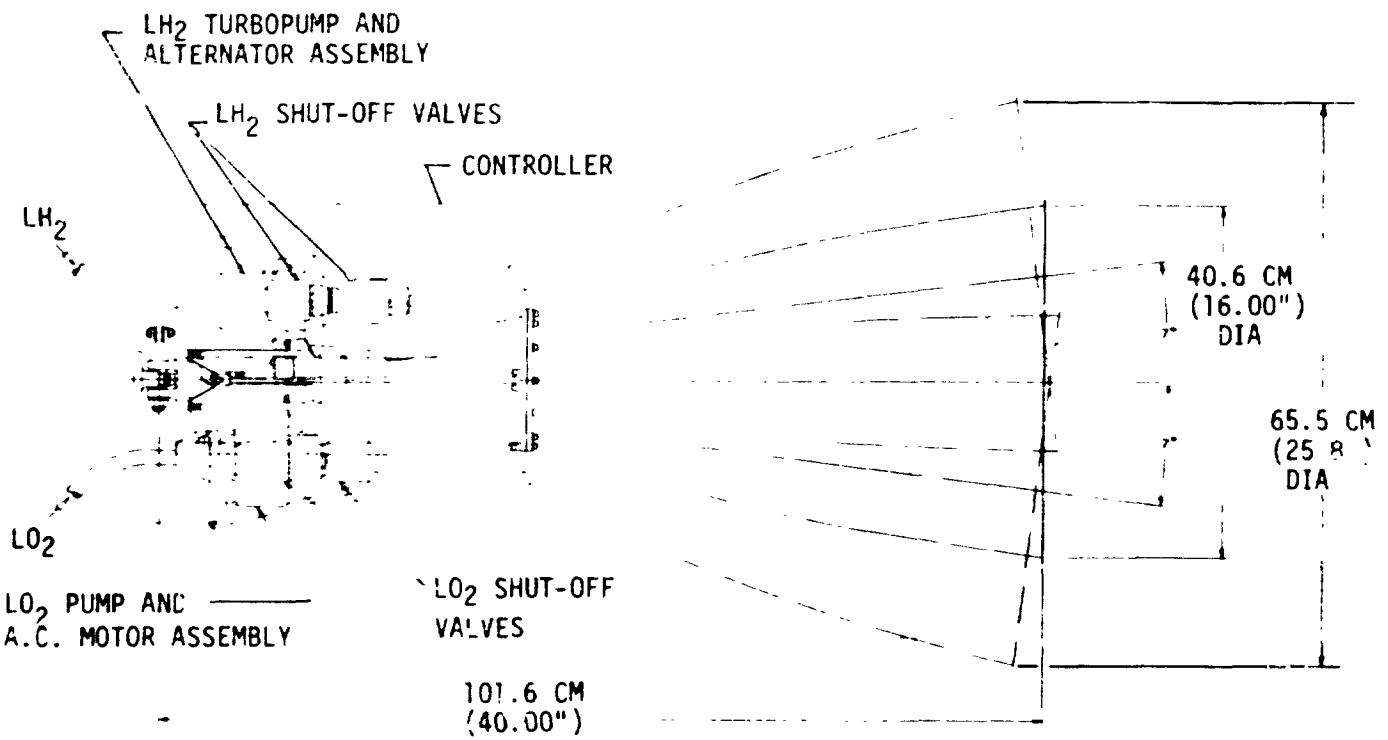

Figure 46. Engine Assembly Layout Drawing (Side View)

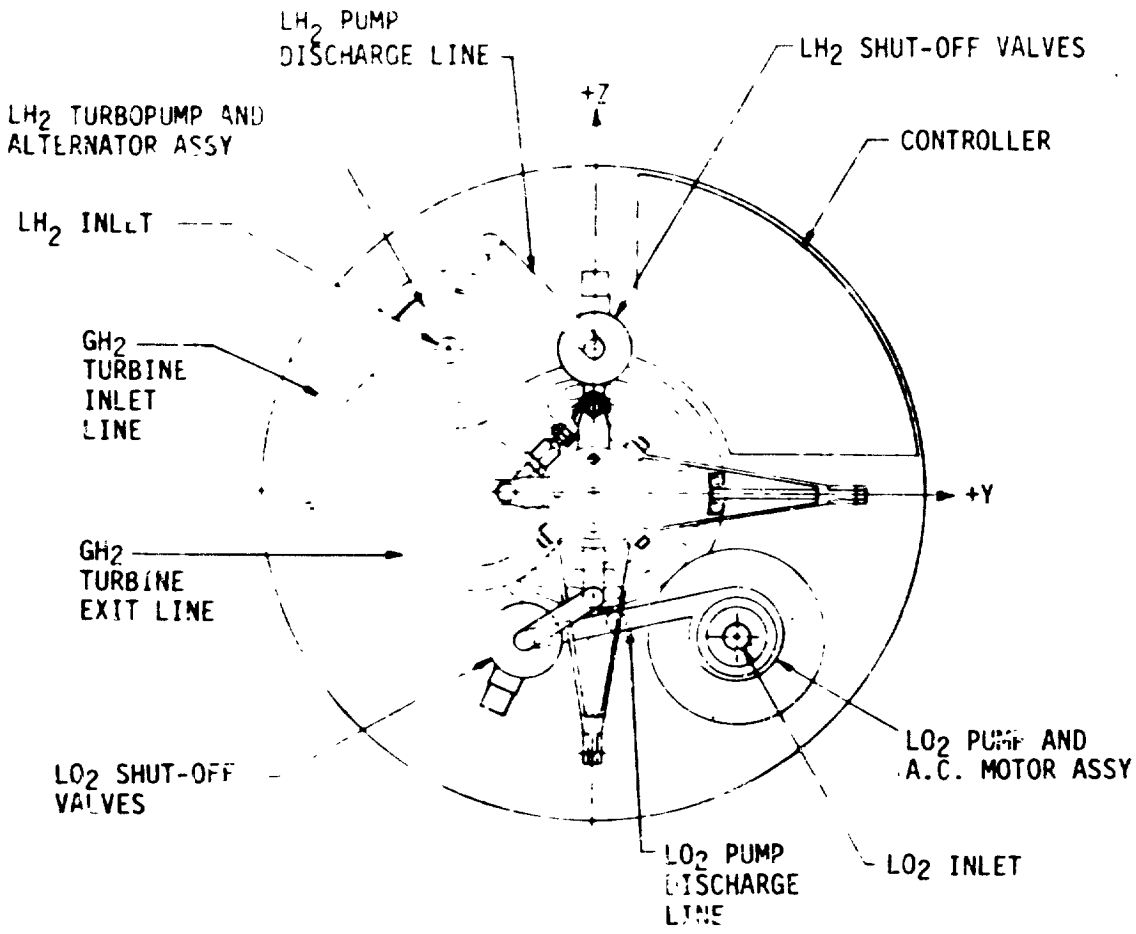

Figure 47. Engine Assembly Layout Drawing (Top View)

A typical engine/vehicle installation drawing is shown in Figure 48. The propellant tank configurations and location of the engine gimbal point were provided by NASA/LeRC for use in determining propellant line lengths and pressure drops from the tank outlets to the engine inlets. The engine inlet lines are only required to be 1.59 cm (5/8 in.) to provide the engine flows. Therefore, these small lines can be flexible. The bends shown in the lines provide for flexibility during engine gimballing.

2. Nominal Operating Point

The baseline engine performance, weight and envelope data resulting from the preliminary design activities are shown in Figure 49. These data were used to update the engine system parametric and power balance model. Typical outputs of the engine model are shown in Tables XIII, XIV, and XV. The outputs shown are the outcome of an iteration to incorporate modifications in component weights, efficiencies, etc., that have resulted from the preliminary design. Therefore, values used to initiate the preliminary design may not be consistent. For example, a hydrogen pump discharge pressure requirement of 64.6 atm (950 psia) was initially estimated, whereas the final iteration shows a fuel pump discharge pressure of 62.6 atm (921 psia).

The engine performance was calculated by using the "JANNAF simplified performance prediction methodology." The original JANNAF procedures were defined in 1968 and were limited in scope to thrust chamber performance and an empirically based method for determining the energy release performance loss. Subsequent work by JANNAF has led to less restrictive procedures and an expanded analytical approach. These updated procedures are defined in CPIA publications 245 and 246 (References 31 and 32 respectively). CPIA 245 contains the specifications for performance test data acquisition and interpretation. CPIA 246 contains the specifications for liquid rocket engine performance prediction and evaluation.

Since the standard procedure is relatively costly in terms of both engineering hours and computer time, there is a great incentive to use simpler, more economical procedures to perform parametric and point design analyses. Such techniques have been developed and are included in the JANNAF procedures (Reference 32).

As described in CPIA 246, the simplified procedure is "less accurate but quicker and less expensive than the "rigorous" method and is thus appropriate for the prelimianry design type analysis required for the baseline engine definition and generation of engine parametric performance data. The accuracy of the simplified procedure can be made nearly equivalent to that of the more rigorous procedure, provided the proper performance efficiencies are defined and shortcut calculational methods or correlations are calibrated or anchored over the parametric range under consideration.

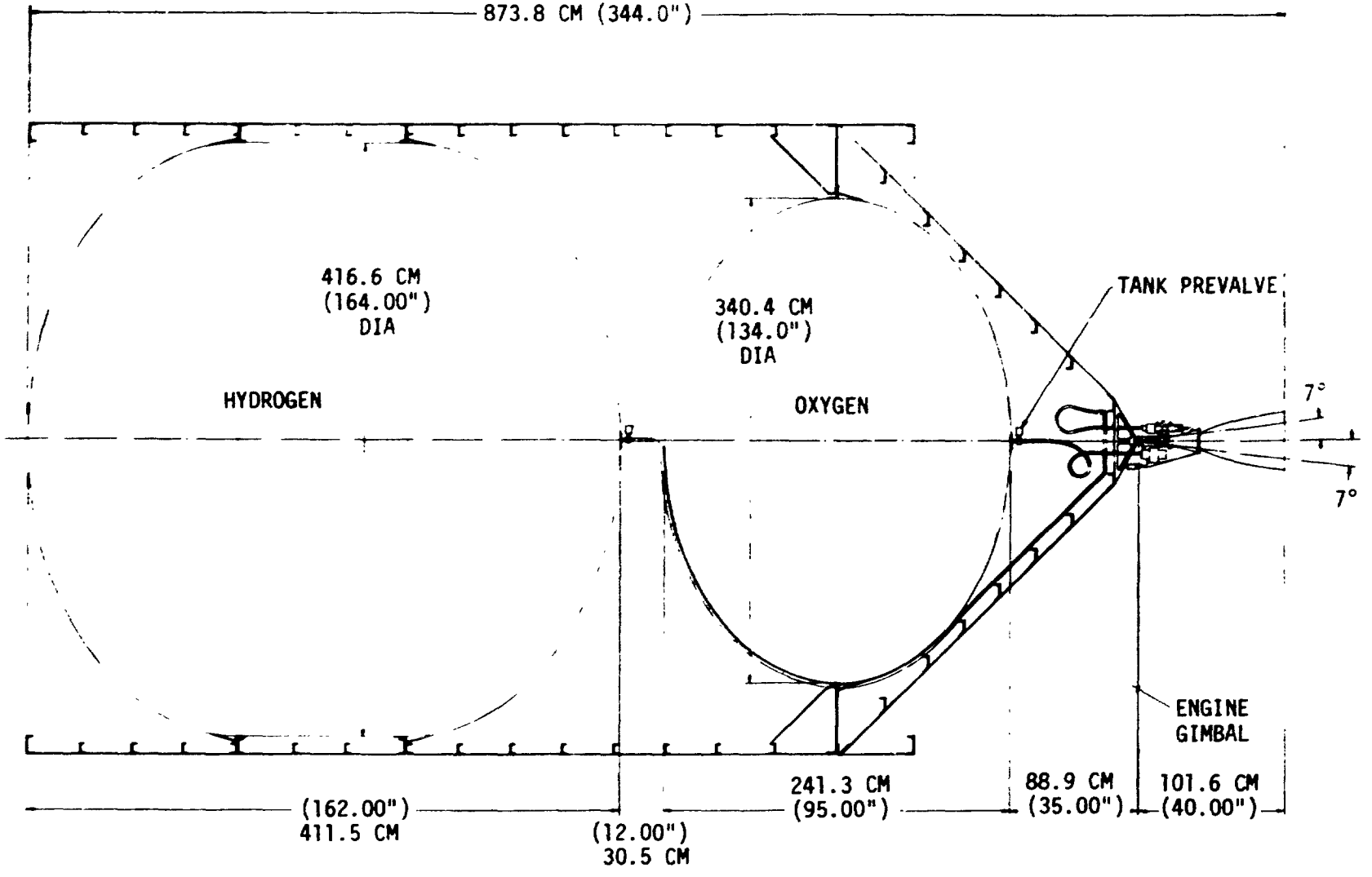

Figure 48. Engine/Vehicle Installation Drawing

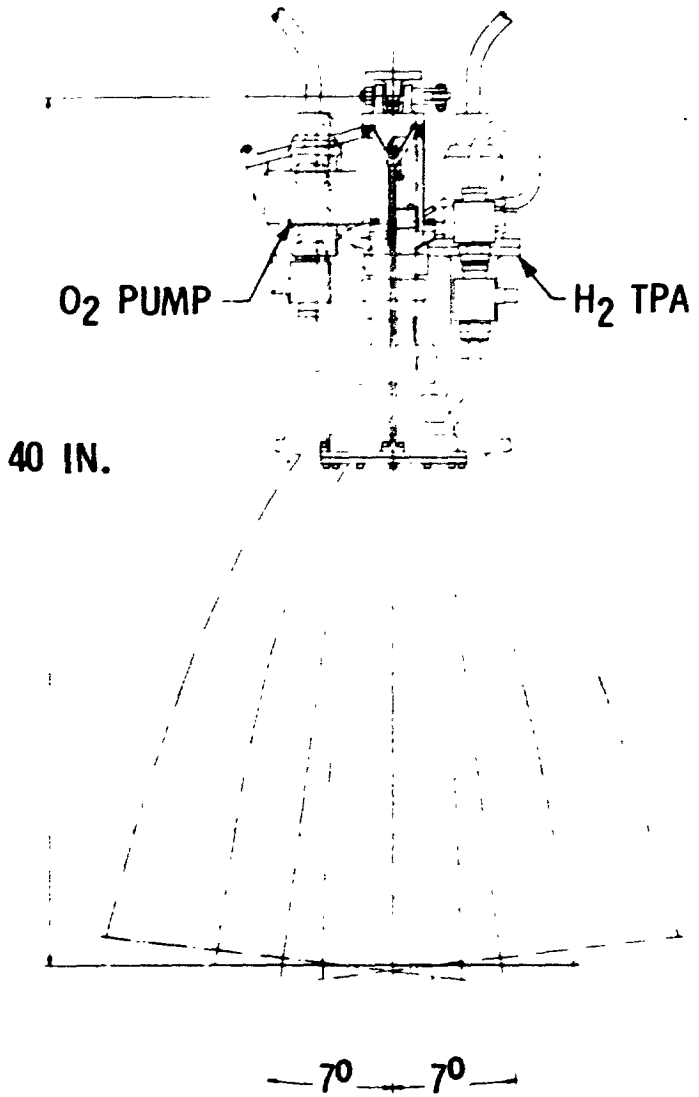

PROPELLANTS	O_2/H_2
VAC. THRUST, N (LB)	2224 (500)
CHAMBER PRESSURE, ATM (PSIA)	34 (500)
ENGINE O/F	6.0
NOZZLE AREA RATIO	400:1
COOLING METHOD	REGEN
COOLANT	H_2
VAC. DELIVERED I_s, SEC	465
ENGINE WEIGHT, kg (LB)	38.8 (85.4)
ENGINE LENGTH, Cm (IN.)	101.6 (40)
STATIC NOZZLE EXIT DIA.,Cm(IN.)	40.6 (16)

Figure 49. Engine Preliminary Design Summary

TABLE XIII. - LOW-THRUST ENGINE MODEL BASELINE PERFORMANCE,

WEIGHT, AND ENVELOPE DATA

(S.I. Units)

PERFORMANCE	
1.THRUST(NEWTONS)	2224.
2.PC(N/M2)	34.0
3.AREA RATIO	400.0
4.ISP-OPT(SEC)	464.8
5.ENERGY REL. EFF.	.994
6.KINETIC EFF.	.987
7.DIVERGENCE EFF.	.996
8.FILM COOL LOSS(SEC)	.0
9.RAD LOSS(SEC)	40.1
10.ISP-DEL(SEC)	465.2
11.TOTAL FLOW(KG/SEC)	.49
12.OX FLOW(KG/SEC)	.42
13.FUEL FLO (KG/SEC)	.07
14.FILM COOL FLOW(KG/SEC)	.00
15.PRESSURE RATIO	6.0

ENVELOPE(METERS)	
IGNITER	.2
INJECTOR	.1
CHAMBER	.2
NOZZLE	.6
TOTAL LENGTH	1.0
EXIT DIAMETER	.4
THROAT RADIUS	.01
CHAMBER CONTR	3.3
AREA RATIO	400.0
PERCENT BELL NOZZLE	80.0
ATTACH RATIO	23.0

WEIGHT BREAKDOWN(KG)

1.HIGH PRESSURE LINES	.5
2.VALVES AND ACTUATORS	5.5
3.INJECTOR	1.0
4.CHAMBER	1.9
5.RAD. COOLED NOZZLE	2.8
6.IGNITER	1.7
7.REGEN COOLED NOZZLE	2.3
8.SEAL AND ACTUATOR SYS	1.8
9.ENGINE CONTROLLER	5.4
10.MISCELLANEOUS	12.6
11.LOW PRESSURE LINES	.6
12.FUEL PUMP	1.7
13.OX PUMP	.7
14.TURBINE ASSEMBLY	1.0
15.A.C. MOTOR	4.1
16.ALTERNATOR	2.0
17.PULSATION DAMPING SYS.	.0
18.TOTAL ENGINE WEIGHT	36.8

TABLE XIII. - LOW-THRUST ENGINE MODEL BASELINE PERFORMANCE, WEIGHT, AND ENVELOPE DATA (cont)

(English Units)

PERFORMANCE	
1.THRUST(LBF)	500.0
2.PC(PSIA)	500.0
3.AREA RATIO	400.0
4.ISP-ODF(SECONDS)	484.9
5.ENERGY REL. EFF.	.994
6.KINETIC EFF.	.987
7.DIVERGENCE EFF.	.996
8.FILM COOL LOSS(SEC)	.0
9.BL LOSS(LBF)	9.0
10.ISP-DEL(SEC)	465.2
11.TOTAL FLOW(LB/SEC)	1.07
12.OX FLOW(LB/SEC)	.92
13.FUEL FLOW(LB/SEC)	.15
14.FILM COOL FLOW(LB/SEC)	.00
15.MIXTURE RATIO	6.0

ENVELOPE(INCHES)	
IGNITER LENGTH	6.0
INJECTOR LENGTH	2.5
CHAMBER LENGTH	6.0
NOZZLE LENGTH	25.5
TOTAL LENGTH	40.0
EXIT DIAMETER	16.0
THROAT RADIUS	.40
CHAMBER CONTR	3.3
AREA RATIO	400.0
PERCENT BELL NOZZLE	90.0
ATTACH RATIO	23.0

COMPONENT WEIGHT BREAKDOWN(LBM)

1.HIGH PRESSURE LINES	1.1
2.VALVES AND ACTUATORS	12.2
3.INJECTOR	2.3
4.CHAMBER	4.1
5.RAD. COOLED NOZZLE	6.1
6.IGNITER	3.8
7.REGEN COOLED NOZZLE	5.2
8.GIMBAL AND ACTUATOR SYS	3.9
9.ENGINE CONTROLLER	12.0
10.MISCELLANEOUS	12.6
11.LOW PRESSURE LINES	1.3
12.FUEL PUMP	3.8
13.OX PUMP	1.5
14.TURBINE ASSEMBLY	2.3
15.A.C. MOTOR	8.9
16.ALTERNATOR	4.3
17.PULSATION DAMPING SYS.	.0
18.TOTAL ENGINE WEIGHT	85.4

TABLE XIV. - LOW-THRUST ENGINE MODEL BASELINE CYCLE

POWER BALANCE DATA

(S.I. Units)

	FLOWRATES (KGM/SEC) TEMP DROP (DEGREES K) CP(JOULES/KG-K) (FC=FUEL CIRCUIT) (OC=OX CIRCUIT) (T-S=TOTAL TO STATIC TEMP) (T=TOTAL TEMP)
1.TURBINE FLOW	.06
2.TURB INLET T(T)	355.56
3.TURB TEMP DROP(T-S)	33.71
4.TURB EXIT T(T)	284.66
5.FUEL MOT REGD POWER	.07
6.OX MOT REGD POWER	3.94
7.GENERATOR REGD POWER	4.38
8.DRIVE GAS GAMMA	1.336
9.DRIVE GAS CP	15181.316

	POWERS (KW) AND EFFICIENCIES (FC=FUEL CIRCUIT) (OC=OX CIRCUIT) (T-S=TOTAL TO STATIC TEMP) (T=TOTAL TEMP)
1.TURB POWER	17.69
2.FUEL PUMP POWER	13.30
3.OX PUMP POWER	3.16
4.TURB EFF	.620
5.FUEL MOT EFF	.900
6.OX MOT EFF	.800
7.FUEL PUMP EFF	.460
8.OX PUMP EFF	.610
9.GENERATOR EFF	.900
10.TOTAL FUEL FLOW	.07
11.TOTAL OX FLOW	.42
12.TURB BYPASS FLOW	.01

TABLE XIV. - LOW-THRUST ENGINE MODEL BASELINE CYCLE

POWER BALANCE DATA (cont)

(English Units)

	FLOWRATES (LBM/SEC) TEMP DROP (DEGREES R) CP(BTU/LB-R) (FC=FUEL CIRCUIT) (OC=OX CIRCUIT) (T-S=TOTAL TO STATIC TEMP) (T=TOTAL TEMP)
1.TURBINE FLOW	.12
2.TURB INLET T(T)	550.00
3.TURB TEMP DROP(T-S)	60.68
4.TURB EXIT T(T)	512.38
5.FUEL MOT REQD HP	0
6.OX MOT REQD HP	5.29
7.GENERATOR REQD SHP	5.88
8.DRIVE GAS GAMMA	1.395
9.DRIVE GAS CP	3.629

	HORSEPOWERS AND EFFICIENCIES (FC=FUEL CIRCUIT) (OC=OX CIRCUIT) (T-S=TOTAL TO STATIC TEMP) (T=TOTAL TEMP)
1.TURB HORSEPOW	23.72
2.FUEL PUMP SHP	17.84
3.OX PUMP SHP	4.24
4.TURB EFF	.620
5.FUEL MOT EFF	1.000
6.OX MOT EFF	.800
7.FUEL PUMP EFF	.460
8.OX PUMP EFF	.500
9.GENERATOR EFF	.900
10.TOTAL FUEL FLOW	.15
11.TOTAL OX FLOW	.92
12.TURB BYPASS FLOW	.03

TABLE XV. - LOW-THRUST ENGINE MODEL

BASELINE PRESSURE SCHEDULE

(S.I. Units)

	PRESSURE SCHEDULE (ATMS)	
	FUEL CIRCUIT	LOX CIRCUIT
1.TANK PRESSURE	1.77	1.57
2.LINE PRESSURE DROP	.20	.20
3.PREVALVE INLET	1.57	1.36
4.PREVALVE PRESSURE DROP	.07	.07
5.PREVALVE OUTLET	1.50	1.29
6.LINE PRESSURE DROP	.20	.20
7.PUMP INLET	1.29	1.09
8.PUMP PRESSURE RISE	61.[illegible]	42.56
9.PUMP DISCHARGE	62.69	43.65
10.LINE PRESSURE DROP	.68	.68
11.SHUTOFF VALVE INLET	62.01	42.97
12.VALVE PRESSURE DROP	.62	.43
13.CHECK VALVE INLET	61.39	42.54
14.CHECK VALVE PRESSURE DROP	.00	.00
15.CHECK VALVE OUTLET	61.39	42.54
16.LINE PRESSURE DROP	.34	.34
17.PULSATION DAMPER INLET	61.05	42.20
18.PULSATION DAMPER PRESSURE DROP	.00	.00
19.PULSATION DAMPER OUTLET	61.05	42.20
20.LINE PRESSURE DROP	.34	.34
21.ENGINE SHUTOFF VALVE INLET PRESSURE	60.71	41.86
22.SHUTOFF VALVE PRESSURE DROP	.61	.42
23.ENGINE SHUTOFF VALVE OUTLET PRESSURE	61.10	41.44
24.LINE PRESSURE DROP	.68	--
25.COOLANT JACKET INLET	59.42	--
26.COOLANT JACKET PRESSURE DROP	1.84	--
27.COOLANT JACKET OUTLET	57.58	--
28.LINE PRESSURE DROP	.68	.68
29.TURBINE INLET	56.90	--
30.TURBINE PRESSURE RATIO(PIN/POUT)	1.511	--
31.TURBINE OUTLET	37.66	--
32.TURBINE OUTLET,TOTAL	39.62	--
33.LINE PRESSURE DROP	.97	--
34.TCA INJECTOR INLET	37.66	40.76
35.TCA INJECTOR PRESSURE DROP	3.01	6.11
36.TCA INJECTOR FACE	34.64	34.64
37.TCA PRESSURE DROP	.62	.62
38.CHAMBER PRESSURE	34.02	34.02

TABLE XV. - LOW-THRUST ENGINE MODEL

BASELINE PRESSURE SCHEDULE (cont)

(English Units)

	PRESSURE SCHEDULE (PSIA)	
	FUEL CIRCUIT	LOX CIRCUIT
1.TANK PRESSURE	26.00	23.00
2.LINE PRESSURE DROP	3.00	3.00
3.PREVALVE INLET	23.00	20.00
4.PREVALVE PRESSURE DROP	1.00	1.00
5.PREVALVE OUTLET	22.00	19.00
6.LINE PRESSURE DROP	3.00	3.00
7.PUMP INLET	19.00	16.00
8.PUMP PRESSURE RISE	902.19	625.42
9.PUMP DISCHARGE	921.19	641.42
10.LINE PRESSURE DROP	10.00	10.00
11.SHUTOFF VALVE INLET	911.19	631.42
12.VALVE PRESSURE DROP	9.11	6.31
13.CHECK VALVE INLET	902.08	625.10
14.CHECK VALVE PRESSURE DROP	.00	.00
15.CHECK VALVE OUTLET	902.08	625.10
16.LINE PRESSURE DROP	5.00	5.00
17.PULSATION DAMPER INLET	897.08	620.10
18.PULSATION DAMPER PRESSURE DROP	.00	.00
19.PULSATION DAMPER OUTLET	897.08	620.10
20.LINE PRESSURE DROP	5.00	5.00
21.ENGINE SHUTOFF VALVE INLET PRESSURE	892.08	615.10
22.SHUTOFF VALVE PRESSURE DROP	8.92	6.15
23.ENGINE SHUTOFF VALVE OUTLET PRESSURE	883.16	608.95
24.LINE PRESSURE DROP	10.00	--
25.COOLANT JACKET INLET	873.16	--
26.COOLANT JACKET PRESSURE DROP	27.00	--
27.COOLANT JACKET OUTLET	846.16	--
28.LINE PRESSURE DROP	10.00	10.00
29.TURBINE INLET	836.16	--
30.TURBINE PRESSURE RATIO(PIN/POUT)	1.511	--
31.TURBINE OUTLET	553.38	--
32.TURBINE OUTLET,TOTAL	567.57	--
33.LINE PRESSURE DROP	14.19	--
34.TCA INJECTOR INLET	553.38	598.95
35.TCA INJECTOR PRESSURE DROP	44.27	89.84
36.TCA INJECTOR FACE	509.11	509.11
37.TCA PRESSURE DROP	9.11	9.11
38.CHAMBER PRESSURE	500.00	500.00

An in-house analysis of the experimental performance results presented in References 33 and 34, with the JANNAF standard analysis techniques (Reference 32) was performed to qualify or anchor the analytical performance procedures when applied to high area ratio (190-400) hydrogen/oxygen rocket engines. This analysis is reported in Reference 30. These procedures, once qualified, were used to develop reasonable predictions of attainable specific impulse for the baseline low-thrust engine. The "calibrated" model predicts an attainable specific impulse of approximately 465.2 sec for the baseline low-thrust engine at nominal operating conditions.

A combustion chamber length of 15.2 cm (6.0 in.) was selected to meet the engine performance and power balance requirements while avoiding cooling limits. With this chamber length, the coolant jacket exit temperature and turbine inlet temperature is 305.6°K (550°R). A longer chamber could increase the turbine inlet temperature (considered beneficial for the power balance), but the coolant jacket pressure drop would also increase. A preliminary trade study was conducted to identify an optimum chamber length at the design point. The thermal data used to conduct the cycle power balances are shown in Figure 50. The fuel pump discharge pressure results from the power balance analysis are shown in Figure 51. The figure shows that the fuel pump discharge pressure could be reduced by approximately 3.4 atm (50 psia) if the thrust chamber length were increased. The short chamber meets the performance requirements and results in a design with more thermal margin, maintaining a lower coolant Mach number. The shorter (15.2 cm/ 6.0 in.) chamber has been baselined and represents a conservative design approach. This chamber length could be increased if other components failed to meet their predicted performance values. The chamber length should be optimized in more detailed engine design studies.

3. Off-Design Mixture Ratio Operation

The results of off-design mixture ratio cycle power balance and performance analysis for the baseline low-thrust engine are presented in Figures 52 and 53.

The two off-design mixture ratios assumed were 5.4 and 6.6, respectively, which represents a ±10% variation from the baseline mixture ratio of 6.0. The analysis assumed that thrust (2224 N/500 lbF) remained constant.

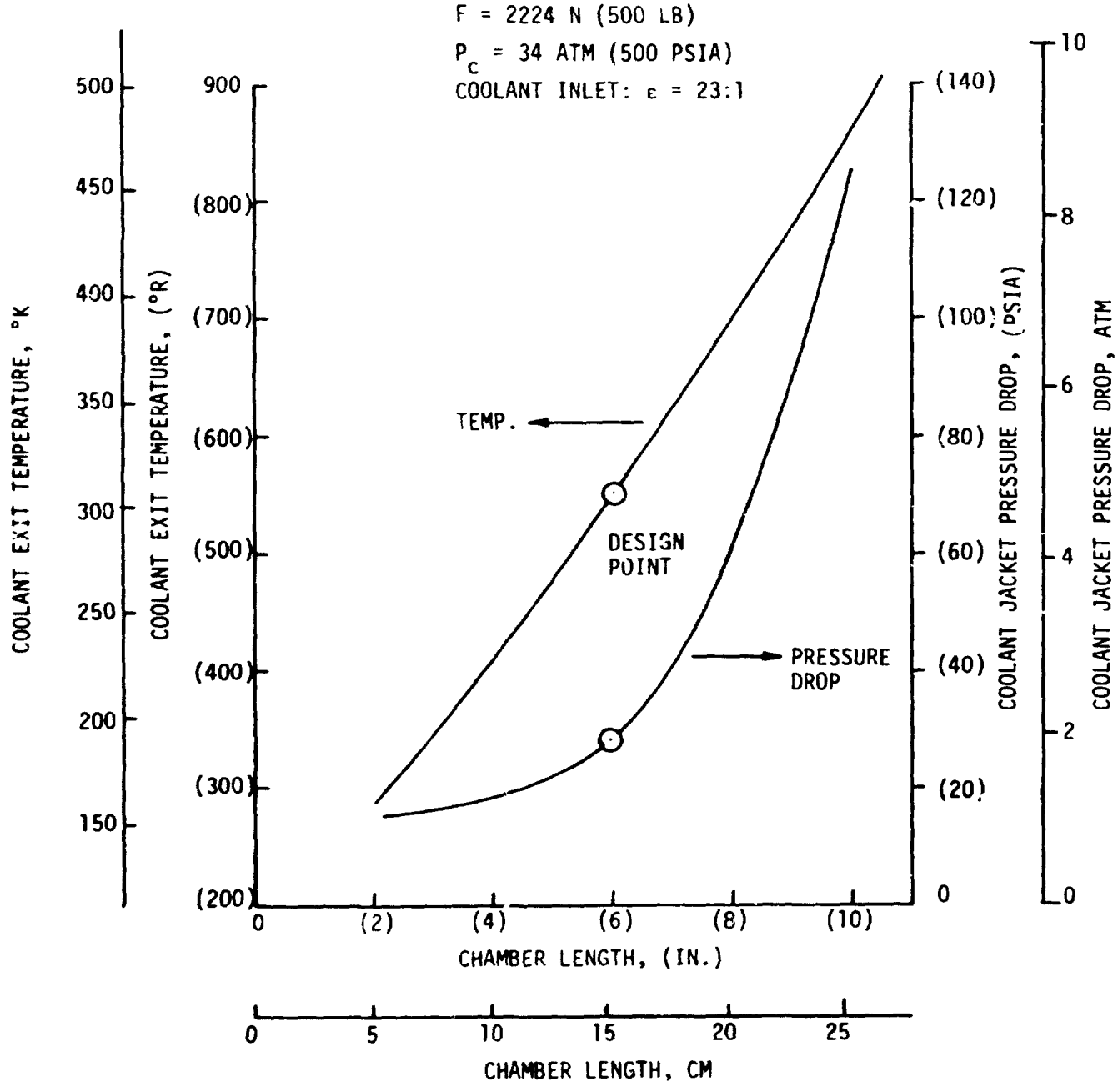

Figure 50. Chamber Coolant Exit Temperature and Pressure Drop vs Chamber Length

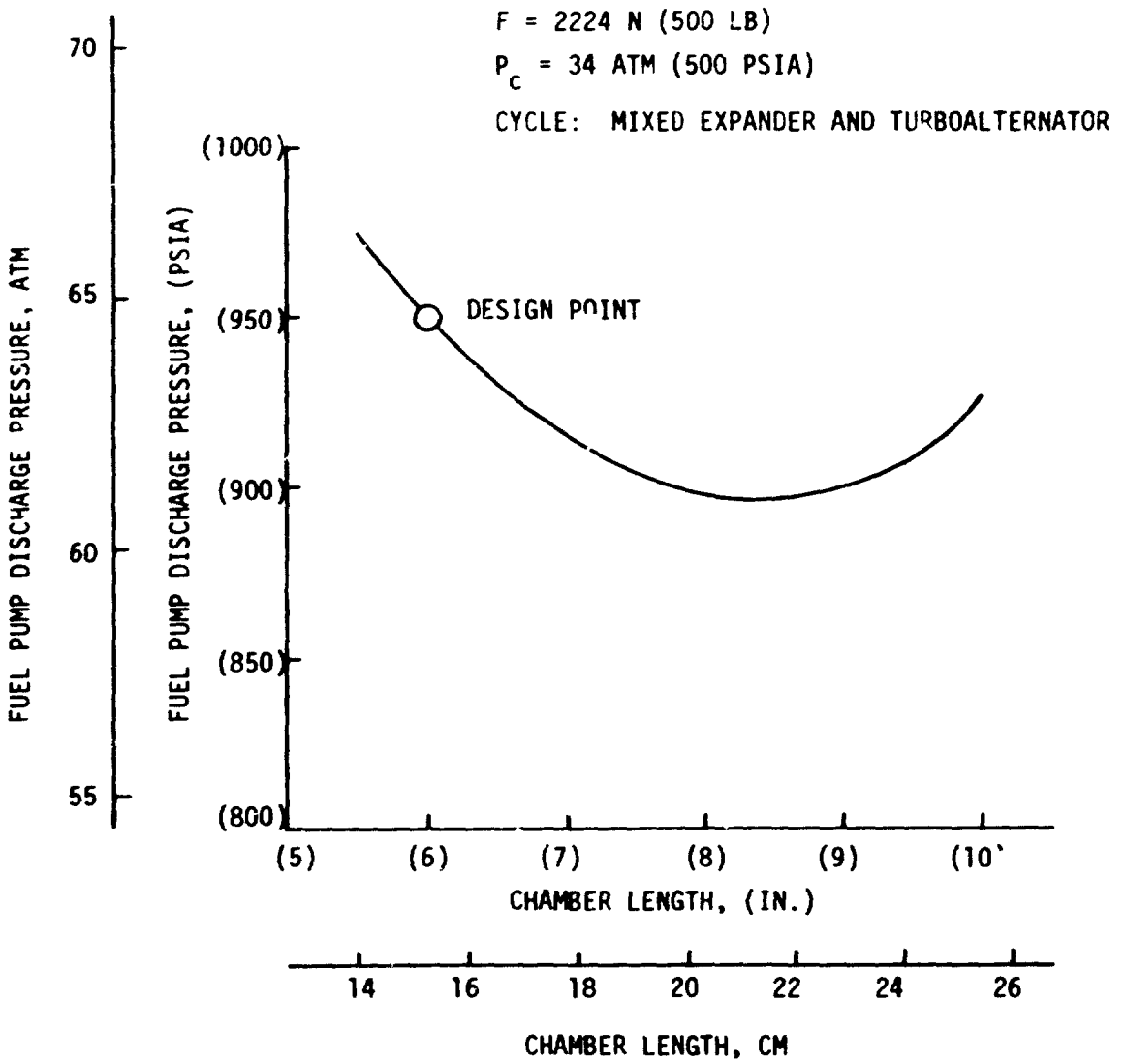

Figure 51. Hydrogen Pump Discharge Pressure Requirement vs Chamber Length

O_2/H_2 EXPANDER/TURBOALTERNATOR CYCLE

ϵ = 400, CHAMBER PRESSURE 34 ATM (500 PSIA), ENGINE THRUST = 2224 N (500 LB)

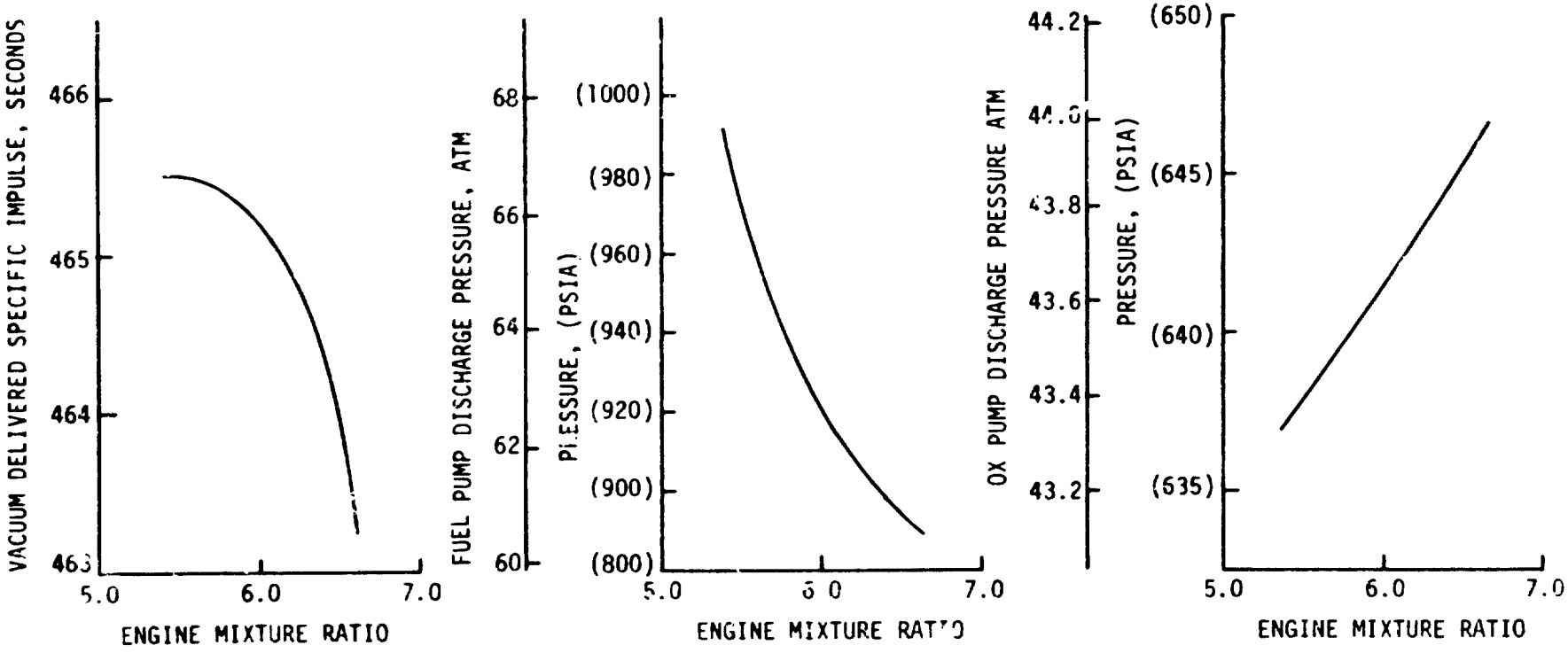

Figure 52. Engine Performance and Pump Discharge Pressure vs Engine Mixture Ratio

ε = 400, CHAMBER PRESSURE = 34 ATM (500 PSIA), ENGINE THRUST = 2224N (500 LB)

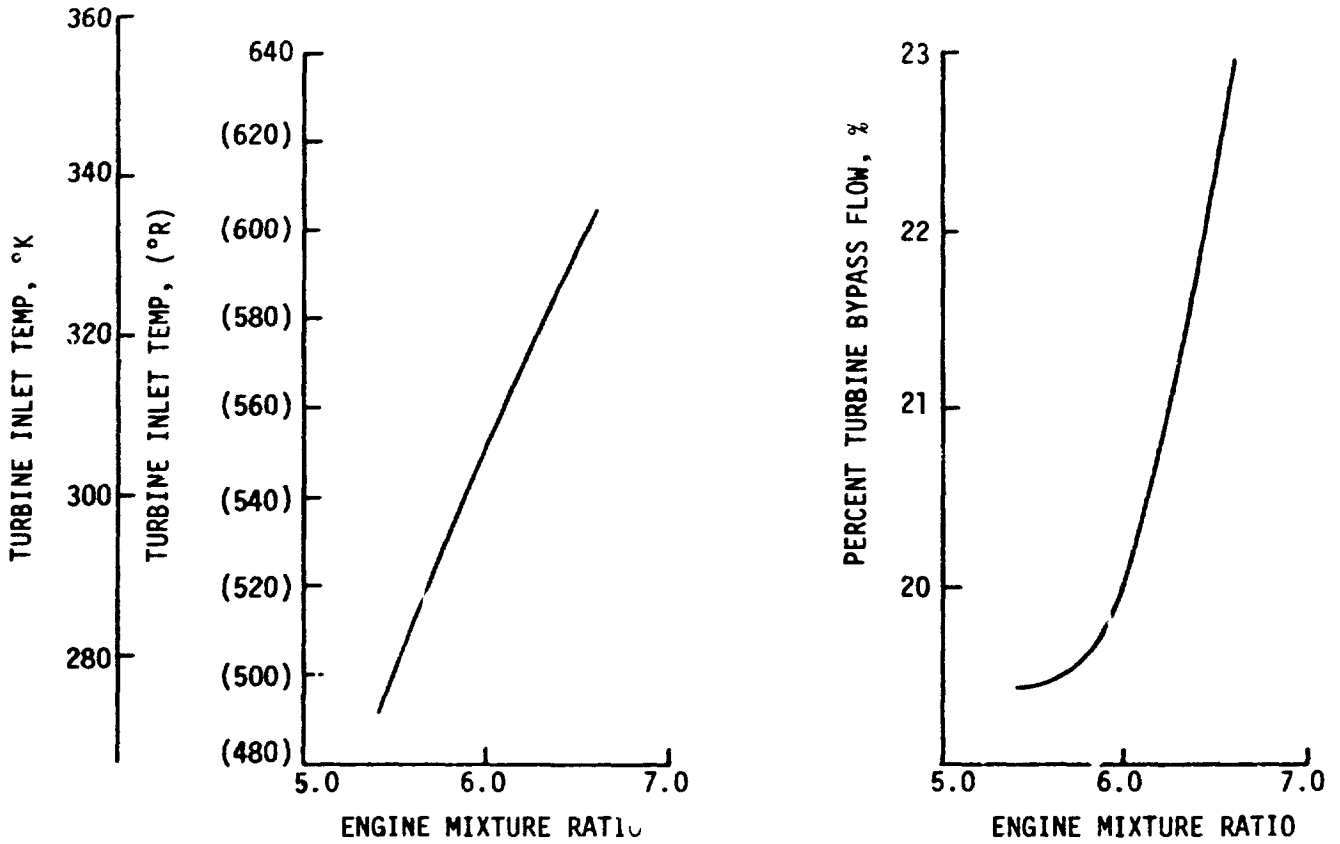

Figure 53. Turbine Inlet Temperature and Percent Turbine Bypass Flow vs Engine Mixture Ratio

The major effect of operating the baseline engine at a mixture ratio of 5.4 was a 32°K (58°R) drop in turbine inlet temperature. This temperature drop is due to the higher fuel coolant flow and the lower chamber combustion temperature. Although the fuel flow is higher, this lower turbine inlet temperature represents a less energetic turbine drive fluid. The higher fuel flow also results in higher pressure drops in the fuel circuit. This requires a higher fuel pump discharge pressure to yield the desired chamber pressure. The reverse of this condition exists in the oxidizer circuit (i.e., less flow) which results in a lower required oxidizer pump discharge pressure. The net result is increased total required pump horsepower at the lower operating mixture ratio. The potential turbine power deficiency is almost entirely compensated for by the increased turbine pressure ratio (due to increased flow through the turbine). The remaining turbine power deficiency is compensated for by decreasing the turbine bypass flow to 19.4% (i.e., increasing turbine flow from 80% to 80.6% of the total fuel flow). This further increase of flow through the turbine increases turbine pressure ratio and, hence, available turbine horsepower to match the required pump horsepower.

The major effects of operating the baseline engine at a mixture ratio of 6.6 are higher turbine inlet temperature and lower delivered specific impulse. The lower specific impulse causes a slightly higher total propellant flow rate, but the higher mixture ratio still results in a net decreased fuel flow and increased oxidizer flow over that of the baseline engine. The higher turbine inlet temperature is the result of this lower fuel flow and the higher chamber combustion temperature. In this case, then, there is less turbine drive fluid available, but the higher temperature represents a more energetic drive fluid. The lower fuel flow also results in reduced fuel circuit pressure drops, thus reducing the required fuel pump discharge pressure. The oxidizer pump discharge pressure on the other hand is higher because of the increased oxygen flow. Since the fuel pump always required proportionally more horsepower than the oxidized pump, the net effect is less total required pump horsepower. The combination of lower turbine pressure ratio and fuel flow and higher turbine inlet temperature and lower required pump horsepower results in a surplus of available turbine horsepower. This surplus power is eliminated by increasing the turbine bypass to 23% (i.e., reducing flow through the turbine to 77% of the total fuel flow).

C. COMPONENT DESIGN ANALYSIS

Layouts of the thrust chamber assembly, and the igniter, injector, and chamber were prepared. In addition, external views of the pumping systems and system valves were drawn to show dimensions and to assist in developing the engine layout.

VI, C, Component Design Analysis (cont.)

This section also contains a discussion of the engine operational sequence, along with the control system narrative.

1. Thrust Chamber Assembly

The overall thrust chamber assembly layout is shown in Figure 54. The engine is head-end gimballed and the gimbal is mounted above the igniter. The cylindrical thrust mount structure is machined from stainless steel and bolted to the injector on the outboard side.

A chamber structural throat support is required because of the thin-walled, small diameter throat and the unusually long chamber and nozzle. To meet this requirement, a conical support structure surrounds the entire chamber to provide a load path for gimbal, start transient, or vibration-induced loads from the nozzle. A secondary function of the conical support structure is to provide for a convenient means of attachment for the other engine components. The support structure is attached to the forward and aft Cres 304L manifolds by electron beam welding. Openings in the cone provide easy access to component attachment points, as well as lower system weight.

The nozzle is radiation-cooled from an area ratio of 23:1 to the exit (ε = 400:1) and bolted to the chamber aft manifold. FS-85 columbium with a silicide coating has been selected as the nozzle extension material because of its high temperature capability. This material has been used recently at ALRC for the OME radiation-cooled nozzle. Detailed design studies should assess the merits of C-103 columbium which is easier to weld although it does not have the temperature capability of FS-85.

2. Igniter, Injector, and Chamber Design

The integrated igniter/injector/chamber design layout is shown in Figure 55.

The injector is designed to accept an igniter which is similar to that used on the Integrated Thruster Assembly (Contract NAS 3-15850) and Extended Temperature Range Thruster Investigation (Contract NAS 3-16775) programs (References 20 and 35, respectively). The igniter incorporates a radial platelet injector which is also a laminate of 304L stainless steel platelets. Ignition occurs in an oxygen-rich core (MR 40) to ensure reliability. The igniter combustion chamber is made of nickel alloy and is slotted on its outer diameter to provide for regenerative cooling with hydrogen. At the converging section of the igniter nozzle, the oxygen-rich core and hydrogen coolant mix and react, entering the chamber at an overall mixture ratio of 6.0. The igniter nozzle is made of nickel alloy and electron-beam-welded to the injector body. Nickel alloy is also used for the spark electrode, and stainless steel is used for the electrode housing. The electrode and the ceramic insulator are sealed to the housing with flexible metal "O" rings, as this design represents a significant improvement over earlier ceramic seal designs.

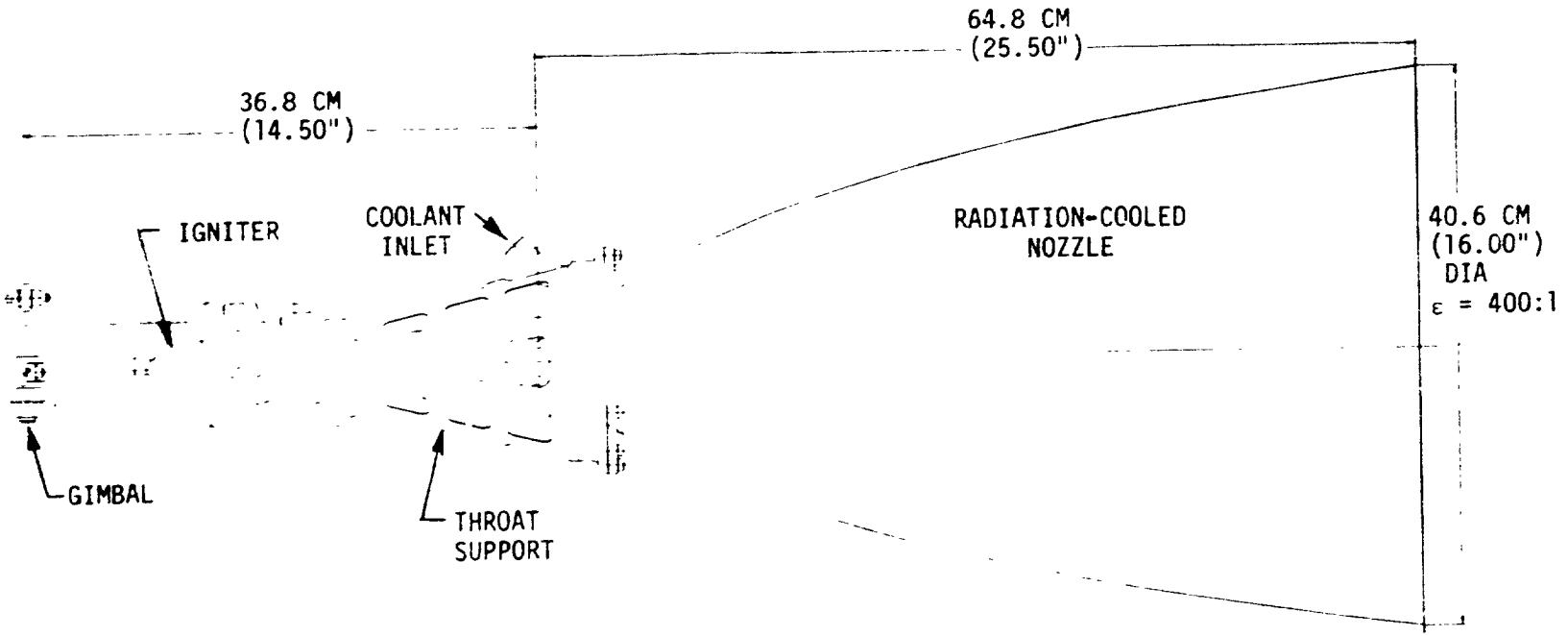

Figure 54. Thrust Chamber Assembly Drawing

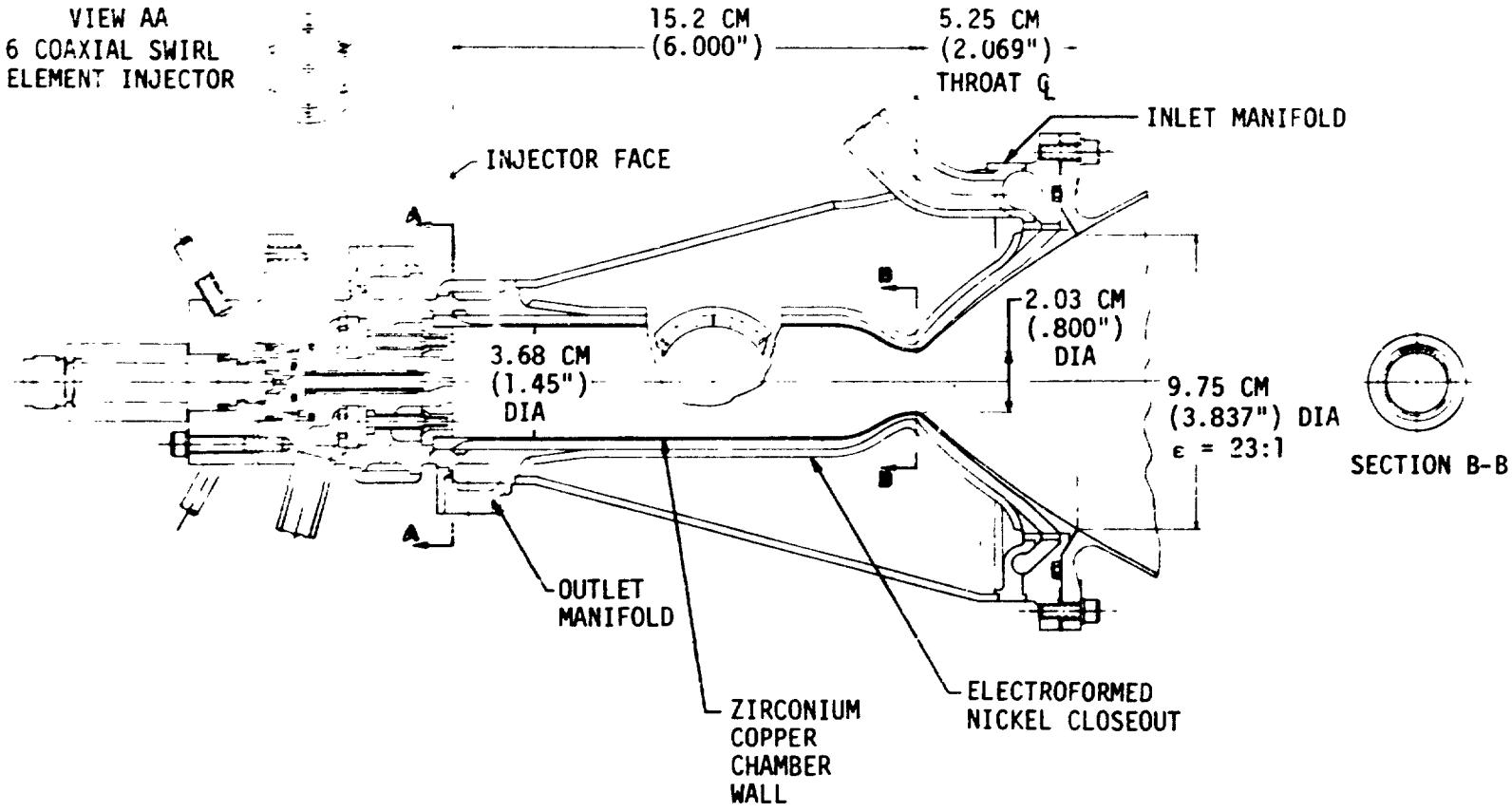

Figure 55. Igniter/Injector/Chamber Drawing

VI, C, Component Design Analysis (cont.)

The injector must satisfy two important criteria. To attain the required cycle life and power balance, the injector must maintain a cool running face and a controlled heat flux to the chamber wall. In addition, excellent vaporization and mixing efficiency are required to achieve the maximum energy release efficiency (ERE). The preliminary injector design shown in Figure 55 is intended to satisfy these requirements.

The injector design utilizes coaxial swirl elements as this type of element has an extensive operating history with GH_2/LO_2 propellants over a broad range of thrust and chamber pressures. As a result of the packaging constraint imposed by the small chamber diameter, there are only six coaxial elements; consequently, the igniter is designed to act as a seventh element. The mass flowrate is divided evenly among the coaxial elements and the igniter.

Combustion is expected to occur close to the injector face, because the hydrogen at 281.7°K (47°F) is injected as a gas and the LO_2 immediately flashes into a gas upon injection. If subsequent design analyses should indicate that injector face cooling is necessary to meet the required cycle life, a platelet stack could easily be incorporated into the face assembly to provide the necessary cooling. It is anticipated that regenerative cooling of the injector face, coupled with discrete fuel film cooling, would provide the most reliable method of ensuring face integrity. The regenerative cooling would be accomplished by the GH_2 flowing through photoetched passages within the platelet stack and in the annuli around the oxidizer tubes. Fuel film-cooling would occur through bleed orifices in the face. The extremely accurate photoetched flow control passages would assure uniform flow across the entire injector face. The platelet stack would be a laminate of 304L stainless steel which, in turn, would be brazed to a stainless steel strongback. Should better thermal properties be required, OFHC could be substituted with only the gas-side platelet being stainless steel.

It is anticipated that the injector face assembly does not have to be physically attached to the injector element oxidizer posts; therefore, the injector face plate is electron-beam-welded at its outer periphery and near the center of the injector body. If subsequent stress analysis should reveal the need for additional support, the face plate could be brazed to the oxidizer posts. The fuel manifold is formed when the injector face plate is welded to the injector body (which is also 304L stainless steel), since the manifold cavity is machined from the face-side of the body.

Uniform propellant mass distribution is necessary to prevent hot streaks from occurring on the chamber wall; consequently, the fuel inlet torus surrounding the injector body is designed for constant flow velocity to assure

uniform fuel distribution into the fuel manifold. Fuel is fed from the inlet torus to the manifold through six equally spaced feed holes located circumferentially in the injector body. The six feed holes are positioned midway between the six coaxial elements. The fuel manifold has sufficient size to provide uniform fuel distribution to the six coaxial elements.

Preliminary dimensions of the injection elements are as follows:

- Ox Tube ID = 0.213 cm (0.084 in.)
- Ox Tube OD/Fuel Annulus ID = 0.318 cm (0.125 in.)
- Fuel Annulus OD = 0.51 cm (0.20 in.)

The oxidizer torus is machined from the face-side of the injector/igniter interface. A metering plate with 24 equally spaced metering holes (12 holes each in 2 rows) is brazed to the injector/igniter interface to enclose the oxidizer torus. The resulting assembly is then electron-beam-welded at its center and at its periphery to the injector body, thereby forming the oxidizer manifold. The oxidizer manifold is fed from the metering plate, providing uniform mass distribution to the oxidizer swirl platelet stack which is located just upstream of the oxidizer tubes.

The oxidizer tubes, recessed approximately 0.178 cm (0.070 in.) from the face, are held concentrically within the fuel discharge orifice by four small tabs integral with the tubes. The tubes can either be integral with the injector body or brazed into the injector body, as both methods have been used in previous applications. Nickel tube tip inserts are brazed to the 304L oxidizer tubes, since nickel has a higher thermal conductivity, thus providing a high thermal margin at the tube tip. In addition, the nickel inserts will be free-floating on the chamber end to prevent thermal stress.

The LO_2 enters the injector oxidizer tubes tangentially, forming a hollow cone spray with a 30° half-angle as it exits from the tube into the surrounding GH_2. The tangential flow of the oxidizer is established by the swirl platelet stack brazed to the upstream side of the injector body. The stack is a laminate of 304L stainless steel platelets.

The injector assembly is electron-beam-welded to the chamber, with the igniter bolting to the injector at the injector/igniter interface.

The chamber, illustrated in Figure 55, is a milled-slot, single-pass design. The chamber contour is comprised of a 3.68 cm (1.45 in.) ID cylindrical section, 13 cm (5.10 in.) long, which converges at a 30° half-angle to a throat diameter of 2.03 cm (0.800 in.). From the throat, the contour diverges along a 90% bell nozzle profile to an area ratio of 23:1, located

5.25 cm (2.069 in.) below the throat. The hydrogen coolant enters the chamber at the 23:1 area ratio and flows toward the forward end along an axial distance of 20.5 cm (8.069 in.). Uniform coolant distribution is necessary within the chamber; therefore, the chamber inlet manifold is designed for constant flow velocity. The coolant collects in a manifold outboard of the cooling channels and exits radially into the chamber outlet manifold. The chamber contraction ratio of 3.3 is the same as that of the Integrated Thruster Design (ITA), Reference 20. It was selected on the basis of both the performance and heat transfer requirements discussed in Section IV,A of this report.

Zirconium copper was selected as the material for the gas-side wall because of the requirement for high conductivity and high strength throughout the cycle life. The inlet manifold flange and the outlet manifold at the aft and forward ends of the chamber, respectively, are made of Cres 304L. These manifolds are designed to be brazed directly to the slotted zirconium copper chamber. Both braze joints are on cylindrical surfaces to facilitate assembly and to assure sound braze joints. Cres 304L was selected for the manifolds primarily because of its excellent electron-beam-welding (EB) characteristics. All subsequent EB-welds are made to either of these two manifolds.

The thrust chamber contains 43 equally spaced coolant slots which are machined into the backside of the zirconium copper liner. To permit a cylindrical (rather than conical) braze joint at the aft end of the chamber, the first coolant slot of approximately 1.91 cm (0.75 in.) length is fabricated by the electrical discharge machining method. The coolant slots are closed out with electroformed copper and nickel. Initially, the slots are closed out with 0.0254 to 0.0508 cm (0.010 to 0.020 in.) thick copper. This copper layer prevents hydrogen embrittlement of the 0.28 to 0.305 cm (0.110 to 0.120 in.) thick structural nickel wall which is subsequently added. No welding or brazing to the electroformed nickel is required, thereby avoiding the possibility of blistering or cracking the electroformed nickel.

3. Rotating Machinery Design

Operating conditions for the turboalternator, fuel pump, electric motor, and oxidizer pump were determined for the mixed expander/turboalternator cycle engine. The operating conditions, within the assumed design limits, dictate a four-stage hydrogen pump and an alternator with a rated power of approximately 4.5 Kw (6 hp) both of which are driven by a single stage 13% partial-admission, axial-flow gas turbine. Acceptable component efficiencies are achievable at a limiting shaft speed of about 200,000 RPM. The oxidizer pump, driven by the electric motor, has two stages and also achieves practical efficiency levels at the minimum NPSH-maximum suction

specific speed limits established in the study. Baseline pump operating characteristics are shown in Table XVI, and the pump drive characteristics are shown in Table XVII. The electric power to drive the oxidizer pump is generated by an alternator that is powered by the fuel turbopump hydrogen gas turbine. The cycle and pump drive selections dictate fuel turbopump operation at some multiple of the oxidizer pump speed.

Maximum design speed for the oxidizer pump is 47,755 RPM. It is set by the maximum suction specific speed limit of 580.9 RPM $(m^3/sec)^{1/2}/m^{3/4}$ (30,000 RPM $GPM^{1/2}/ft^{3/4}$) with a minimum NPSH of 0.61 m (2 ft), and a thermodynamic suppression head (THH) of 1.22 m (4 ft). Maximum allowable design speed for the fuel turbopump-alternator is 200,000 RPM. This is set by the maximum rolling contact bearing DN value of 2×10^6 (mm x RPM) and the minimum bearing size of 10 mm. Suction specific speed is not limiting if the potential of the hydrogen thermodynamic suppression head is assumed at a temperature of 21°K (37.8°R). The design operating speed of 191,320 RPM is predicated on four times oxygen pump speed (plus slip differences) for the fuel turbopump-alternator assembly. The hydrogen pump speed was selected after evaluating its effect upon component efficiencies, sizes, number of pump stages, and alternator rotor stress and shaft bending critical speed. The operating speed selection results in high efficiencies and practical sizes while avoiding the bearing DN limit of 2×10^6 mm x RPM. The resulting operating conditions yield a fuel pump efficiency of approximately 46% and an oxidizer pump efficiency of 50%, as shown in Table XVI and Figure 56.

External views of the hydrogen turbopump and alternator assembly and the oxygen pump and AC motor assembly are shown in Figures 57 and 58, respectively. The hydrogen pump and turbine weigh 2.7 kg (6.1 lb), and the alternator weighs 2.0 kg (4.3 lb). The oxygen pump and AC motor assembly weighs 4.7 kg (10.4 lb).

Estimates for "off-design" head-capacity characteristics of the multistaged hydrogen and oxygen pumps are shown in Figures 59 and 60, respectively. Estimates for "off-design" pump-head loss due to cavitation as a function of suction specific speed is plotted on Figure 61. The slope of the curve is based upon empirical data. The assumed loss is based upon a 5% head loss at design maximum suction specific speed.

The turbine drive required a 1.472 pressure ratio at the maximum available hydrogen flowrates (0.14 lb/sec). Efficiency is estimated at 62% for a 13% partial-admission, axial-flow turbine. The turbine performance curve is shown in Figure 62.

TABLE XVI. - BASELINE PUMP OPERATING CHARACTERISTICS

(S.I. UNITS)

PUMPS	DIMENSIONS	FUEL	OXIDIZER
Stages		4	2
Net Positive Suction Head	m	4.57	0.61
Suction Specific Speed	$\frac{(rpm)(m^3/sec)^{1/2}}{(m)^{3/4}}$	351	581
Vapor Pressure	atm	1.22	1.02
Thermodynamic Supression Head	atm	8.84	0.272
Shaft Speed	rpm	191,320	47,755
Total Discharge Pressure	atm	64.9	43.5
Total Head Rise (Stage)	m	9509 (2377)	385 (192)
Capacity	m^3/sec	9.91×10^{-4}	3.66×10^{-4}
Specific Speed (Based on Stage Head)	$\frac{rpm(m^3/sec)^{1/2}}{(m)^{3/4}}$	17.66	17.67
Efficiency	%	45.8	50.3
Shaft Power	KW	13.87	3.13
Impeller Diameter	cm	2.18	2.49

(ENGLISH UNITS)

Stages		4	2
Net Positive Suction	ft	15	2.0
Suction Specific Speed	$\frac{rpm \times gpm^{1/2}}{ft^{3/4}}$	18,114	30,000
Vapor Pressure	psia	18	15
Thermodynamic Suppression Head	ft	130	4
Shaft Speed	rpm	191,320	47,755
Total Discharge Pressure	psia	950	640
Total Head Rise (Stage)	ft	31,196 (7799)	1,262 (631)
Capacity	gpm	15.7	5.8
Specific Speed (Based on Stage Head)	$\frac{rpm \times gpm^{1/2}}{ft^{3/4}}$	912	913
Efficiency	%	45.8	50.3
Shaft Horsepower	hp	18.6	4.24
Impeller Diameter	in.	0.86	0.98

TABLE XVII. - BASELINE PUMP DRIVE OPERATING CHARACTERISTICS

(S.I. UNITS)

DRIVE	DIMENSIONS	GAS TURBINE	ELECTRIC MOTOR
Stages		1	
Gas		GH_2	
Shaft Power	KW	18.87	3.97
Gas Weight Flow (Max)	kg/sec	.0635	
Gas Inlet Total Temperature	°C/°K	32.2/305.6	
Gas Inlet Total Pressure	atm	58.8	
Pressure Ratio	---	1.472	
Shaft Speed	rpm	191,320	
Efficiency	%	62	80
Admission	%	13	
Rotor Diameter	cm	3.89	
Blade Height	cm	0.40	
Alternator Efficiency	%	90	

(ENGLISH UNITS)

Stages		1	
Gas		GH_2	
Shaft Power	hp	25.3	5.33
Gas Weight Flow (Max)	lb/sec	0.14	
Gas Inlet Total Temperature	°F/°R	90/550	
Gas Inlet Total Pressure	psia	865	
Pressure Ratio		1.472	
Shaft Speed	rpm	191,320	
Efficiency	%	62	80
Admission	%	13	
Rotor Diameter	in.	1.53	
Blade Height	in.	0.157	
Alternator Efficiency	%	90	

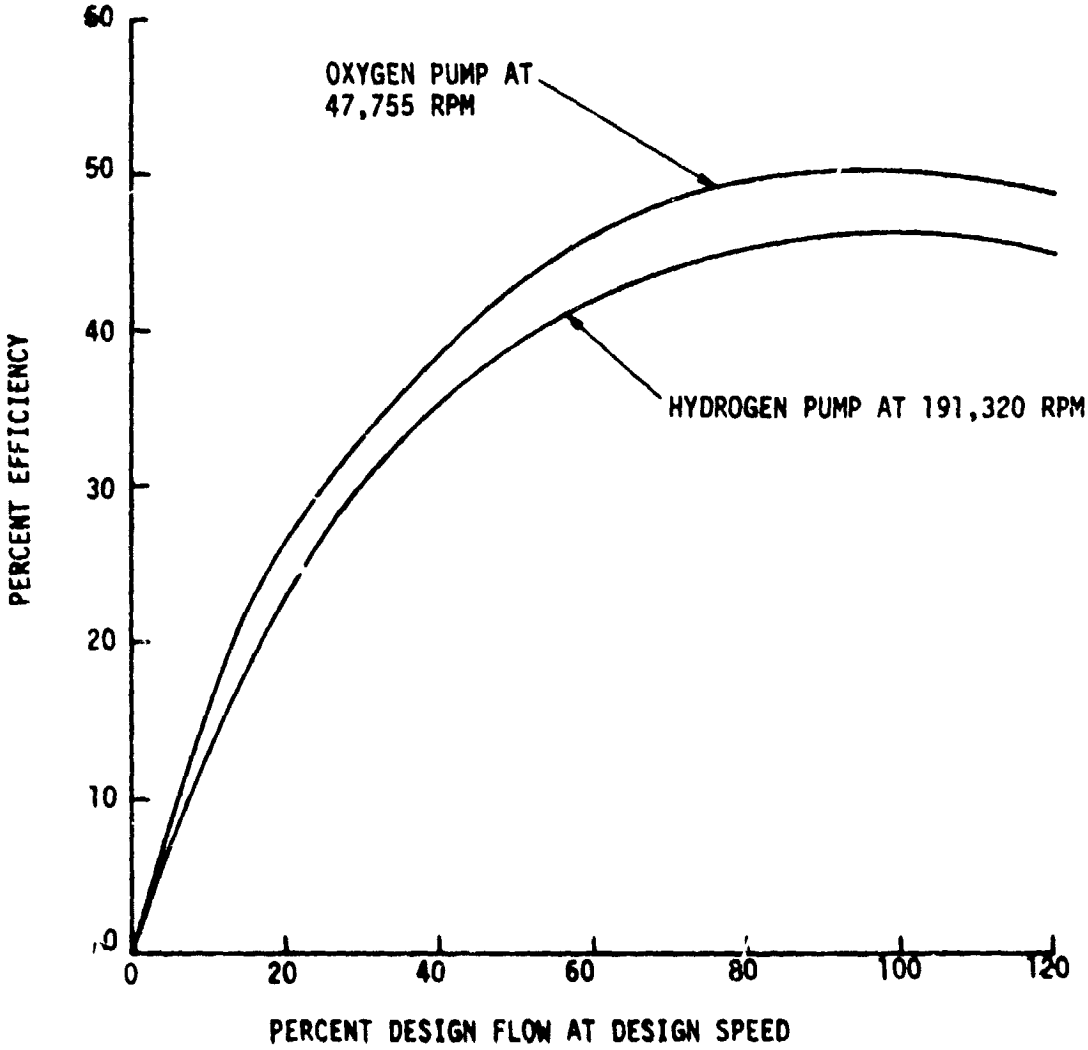

Figure 56. Pump Efficiencies at Design Speed

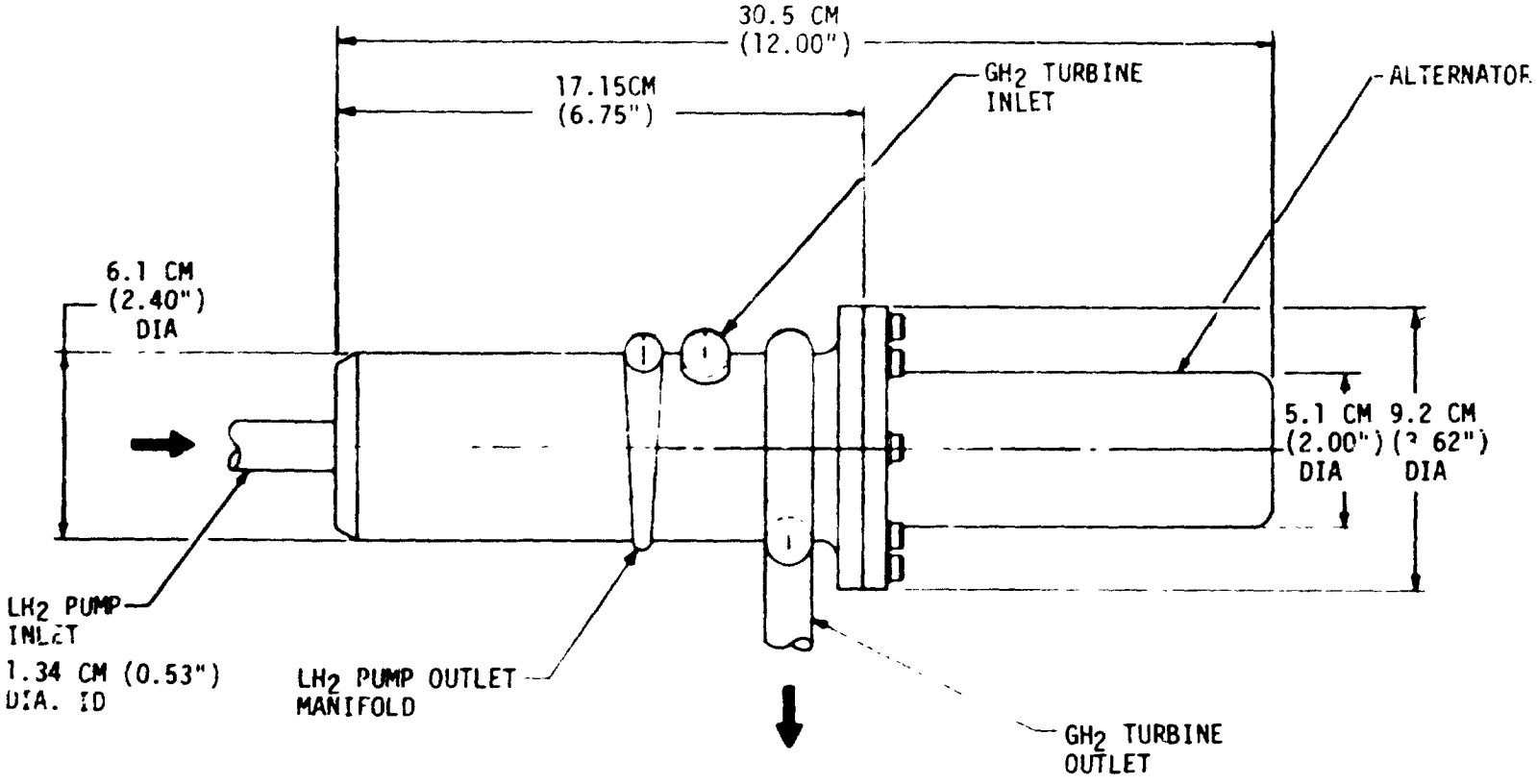

Figure 57. LH_2 Turbopump/Alternator Assembly

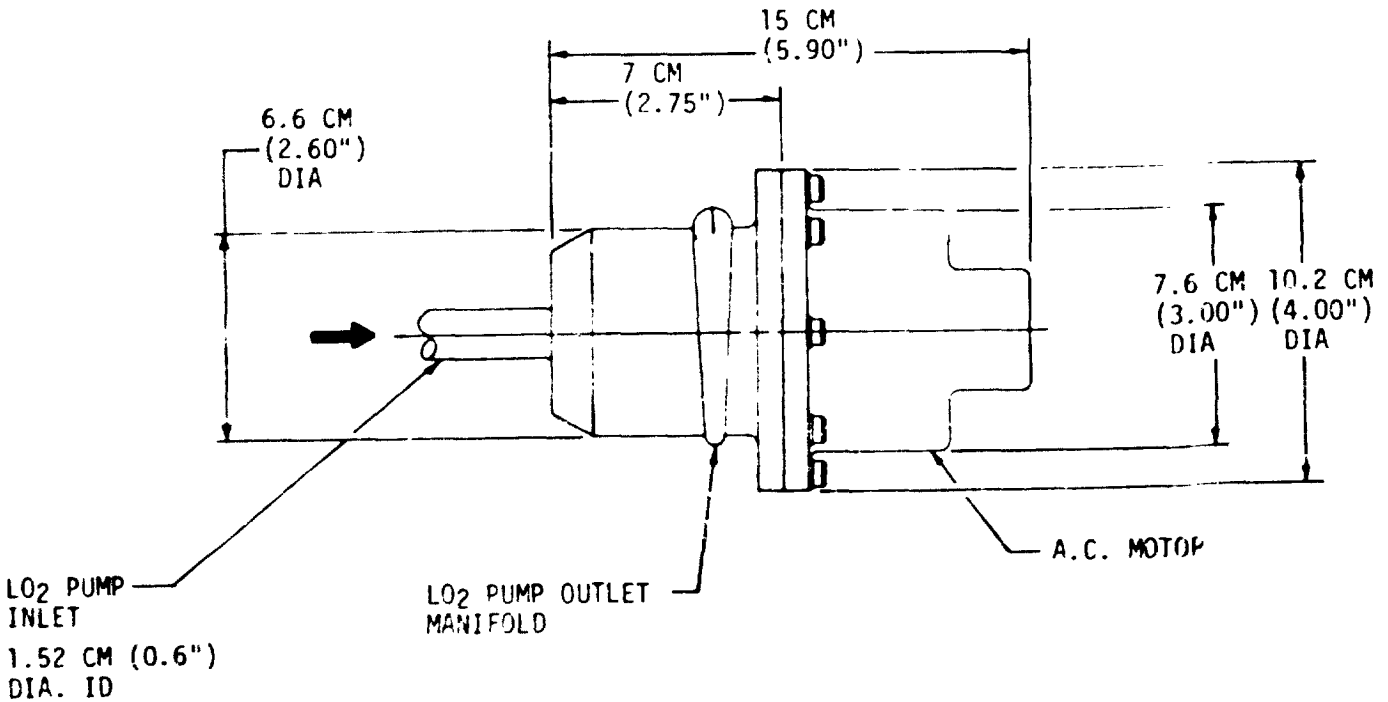

Figure 58. LO_2 Pump and AC Motor Assembly

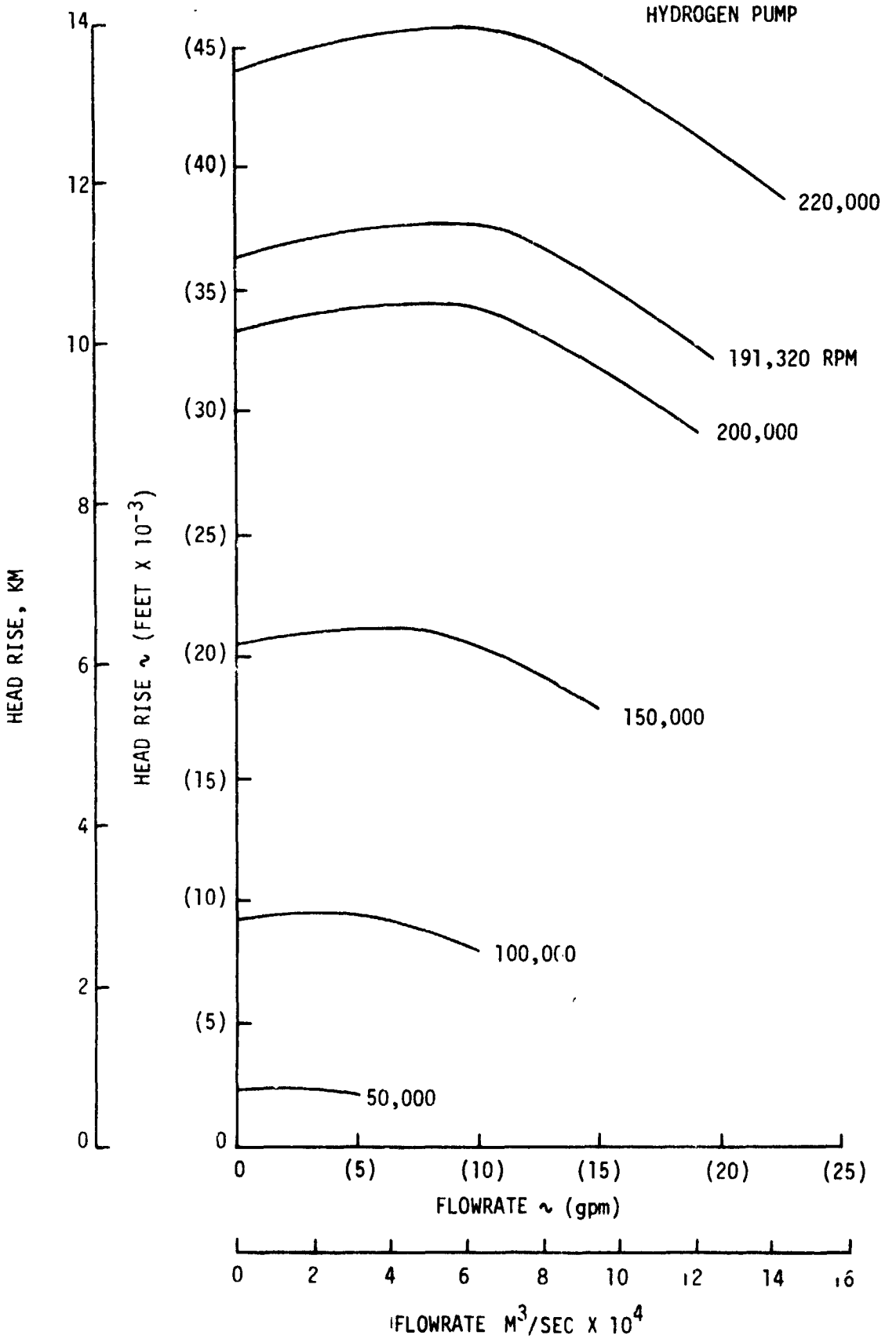

Figure 59. Hydrogen Pump Head-Capacity Characteristics

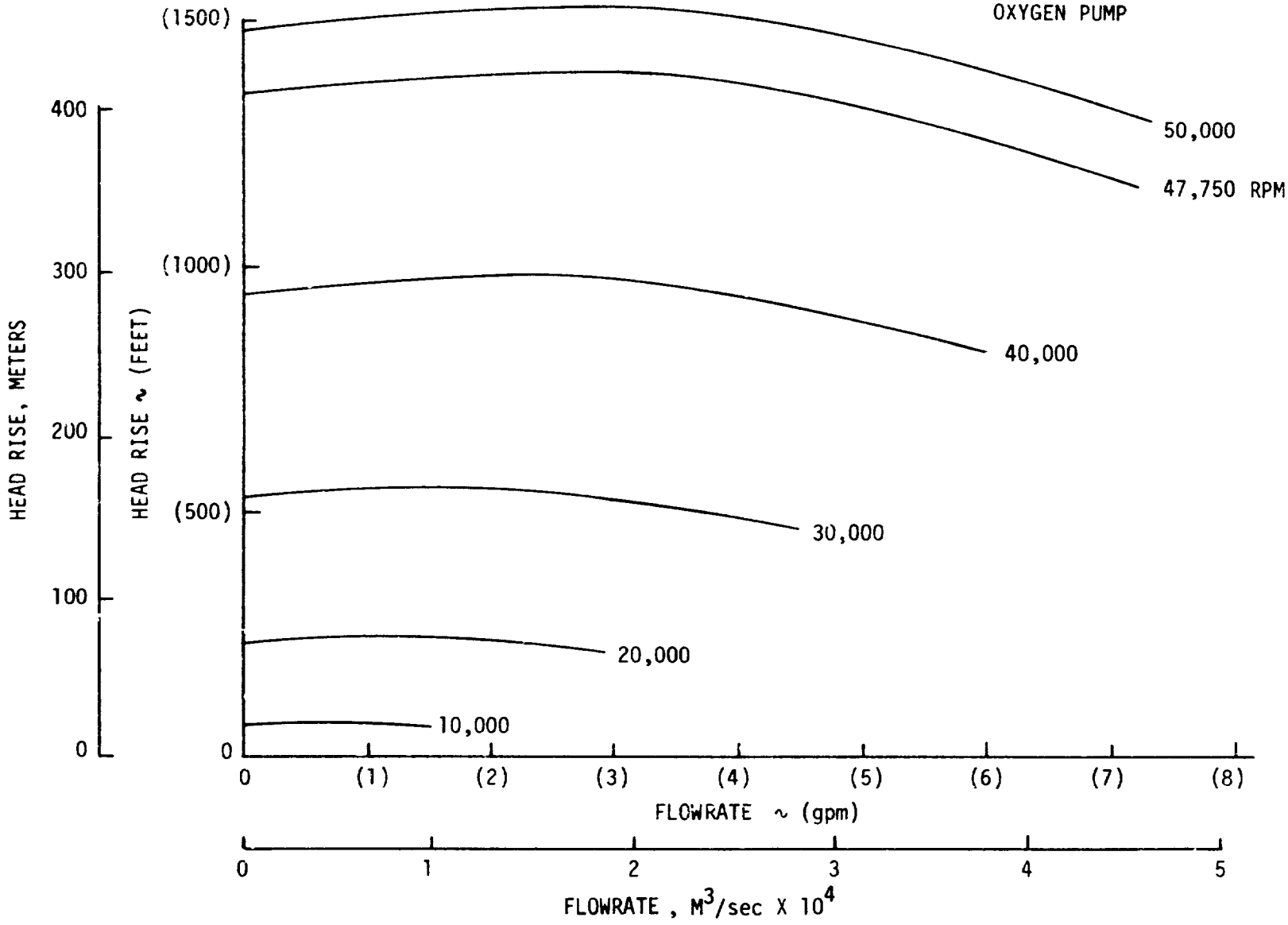

Figure 60. Oxygen Pump Head-Capacity Characteristics

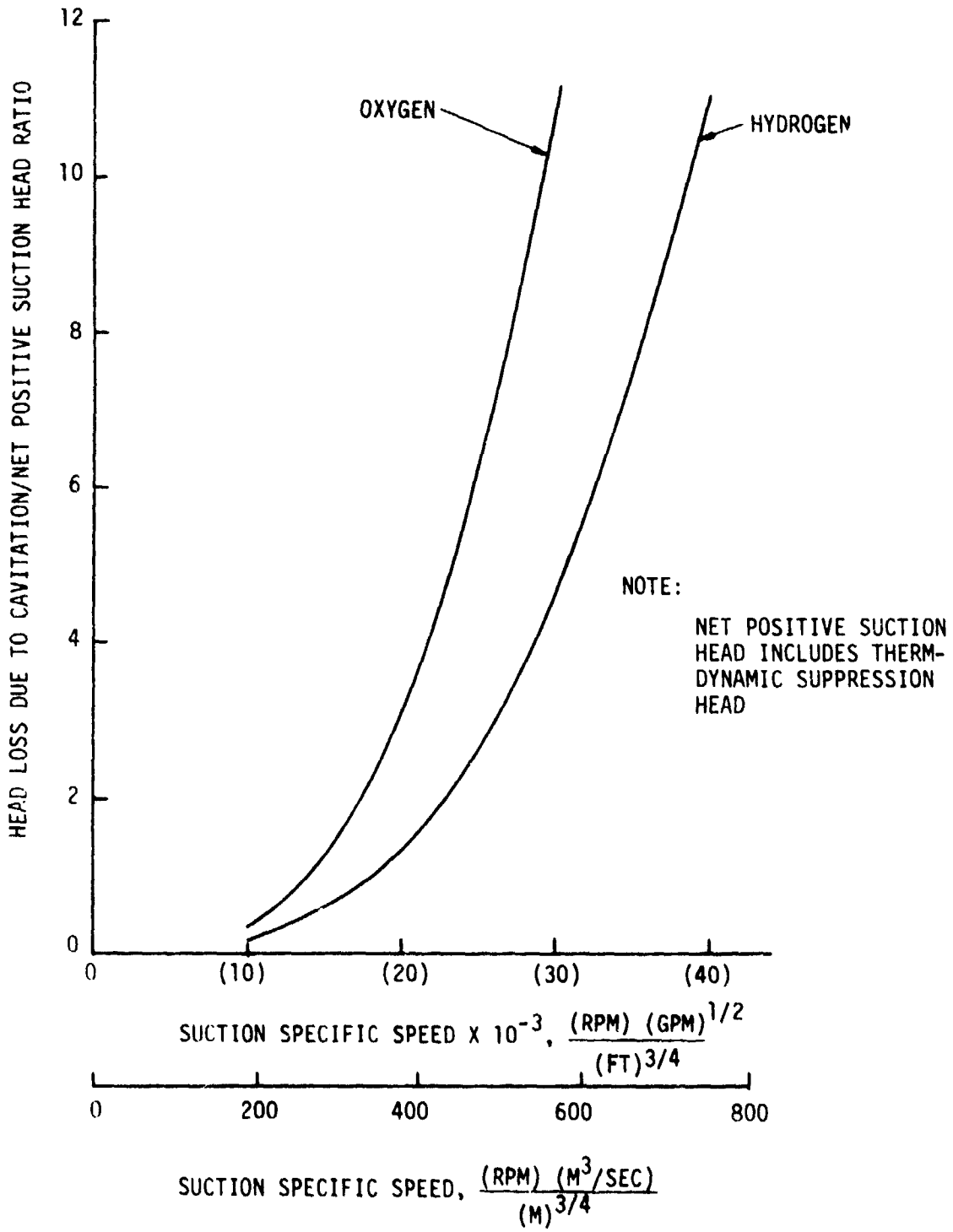

Figure 61. Pump Overall Head Loss Due to Cavitation

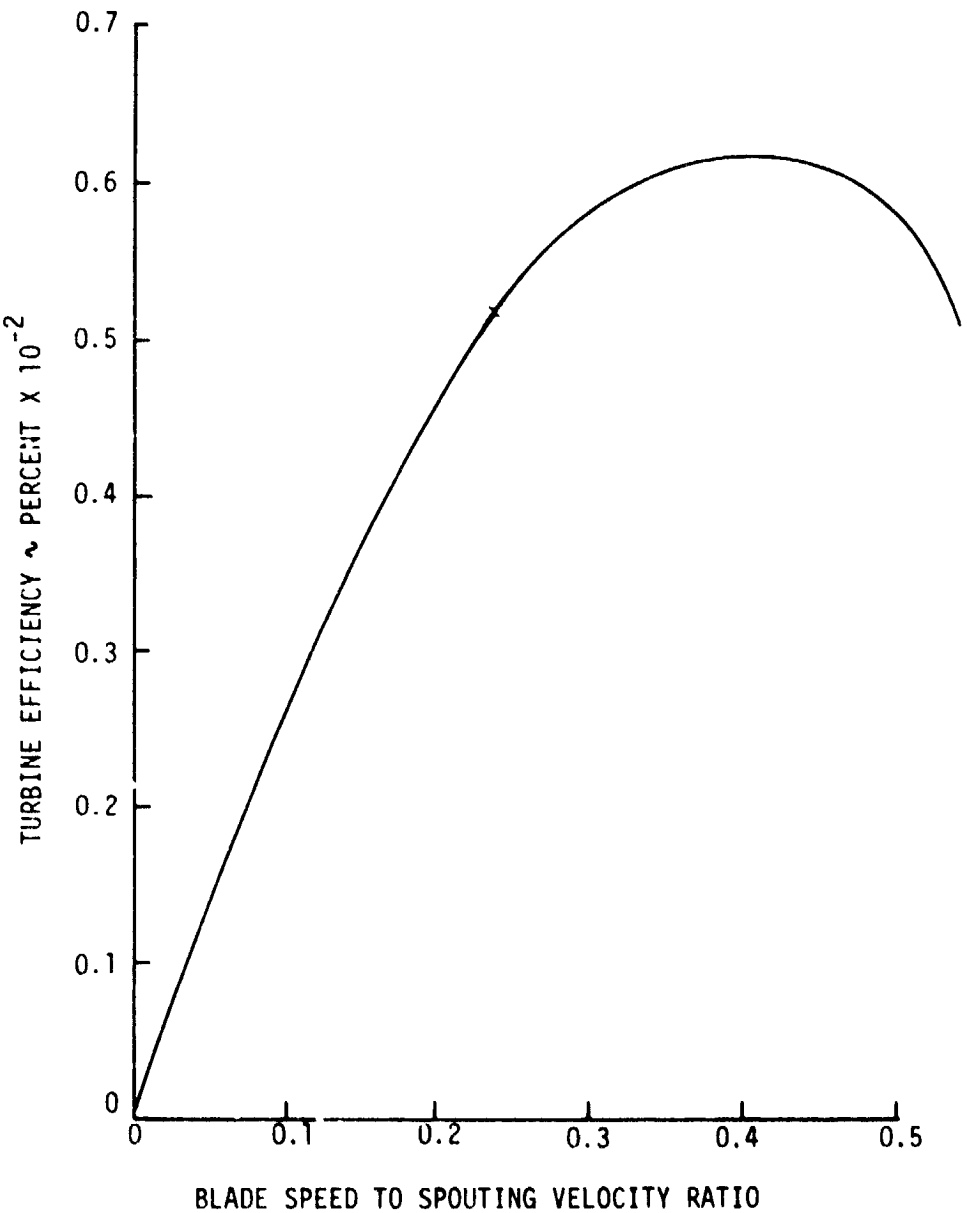

Figure 62. Hydrogen Gas Turbine Performance

4. Controls System Design

The primary objective of the control systems design analysis effort during this phase of the engine study was to provide envelope and flow port sizing data for the valves and to define the basic engine operational sequence.

A definition of the engine system valve locations and nomenclature is given in Figure 63. Prior to engine operation, the fuel and oxidizer propellant lines must be purged to ensure that no moisture or condensible gases are present in the engine system. The lines and components required for the engine purge and relief system and the igniter system should be determined during future more detailed engine system design efforts.

After the engine is purged, it is chilled down and the operating sequence is initiated. The sequence which follows assumes that the engine prevalves (valves ① and ②) are open and the engine is chilled and bled-in to the pump discharge valves.

- Close fuel turbine bypass valve ③.
- Open fuel pump discharge and engine fuel shutoff valves ④ and ⑤.
- Energize engine igniter system.
- Open LO_2 pump discharge and engine LO_2 shutoff valves ⑥ and ⑦.
- As the fuel pump speed increases, the fuel pump alternator output is controlled to increase the oxidizer pump motor speed at a specified ramp rate, and the fuel turbine bypass valve ③ is shuttled to the nominal operating position.
- Engine steady-state mixture ratio is controlled by sensing fuel and oxidizer system mass flowrates. This input is compared to set-point parameters, and the error signal is processed by the controller to adjust the fuel turbine bypass valve ③ position and the power input to the LO_2 pump drive motor.

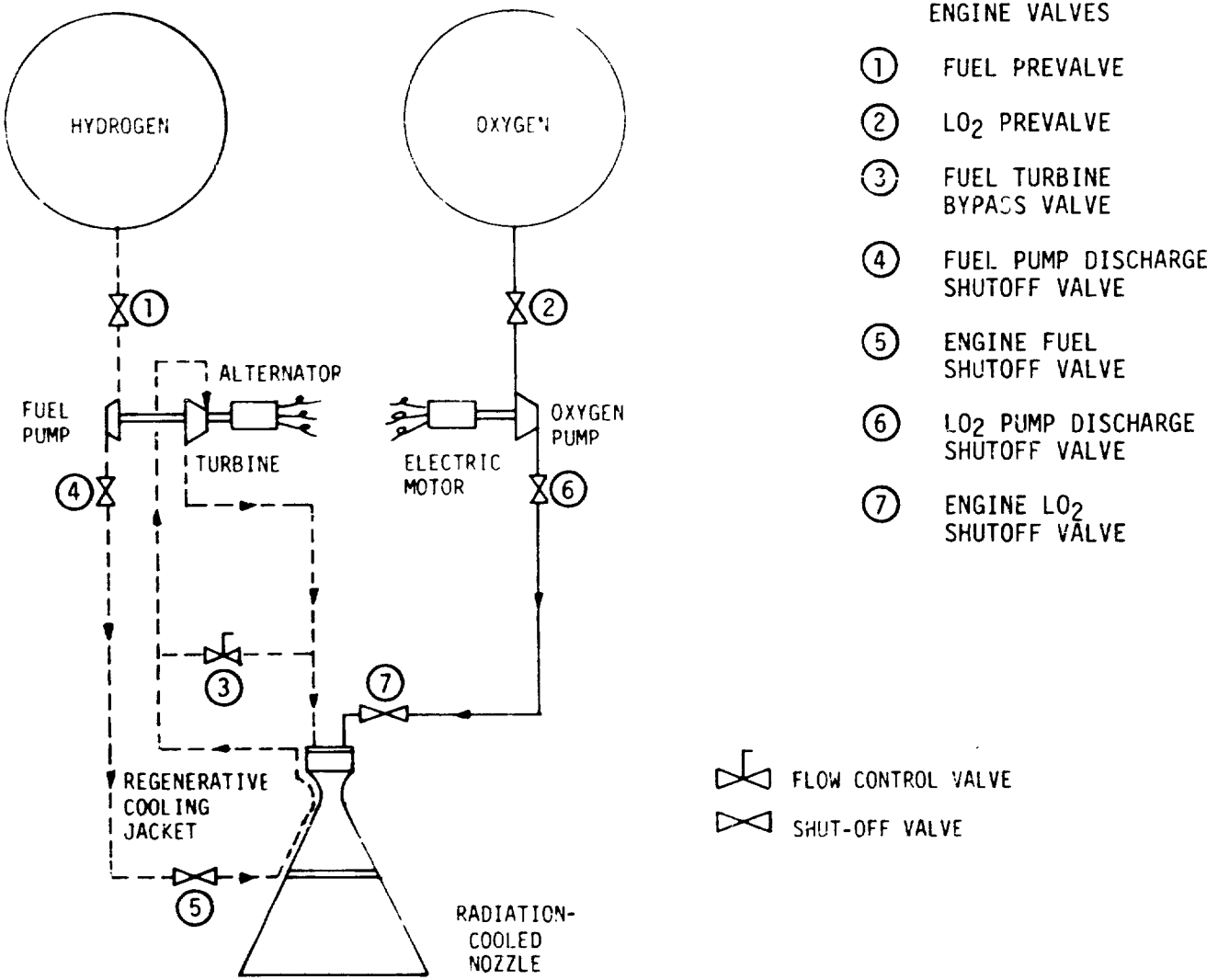

Figure 63. Engine System Valve Locations

VI, C, Component Design Analysis (cont.)

To terminate engine operation, the valves are actuated in the following sequence:

- Close engine LO_2 shutoff valve (7)
- Close LO_2 pump discharge valve (6)
- Close engine fuel shutoff valve (5)
- Close fuel pump discharge valve (4)
- Open fuel turbine bypass valve (3)
- De-energize engine igniter system

If engine restart is not scheduled within a specified period of time, the fuel and LO_2 prevalves are also closed.

To prevent excessive pressure rise as the engine system warms up after shutdown, pressure relief provisions can be designed into the pump discharge valves (4) and (6) and the prevalves (1) and (2), or relief valves can be added to the system.

Based on the relatively small engine size and moderate operating pressures, it is assumed that the engine valves will be solenoid-operated. The tradeoff is solenoid weight versus the size and weight of a pneumatic actuation system which would probably have to be quite large to supply gas during the anticipated multiple restarts for the intended mission. This assumption should be reevaluated if it is later determined that actuation gas could be supplied by the vehicle tank pressurization system. It should be noted that power input to the solenoids can be minimized by reducing the applied voltage (i.e., from 28 VDC to 10 VDC) after a valve has been opened, or by using mechanical latching solenoids.

The preliminary valve flow port sizing was calculated on the basis of the predicted flowrates and pressure drops from the engine pressure schedule, (Table XIV) and the cycle power balance data (Table XV). The resultant valve flow port sizing and equivalent sharp edge orifice diameters (ESEOD) are presented in Table XVIII.

Based on a review of valve vendor literature, it was determined that the coaxial solenoid poppet valve configuration is desirable in terms of compact envelope size, high reliability, and cycle life. As a result, this configuration was chosen for the engine pump discharge and shutoff valves. The approximate envelope dimensions for the fuel and LO_2 pump discharge and engine shutoff valves are shown in Figure 64. It is anticipated that opening response requirements for these valves will not be critical because they will be opened during the start transient while system pressures are relatively low. The valves are spring-loaded and will fail-safe to the normally closed position.

TABLE XVIII. - ENGINE VALVE FLOW PORT SIZING

Valve	Type	Flow Port Dia. cm (in.)	ESEOD* CD = .65 cm (in.)
Fuel Pump Discharge Shutoff Valve	Coaxial Solenoid	.95 (3/8)	.66 (.26)
Engine Fuel Shutoff Valve	Coaxial Solenoid	.95 (3/8)	.66 (.26)
LO_2 Pump Discharge Shutoff Valve	Coaxial Solenoid	1.27 (1/2)	.91 (.36)
Engine LO_2 Shutoff Valve	Coaxial Solenoid	1.27 (1/2)	.91 (.36)
Fuel Turbine Bypass Valve	Poppet-Control	.64 (1/4)	.25 (.10)
Fuel Prevalve	Balanced Poppet or Gate	1.27 (1/2)	1.17 (.46)
LO_2 Prevalve	Balanced Poppet or Gate	1.91 (3/4)	1.45 (.57)

*Equivalent Sharp Edged Orifice Diameter

- VALVE TYPE - COAXIAL SOLENOID

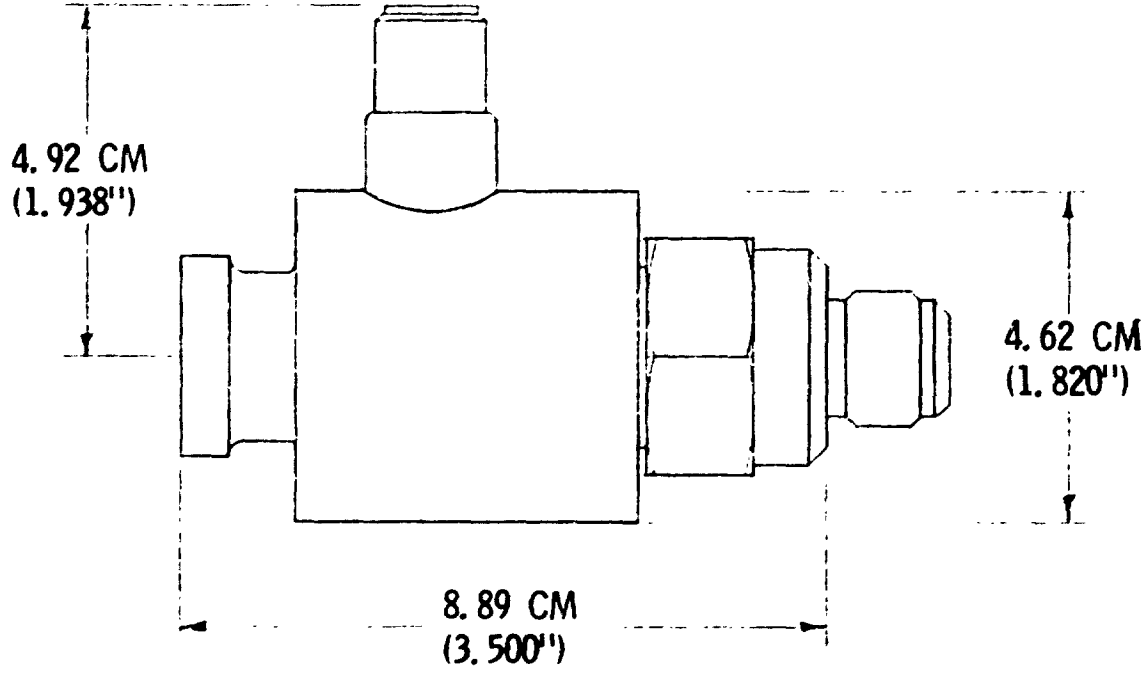

- APPROXIMATE CONFIGURATION FOR THE LO_2 AND LH_2 PUMP DISCHARGE AND ENGINE SHUT-OFF VALVES

Figure 64. Envelope Dimensions for Engine Valves

The fuel turbine bypass valve is a poppet type control valve with the same overall dimensions as the engine shutoff valves.

Consideration was given to utilizing the coaxial configuration for the prevalves; however, a coaxial solenoid valve with a 1.45 cm (.57 in.) ES-EOD would result in a heavy solenoid when the necessary number of ampere turns are wound on the larger valve diameter. Therefore, a balanced poppet or gate solenoid valve was selected for this location. Approximate valve envelope dimensions for the fuel and LO_2 prevalves are shown in Figure 65.

D. PARAMETRIC DATA UPDATE

Based upon the results of the preliminary design, the engine parametric data were updated and generated over a nozzle area ratio range from 200 to 1000:1.

As shown in Table XIX, in some cases, the individual component weights exhibited significant differences from the preliminary estimates. However, the total engine weight remained about the same. Changes to the envelope calculations were minor, and the performance is the same as presented for the conceptual analysis. Therefore, all the parametric data presented in Section V,C are valid.

The parametric performance, weight, and envelope data are summarized in Figures 66, 67, 68, and 69 as a function of thrust and nozzle area ratio at the baseline chamber pressure of 34 atm (500 psia). At this chamber pressure, engines at thrust levels of 890 N (200 lb) or less are not feasible to cool within the study guidelines.

Figure 66 shows that performance gains beyond an area ratio of 400:1 are relatively small, but that significant increases in the 200:1 to 400:1 range can be obtained.

The engine weight data shown in Figure 67 was generated by inputting the new baseline component weights in the engine model weight sealing equations.

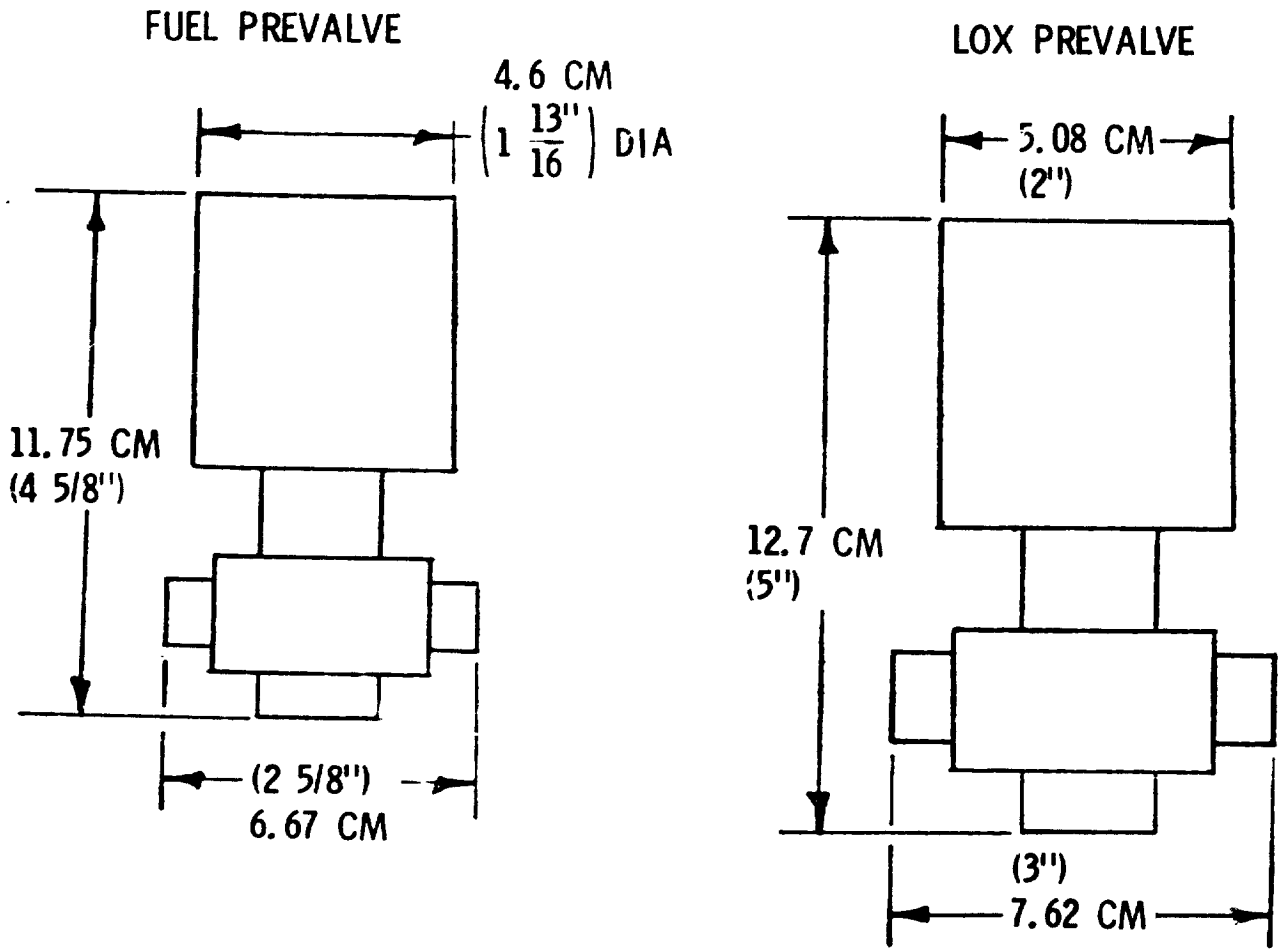

Figure 65. Prevalve Envelope Dimensions

TABLE XIX. - CURRENT VS INITIAL ENGINE WEIGHT STATEMENT

COMPONENT DESCRIPTION	INITIAL ESTIMATE,[1] kg (lbs)	CURRENT ESTIMATE[2] kg (lbs)	CURRENT ESTIMATION BASIS
1. High Pressure Lines	0.50 (1.1)	0.50 (1.1)	(1)
2. Valves and Actuators	1.86 (4.1)	5.53 (12.2)	(2)
3. Injector	0.54 (1.2)	1.04 (2.3)	(2)
4. Chamber	0.86 (1.9)	1.86 (4.1)	(2)
5. Rad.-Cooled Nozzle	3.22 (7.1)	2.77 (6.1)	(2)
6. Igniter	2.04 (4.5)	1.72 (3.8)	(2)
7. Regen-Cooled Nozzle	0.77 (1.7)	2.36 (5.2)	(2)
8. Gimbal and Actuator Sys	0.91 (2.0)	1.77 (3.9)	(2)
9. Engine Controller	5.44 (12.0)	5.44 (12.0)	(1)
10. Miscellaneous	5.72 (12.6)	5.72 (12.6)	(1)
11. Low Pressure Lines	0.14 (.3)	0.59 (1.3)	(2)
12. Fuel Pump	3.49 (7.7)	1.72 (3.8)	(2)
13. Ox Pump	2.45 (5.4)	0.68 (1.5)	(2)
14. Turbine Assembly	4.85 (10.7)	1.04 (2.3)	(2)
15. A.C. Motor	2.63 (5.8)	4.04 (8.9)	(2)
16. Alternator	2.27 (5.0)	1.95 (4.3)	(2)
17. Total Engine Weight	37.7 (83.1)	38.7 (85.4)	(2)

[1] Computer model scaling of historical designs and data

[2] Based upon preliminary design results

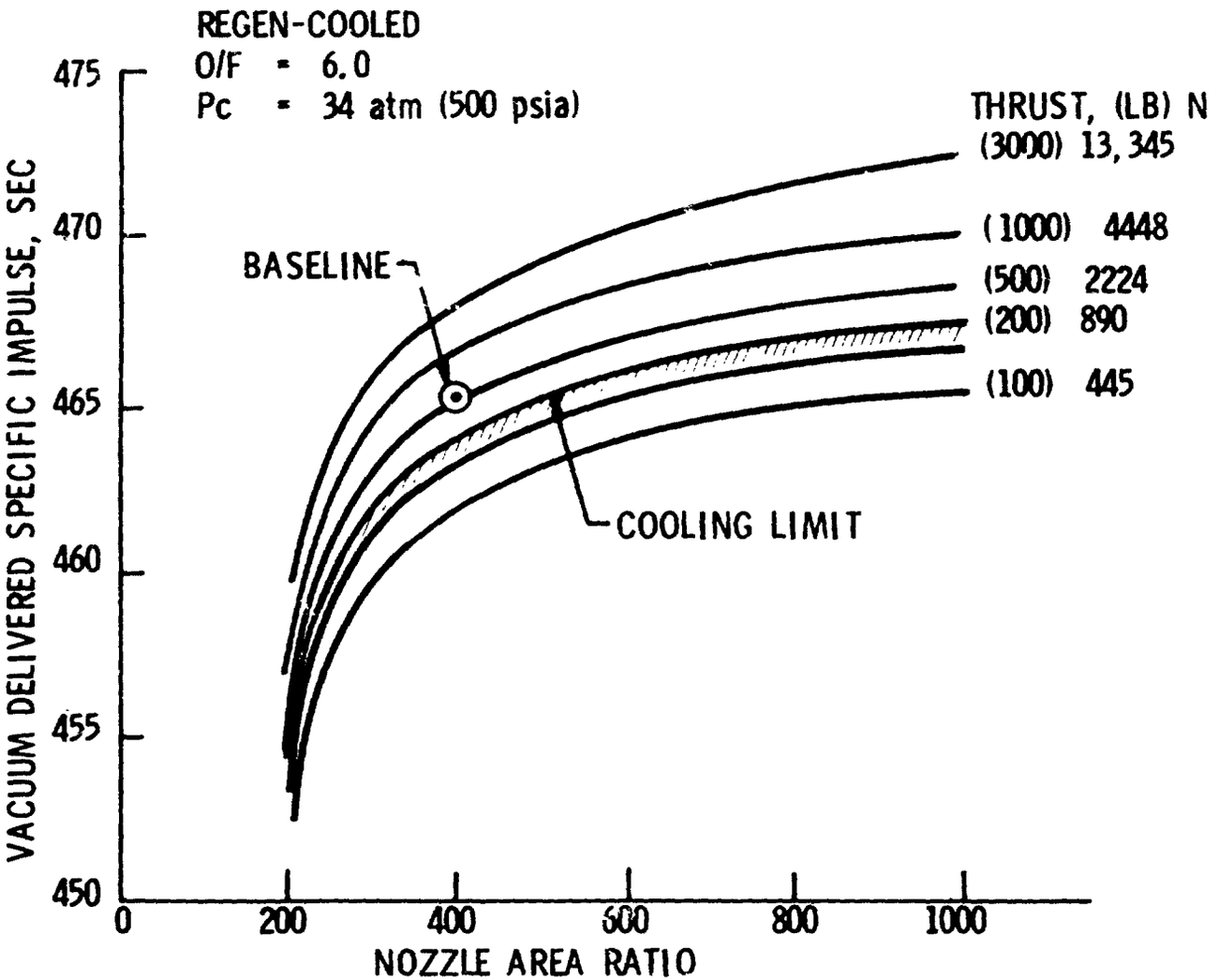

Figure 66. Updated O_2/H_2 Engine Performance Parametric Data

EXPANDER/TURBOALTERNATOR CYCLE
O/F = 6.0
CHAMBER PRESSURE = 34 ATM (500 PSIA)

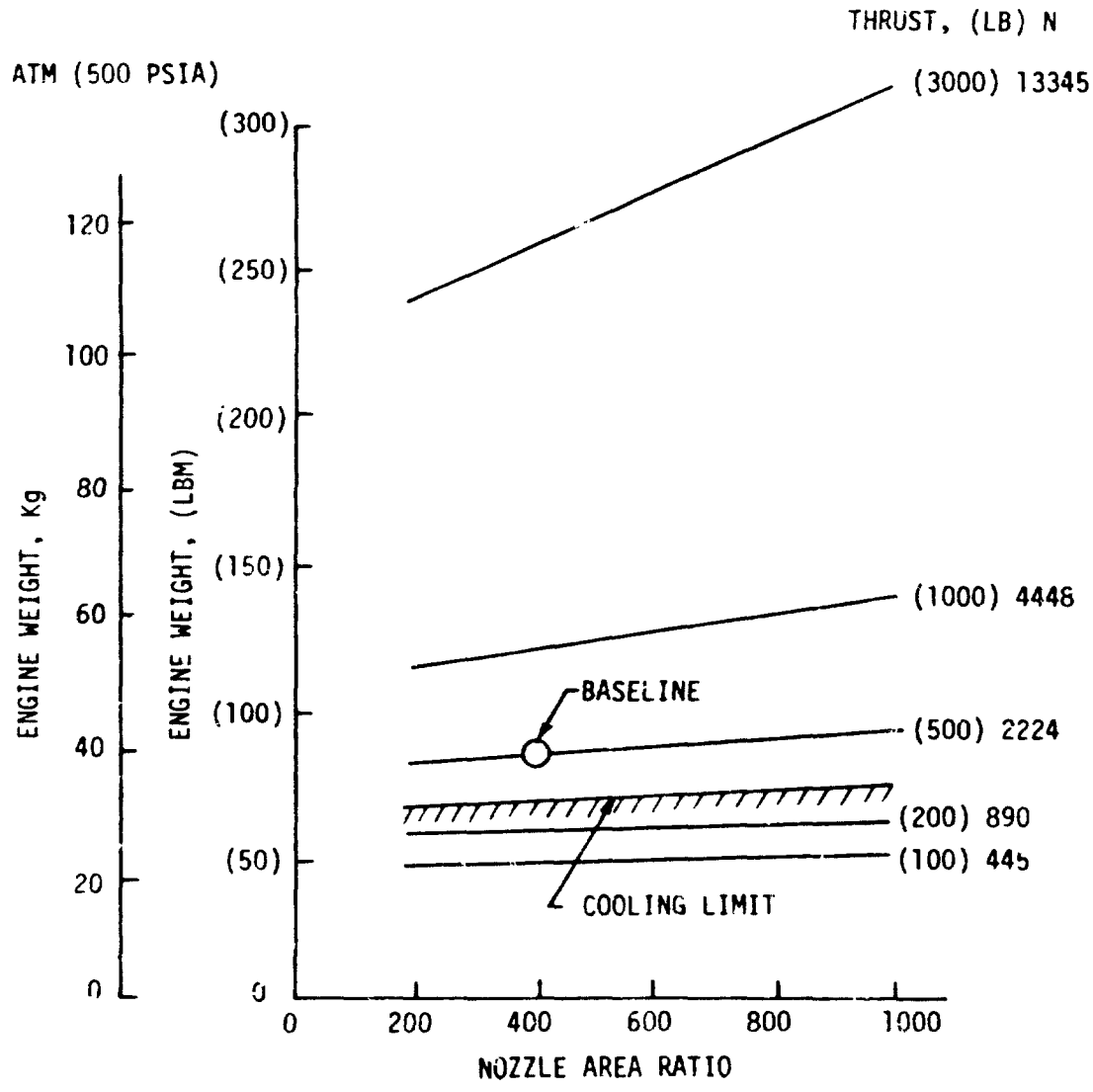

Figure 67. Updated O_2/H_2 Engine Weight Parametric Data

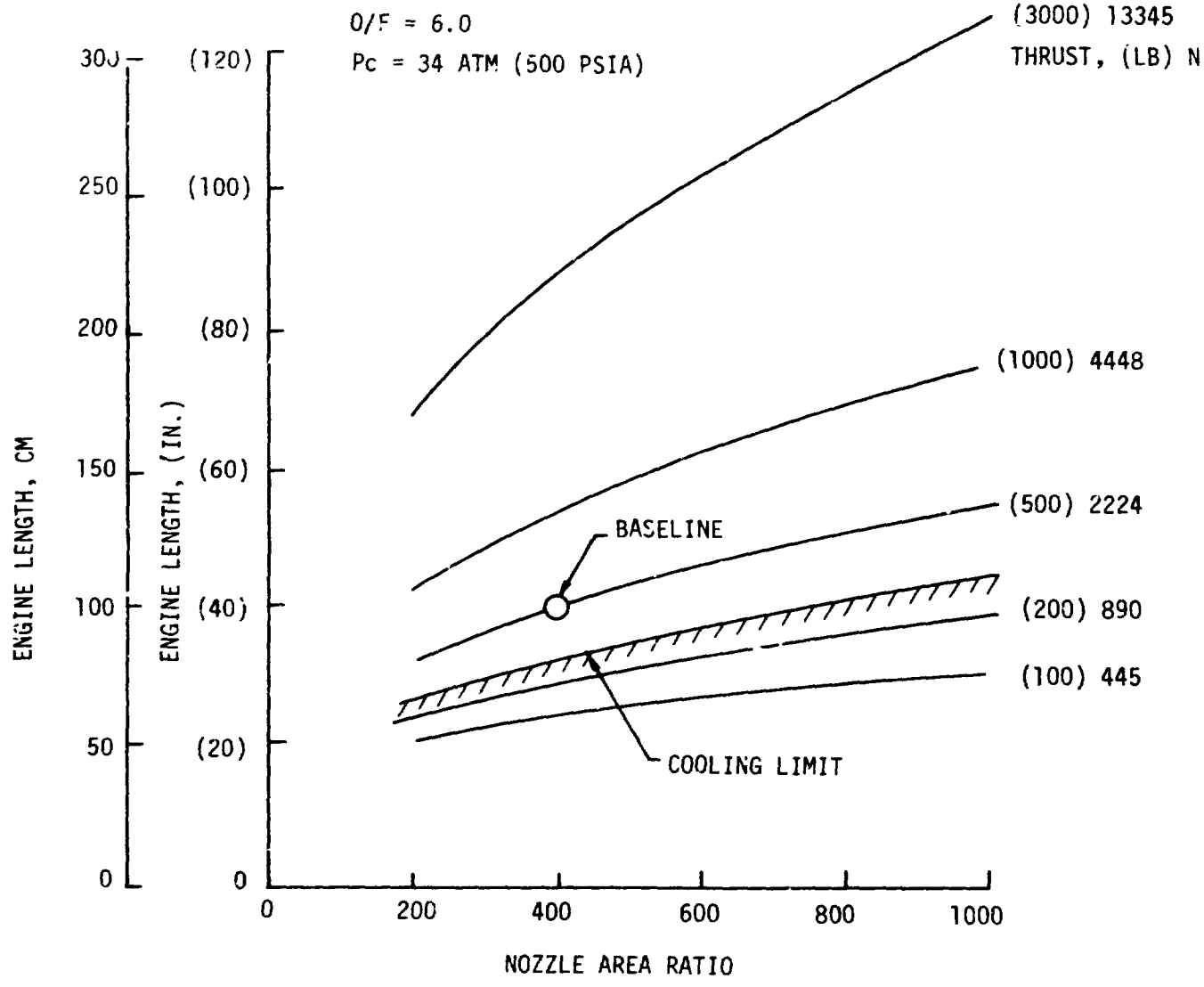

Figure 68. Updated O_2/H_2 Engine Length Parametric Data

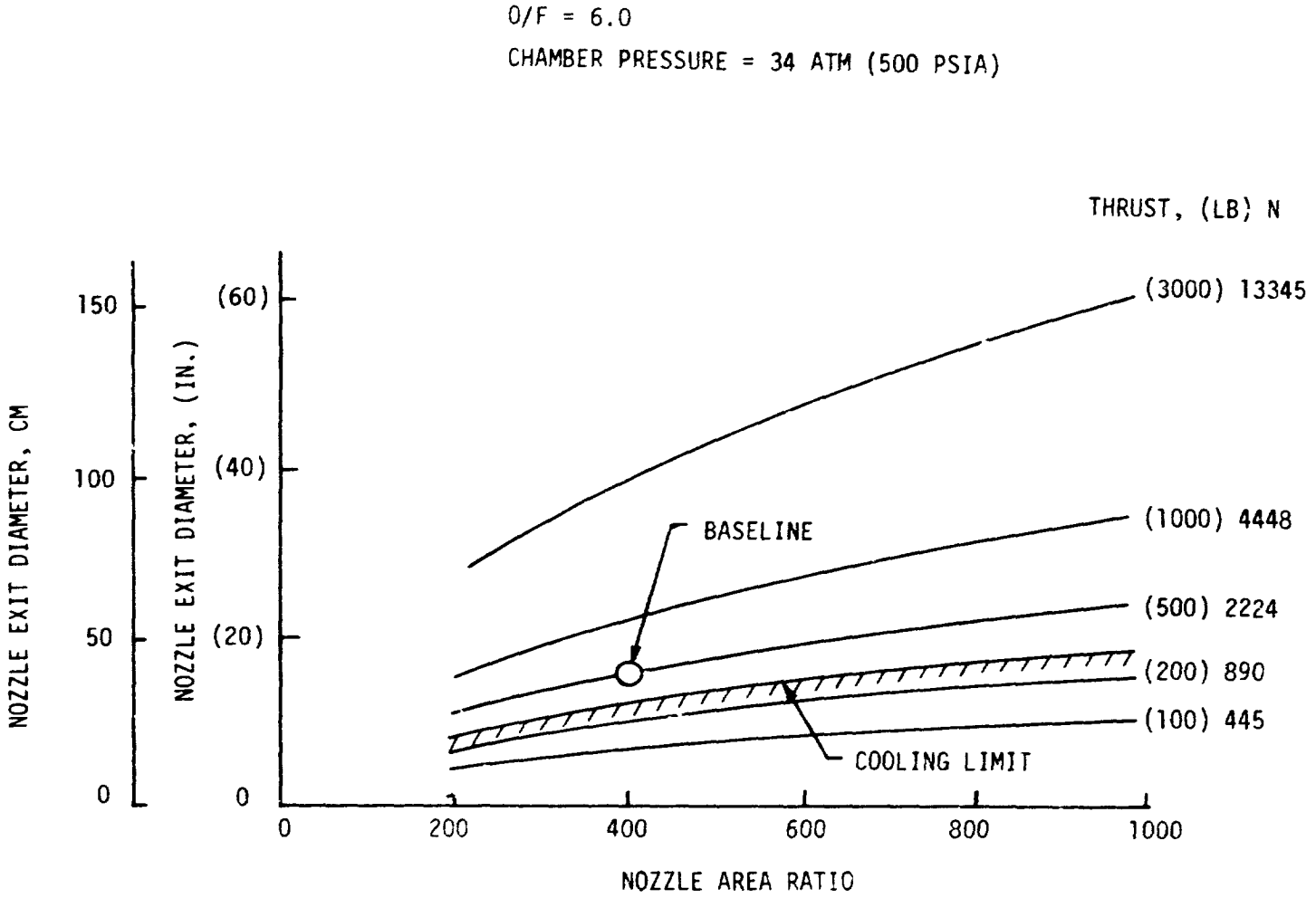

Figure 69. Updated O_2/H_2 Nozzle Exit Diameter Parametric Data

SECTION VII

CONCLUSIONS AND RECOMMENDATIONS

The conclusions and recommendations derived from the results of this study are summarized in Table XX and discussed herein.

Hydrogen regeneratively cooled O_2/H_2 engines provide the largest feasible thrust and chamber pressure ranges with use of conventional cooling methods and criteria. These engines are also applicable to a large number of system concepts and pump-fed systems as the availability of heated hydrogen for a turbine drive fluid makes them relatively easy to power balance.

Film-cooled systems are only applicable in high-thrust (i.e., >4.45 KN (1000 lbF) and low chamber pressure operating regions. The film-cooling losses as well as the low operating chamber pressures make these engines unattractive.

Methane regeneratively cooled O_2/CH_4 engines provide a large, feasible operating thrust and chamber pressure regime. To avoid the two-phase region, the coolant jacket outlet pressure must be held above the critical pressure (i.e., 45.4 atm (667 psia)) of CH_4. This limits the number of system concepts for which methane appears attractive.

RP-1 regeneratively cooled O_2/RP-1 systems are feasible for cooling over small ranges provided that measures are taken to reduce the coolant temperature rise and purified RP-1 with a high coking temperature is assumed. This limitation is changed if a carbon deposit is assumed. With a carbon deposit, the total thrust and chamber pressure range was found to be feasible to cool. Experimental data findings do not currently support the carbon deposition correlations found in the literature. Therefore, further evidence of the benefits of carbon must be obtained before this design approach can be recommended.

Pump-fed O_2/H_2, hydrogen regeneratively cooled engines are the highest-performing system candidates. Their high performance occurs not only because of the high theoretical performance of the propellant combination itself, but also because operation at high chamber pressures are feasible. Operation at low thrusts and high chamber pressures make these engines the lightest and shortest concepts. In the length-limited Shuttle Orbiter application, the length advantage peculiar to this system could be very important.

It is recommended that component technology programs be initiated on a low-thrust O_2/H_2, pump-fed hydrogen regeneratively cooled engine. These technologies are discussed in the next section of this report. In addition, advanced cooling studies and evaluations should be conducted to remove the restrictions imposed by current design criteria, manufacturing techniques, and cooling configurations.

TABLE XX. - CONCLUSIONS AND RECOMMENDATIONS

- Viable Concepts with Conventional Cooling Methods
  - O_2/H_2, H_2 Regen-Cooled - Largest F & P_c Ranges
  - O_2/H_2, H_2 Film-Cooled - Small, Low Performance Range
  - O_2/CH_4, CH_4 Regen-Cooled - Maintain CH_4 above Critical
- Advanced Coolant Schemes and Concepts are Required for O_2/RP-1, RP-1 Cooled Engines.
- Carbon Deposition Assumption Creates a Major Impact on the Study Results.
- Pump-Fed O_2/H_2 Regen-Cooled Engines are the Highest Performance Option.
- Pump-Fed O_2/H_2 Regen-Cooled Engines Have the Largest F & P_c Feasible Design Ranges.
- O_2/H_2 Pump-Fed, Regen-Cooled Engine Component Critical Technology Programs Should be Initiated to:
  - Reduce Risk
  - Verify Power Balance
  - Verify Performance
- Advanced Cooling Design Experimental Evaluations Should be Conducted to Permit Lower Thrust and Higher Chamber Pressure Designs.

SECTION VIII

TECHNOLOGY ITEMS

During the course of this study, recommendations for an advanced technology program which would enhance the low-thrust engine concepts or general technologies required to improve design and analysis techniques were identified.

These engine technologies, depicted on Figure 70, cover every major engine component. The major technology items identified are also summarized in Table XXI and discussed briefly herein.

If the recommended pump-fed system is ultimately selected for the low-thrust mission, demonstrations of high-efficiency pumps and gas turbines are required. Experience and/or data in the size ranges covered by this study is either very limited or nonexistent. These turbomachinery programs should then be followed by an experimental demonstration of the pumps and drives for the mixed expander/turboalternator cycle to verify the rotating machinery system performance and to obtain further data on system interactions.

Current turbomachinery designs are limited in speed and performance by the use of conventional bearings and seals. Substitution of hydrostatic bearings and seals offers the potential of substantially increasing running speeds. Technology studies should be undertaken to obtain experimental data on the hydrostatic bearings and seals so that the performance and life of the rotating machinery components can be increased.

The injector and combustion chamber are critical components in an expander or turboalternator cycle because the system power balance is dependent upon the coolant jacket pressure drop and coolant temperature rise. Verification of cooling model design predictions is required to assure that the selected engine design point chamber pressure and thrust can be achieved.

Unique chamber designs should also be evaluated to assess the possibility of increasing the coolant temperature while still maintaining low coolant pressure drops. These thermally enhanced chamber designs would improve the engine cooling margin and life and permit operation at higher chamber pressure or provide more power balance margin.

Although much work has been accomplished in past H/O torch igniter programs, data should be obtained for this pressure-diameter size range. Long life and reliable ignition and restart capability must be demonstrated for this application.

The data base on high area ratio (400:1 or greater) nozzle performance is very small. A test program should be conducted with small hardware to verify the performance predictions. Of particular concern are the boundary layer and kinetic loss evaluations.

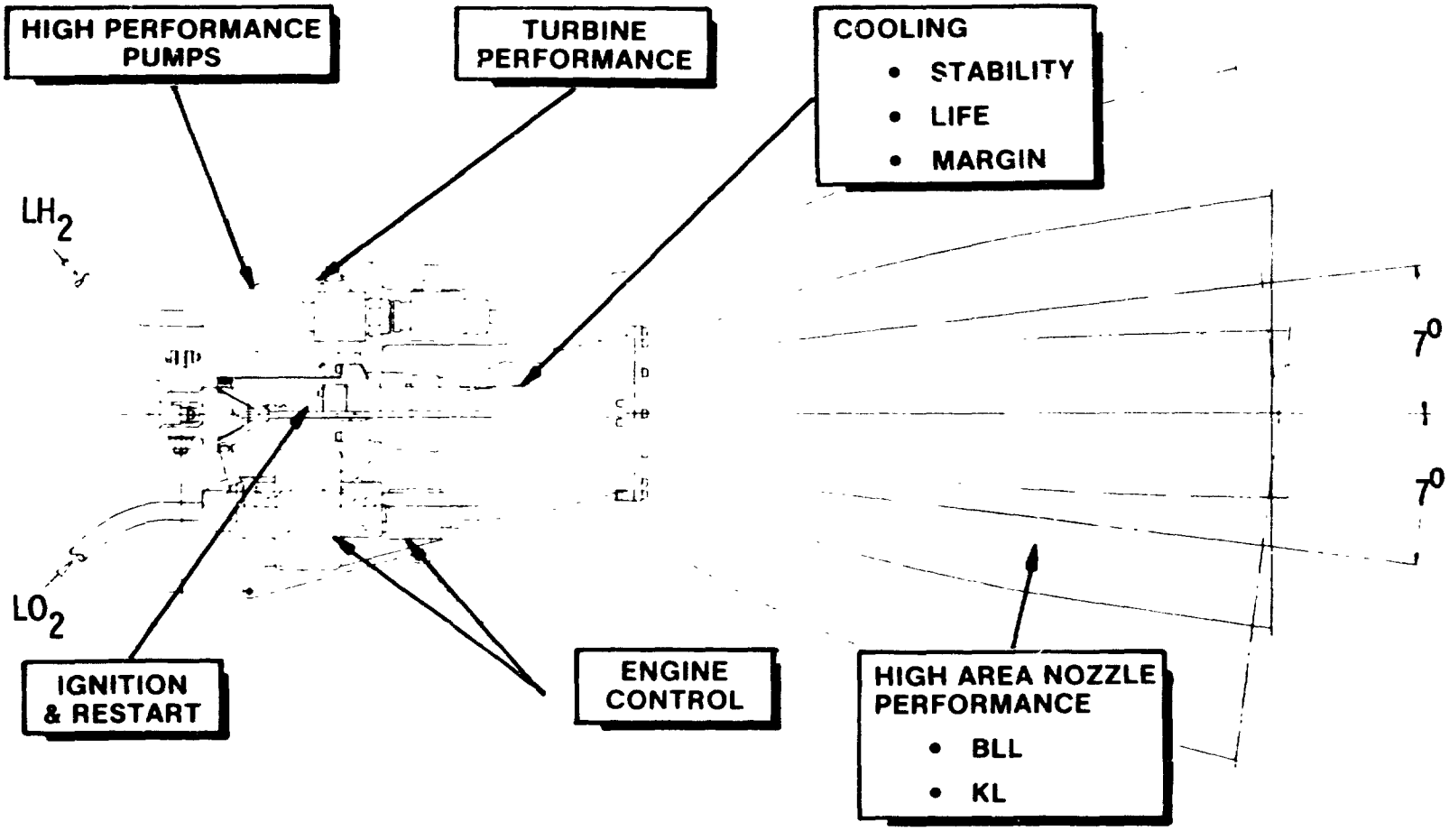

Figure 70. Technology Areas Summary

TABLE XXI. - MAJOR TECHNOLOGY ITEMS

- PUMPS AND DRIVES
  - Demonstrate the Performance of Low Specific Speed, High Head Rise, Low-Flow, Multi-Stage Centrifugal Pumps
  - Experimentally Verify the Performance of Small, Low-Flow, Hydrogen Partial Admission Gas Turbines
  - Conduct a Design and Demonstration Program on Pumps and Drives for the Mixed Expander/Turboalternator Cycle
  - Evaluate the use of Hydrostatic Bearings and Seals in the Turbomachinery Design: to Increase Life & Performance
- THRUST CHAMBER ASSEMBLY
  - Experimentally Verify the Forecasted Injector/Chamber Performance for use in an Expander Cycle
  - Evaluate Thermally Enhanced High-Flux Chambers to Extend Life, Operating Capability and Cooling Margin
  - Evaluate and Demonstrate High-Altitude Ignition and Restart
- PERFORMANCE
  - Experimentally Verify High Area Ratio Nozzle Performance (Boundary Layer & Kinetic Losses)
- ENGINE ASSEMBLY
  - Conduct a Point Design Engine Optimization Study to Drive Out Design and Technology Issues
    - Performance
      Life
    - Risk
    - Power
  - Evaluate Methods to Achieve Thrust and O/F Control and Optimize the Control System
- COOLING
  - Experimentally Evaluate Single-Channel Flow Stability for Changing Area Channels with Heat Addition
  - Develop a Flow Stability Computer Model that Simulates the Chamber Designs
  - Evaluate Two-Phase and Transition from Two-Phase to Single-Phase Flow on Heat Transfer
  - Assess Significance of Nucleate Boiling with Subcritical Cryogens
  - Verify the Liquid Film Cooling Model Extension to Higher Liquid Entrainment Rates and Account for Boundary Layer Development (i.e., Short Liquid Films)
  - Obtain Film Cooling Data for Dense Supercritical and Near Critical Coolants

The engine design should be carried to the next logical iteration or point design phase to further optimize the engine design, drive out additional technology issues, and evaluate component performance. Pump leakage and recirculation flows should be established so that the overall efficiency can be determined. This should be undertaken in conjunction with the cooling evaluations so that the turbine bypass flow requirements can be defined and the feasibility of the cycle power balance and design point can be established. The control system and controller requirements must be defined, and the best method to achieve mixture ratio control with a mixed expander/ turboalternator cycle should be determined.

The successful completion of the engine component technology programs will permit entry into the engine development phase with high confidence.

In addition to the engine technologies, several general technologies were identified in the cooling area. These technologies address shortcomings in analytical models and are listed in Table XXI.

Models which are available to predict flow instability are based upon data obtained from constant diameter heated tube tests. Data should be obtained with specimens simulating a real chamber configuration and then incorporated into the computer models.

A film boiling model should be incorporated and checked out in engine regenerative cooling design correlations. This work should include an assessment of the transition from two-phase to single-phase flow. Further effort is needed to evaluate pressure drop for two-phase flow to better prescribe pressure drop prediction formulation.

Although film-cooled engines were not recommended by this study, they should not be ruled out for other applications. The use of available film-cooling models to analyze the study coolants over the ranges of pressures and engine thrusts suggests a need for additional information to improve the analysis. Film-cooling data for dense supercritical and near-critical coolants are needed to evaluate the models and demonstrate their applicability in this region. In addition, experimental verification of the analytical extension of the liquid film mode to higher liquid entrainment rates is needed. This should include accounting for boundary layer development with short liquid films.

REFERENCES

1. McCarty, R.D. and Weber, L.A., Thermophysical Properties of Oxygen From the Freezing Line to 600°R for Pressures to 5000 psia, NBS Tech. Note 384, National Bureau of Standards, Cryogencis Div., Boulder, CO, July 1971.

2. Roder, H.M. and Weber, L.A., ASRDI Oxygen Technology Survey: Volume I, Thermophysical Properties, NASA SP-3071, National Aeronautics and Space Administration, Washington, D.C., 1972.

3. Weber, L.A., Extrapolation of Thermophysical Properties Data for Oxygen to High Pressures (5000 to 10,000 psia) at Low Temperatures (100-600°R), NASA CR-133858, NBS-10727, National Bureau of Standards, Cryogenics Div., Boulder, CO, November 1971.

4. Hanley, H.J., McCarty, R.D., and Sengers, J.V., Viscosity and Thermal Conductivity Coefficients of Gaseous and Liquid Oxygen, NASA CR-2440, National Aeronautics and Space Administration, Washington, D.C., August 1974.

5. McCarty, R.D. and Weber, L.A., Thermophysical Properties of Parahydrogen from the Freezing Liquid Line to 5000°R for Pressures to 10,000 psia, NBS Tech. Note 617, National Bureau of Standards, Cryogenics Div., Boulder, CO, April 1972.

6. Liquid Propellants Manual: Unit 20, RP-1, Chemical Propulsion Information Agency, The John Hopkins University Applied Physics Laboratory, Silver Springs, MD, January 1966.

7. Dean, L.E. and Shurley, L.A., Characteristics of RP-1 Rocket Fuel, Tech. Report TCR-70, Contract F04(645)-8, Weapon System 107A, Aerojet-General Corporation, Sacramento, CA, 14 February 1957.

8. Goodwin, R.D., The Thermophysical Properties of Methane, from 90 to 500°K at Pressures to 700 Bar, NBS Technical Note 653, Cryogenics Div., National Bureau of Standards, Boulder, CO, 1974

9. Huang, E.T.S., Swift, G.W., and Kurata, F., "Viscosities of Methane and Propane at Low Temperatures and High Pressures," A.I.Ch.E. Journal, 12, No. 5 (1966), 932-36.

10. Swift, G.W., Lohrenz, J, and Kurata, F, "Liquid Viscosities Above the Normal Boiling Point for Methane, Ethane, Propane, and n-Butane," A.I.Ch.E. Journal, 6, No. 3 (1960), 415-19.

11. Ikenberry, L.D. and Rice, S.A., "On the Kinetic Theory of Dense Fluids XIV. Experimental and Theoretical Studies of Thermal Conductivity in Liquid Ar, Kr, Xe," J. Chem. Phys., 39, No. 6 (1963) 1561.

12. Svehla, R.A. and McBride, B.J., Fortran IV Computer Program for Calculation of Thermodynamic and Transport Properties of Complex Chemical Systems, NASA TN D-7056, January 1973.

13. Low-Thrust Chemical Rocket Engine Study, Monthly Technical Progress Narrative No. 1, Contract NAS 3-21940, ALRC, 10 September 1979.

14. Friedly, J.C., et al, Stability Investigation of Thermally Induced Flow Oscillations in Cryogenic Heat Exhangers, Final Report, Contract NAS 8-21045, General Electric Research and Development Center Report S-68-1023, October 1967.

15. Friedly, J.C., et al, "Approximate Criterion for Prediction of Flow Oscillations in Supercritical Fluid Heat Exchangers," Advances in Cryogenic Engineering, 14 (1969), 258-270.

16. Zuber, N., An Analysis of Thermally Induced Flow Oscillations in the Near-Critical and Supercritical Thermodynamic Region, Final Report, Contract NAS 8-11422, General Electric Research and Development Center Report, May 1966.

17. Thurston, R.S., "A Time-Delay Analog for Thermal-Acoustic Oscillations," Advances in Cryogenic Engineering, 15 (1970), 364-367.

18. Edeskuty, F.J. and Thurston, R.S., Similiarity of Flow Oscillations Induced by Heat Transfer in Cryogenic Systems. Los Alamos Scientific Laboratory Report LA-DC-8595.

19. Rogers, J.D., Oscillations in Flowing and Heated Subcritical Hydrogen, Los Alamos Scientific Laboratory Report LA-DC-8726, August 1967. Printed also in Advances in Cryogenic Engineering, 13 (1968), 223-231.

20. Integrated Thruster Assembly Program, Final Report, Contract NAS 3-15850, NASA CR-134509, ALRC, November 1973.

21. Cock, R.T., Advanced Cooling Techniques for High-Pressure Hydrocarbon Fueled Engines, Final Report, Contract NAS 3-21381, NASA CR-159790, Rocketdyne Division, Rockwell International, October 1979.

22. LaBotz, R.J., Rousar, D.C., and Valler, H.W., High Density Fuel Combustion and Cooling Investigation, Final Report, Contract NAS 3-21030, NASA CR 165177, ALRC, September 1980.

23. Spencer, R.G. and Rousar, D.C., Supercritical Oxygen Heat Transfer, Contract NAS 3-20384, NASA CR-135339, ALRC, November 1977.

24. Gross, R.G., Combustion Performance and Heat Transfer Characterization of LOX/Hydrocarbon Type Propellants, Monthly Progress Report 15958-M-8, Contract NAS 9-15958, ALRC, June 1980.

REFERENCES (cont.)

25. Hess, H.L., and Kunz, H.R., "A Study of Forced Convection Heat Transfer to Supercritical Hydrogen," Journal of Heat Transfer, 87, No. 1 (1965), 41-48.

26. Ewen, R.L., Hydrogen Film/Conductive Cooling, Contract NAS 3-14343, NASA CR-120926, ALRC, November 1972.

27. Rousar, D.C., and Ewen, R.L., Hydrogen Film Cooling Investigation, Contract NAS 3-15344, NASA CR-121235, ALRC, August 1973.

28. Rousar, D.C. and Ewen, R.L., Combustion Effects on Film Cooling, Contract NAS 3-17813, NASA CR-135052, ALRC, Nobember 1976.

29. Gater, R.A., and L'Ecuyer, M.R., A Fundamental Investigation of the Phenomena that Characterize Liquid Film Cooling, Purdue University Jet Propulsion Center, Report TM-69-1, January 1969.

30. Mellish, J.A., Orbit Transfer Vehicle (OTV) Advanced Expander Cycle Engine Point Design Study, Final Report, Vol. II: Study Results, Contract NAS 8-33574, ALRC, 10 December 1980.

31. JANNAF Rocket Engine Performance Test Data Acquisition and Interpretation Manual, CPIA Publication 245, December 1973.

32. JANNAF Liquid Rocket Engine Performance Prediction and Evaluation Manual, CPIA Publication 246, April 1975.

33. Dennies, P.C., Marker, H.E., and Yost, M.C., Advanced Thrust Chamber Technology, Final Report, Contract NAS 3-17825, NASA CR-135221, Rocketdyne Division, Rockwell International, July 1977.

34. Yost, M.C., Preburner of Staged Combustion Rocket Engine, Final Report, Nas 3-19713, NASA CR-135356, Rocketdyne Division, Rockwell International, February 1978.

35. Blubaugh, A.L., and Schoenman, L., Extended Temperature Range Thruster Investigation, Final Report, Contract NAS 3-16775, NASA CR-134655, ALRC, August 1974.